FOUNDATION ENGINEERING II

Lecture
Ahmed H. Abdulkareem

2017

University of Anbar
Engineering College
Civil Engineering Department

CHAPTER ONE

DRILLED-SHAFT AND CAISSON FOUNDATIONS

LECTURE
DR. AHMED H. ABDULKAREEM
2017

1.1 Introduction

The terms *caisson, pier, drilled shaft,* and *drilled pier* are often used interchangeably in foundation engineering; all refer to a *cast-in-place pile generally having a diameter of about 750 mm* or more, with or without steel reinforcement and with or without an enlarged bottom. Sometimes the diameter can be as small as 305 mm.

The use of drilled-shaft foundations has several advantages:

1. A single drilled shaft may be used instead of a group of piles and the pile cap.
2. Constructing drilled shafts in deposits of dense sand and gravel is easier than Driving piles.
3. Drilled shafts may be constructed before grading operations are completed.
4. When piles are driven by a hammer, the ground vibration may cause damage to nearby structures.
5. Piles driven into clay soils may produce ground heaving and cause previously driven piles to move laterally.
6. There is no hammer noise during the construction of drilled shafts**.**
7. Because the base of a drilled shaft can be enlarged, it provides great resistance to the uplifting load.
8. The surface over which the base of the drilled shaft is constructed can be visually inspected.
9. The construction of drilled shafts generally utilizes mobile equipment.
10. Drilled shafts have high resistance to lateral loads.

1.2 Types of Drilled Piers

Drilled piers may be described under four types. All four types are similar in construction technique, but differ in their design assumptions and in the mechanism of load transfer to the surrounding earth mass. These types are illustrated in **Fig. 1.1** and as following:

1. *Straight –shaft end-bearing piers* develop their support from end-bearing on strong soil, " hardpan" or rock. The overlying soil is assumed to contribute nothing to the support of the load imposed on the pier**[Fig.1.1(a)]**.
2. *Straight-shaft side wall friction piers* pass through overburden soils that are assumed to carry none of the load, and penetrate far enough into an assign bearing stratum to develop design load capacity by side wall friction between the pier and bearing stratum to develop design load capacity by side wall friction between the pier and bearing stratum**[Fig. 1.1(b)]**.
3. *Combination of straight shaft side wall friction and end bearing piers* are of the same construction as the two mention above, but with both side wall friction and end bearing assigned a role in carrying the design load. When carried into rock, this pier may be referred to as a socketed pier or a " drilled pier with rock socket"**[Fig. 1.1(c)]**.

4. *Belled or underreamed piers* with a bottom bell or underream[Fig.1.1(d)]. A greater percentage of the imposed load on the pier top is assumed to be carried by the base.

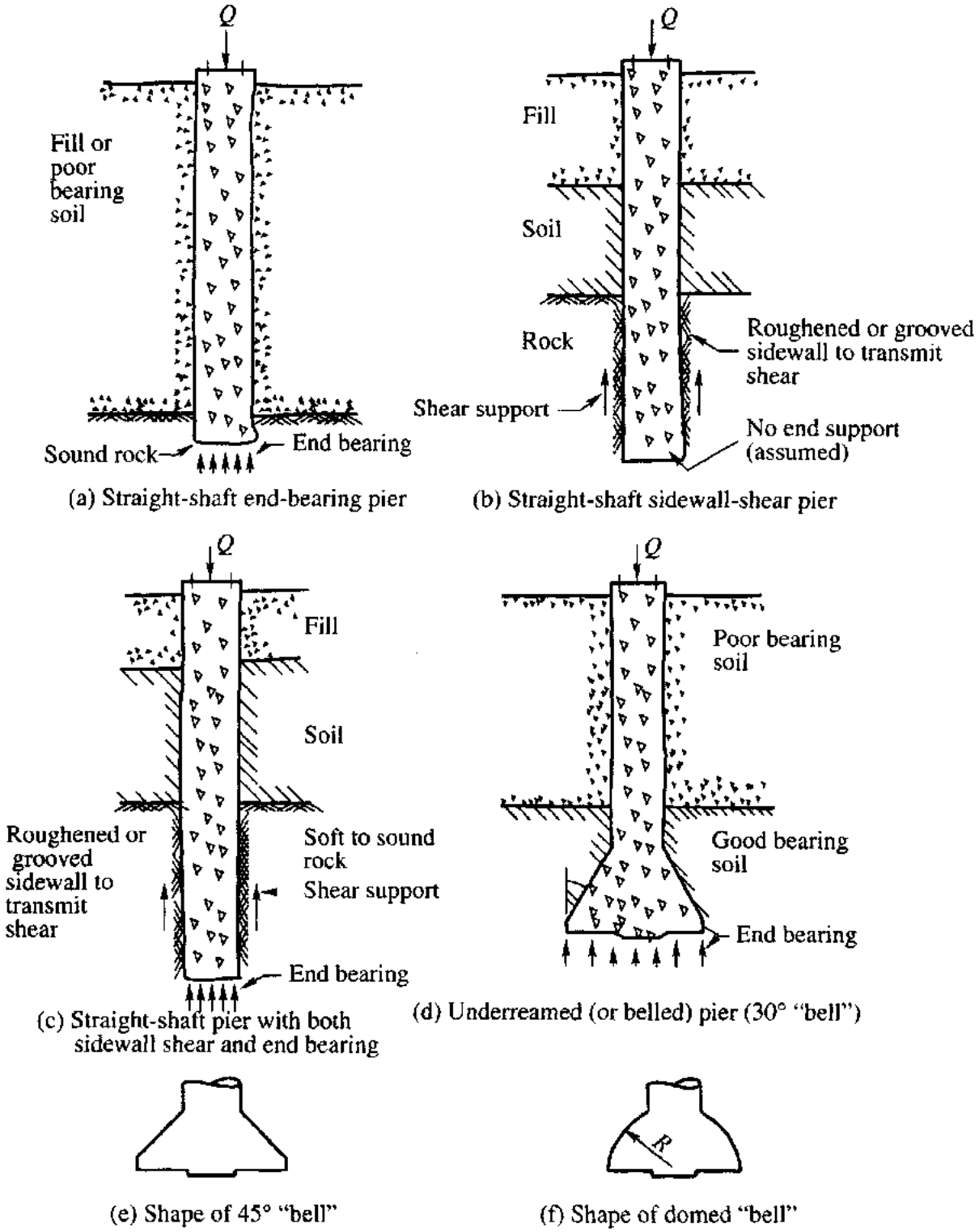

Fig 1.1 Types of drilled piers and underream shapes (Woodward et al., 1972)

1.3 Advantages and Disadvantages of Drilled Pier Foundations

Advantages

1. Pier of any length and size can be constructed at the site
2. Construction equipment is normally mobile and construction can proceed rapidly
3. Inspection of drilled holes is possible because of the larger diameter of the shafts
4. Very large loads can be carried by a single drilled pier foundation thus eliminating the necessity of a pile cap
5. The drilled pier is applicable to a wide variety of soil conditions
6. Changes can be made in the design criteria during the progress of a job
7. Ground vibration that is normally associated with driven piles is absent in drilled pier construction
8. Bearing capacity can be increased by underreaming the bottom (in non-caving materials)

Disadvantages

1. Installation of drilled piers needs a careful supervision and quality control of all the materials used in the construction
2. The method is cumbersome. It needs sufficient storage space for all the materials used in the construction
3. The advantage of increased bearing capacity due to compaction in granular soil that could be obtained in driven piles is not there in drilled pier construction
4. Construction of drilled piers at places where there is a heavy current of ground water flow due to artesian pressure is very difficult

1.4 Construction Procedures

There are three major types of construction methods: the dry method, the casing method,
and the wet method.

Dry Method of Construction

This method is employed in soils and rocks that are above the water table and that will not cave in when the hole is drilled to its full depth. The sequence of construction, shown in **Figure 1.2**, is as follows:

Step 1. The excavation is completed (and belled if desired), using proper drilling tools, and the spoils from the hole are deposited nearby. **(See Fig. 1.2a.)**

Step 2. Concrete is then poured into the cylindrical hole. **(See Fig. 1.2b.)**

Step 3. If desired, a rebar cage is placed in the upper portion of the shaft. **(See Fig. 1.2c.)**

Step 4. Concreting is then completed, and the drilled shaft will be as shown in **Fig. 1.2d**.

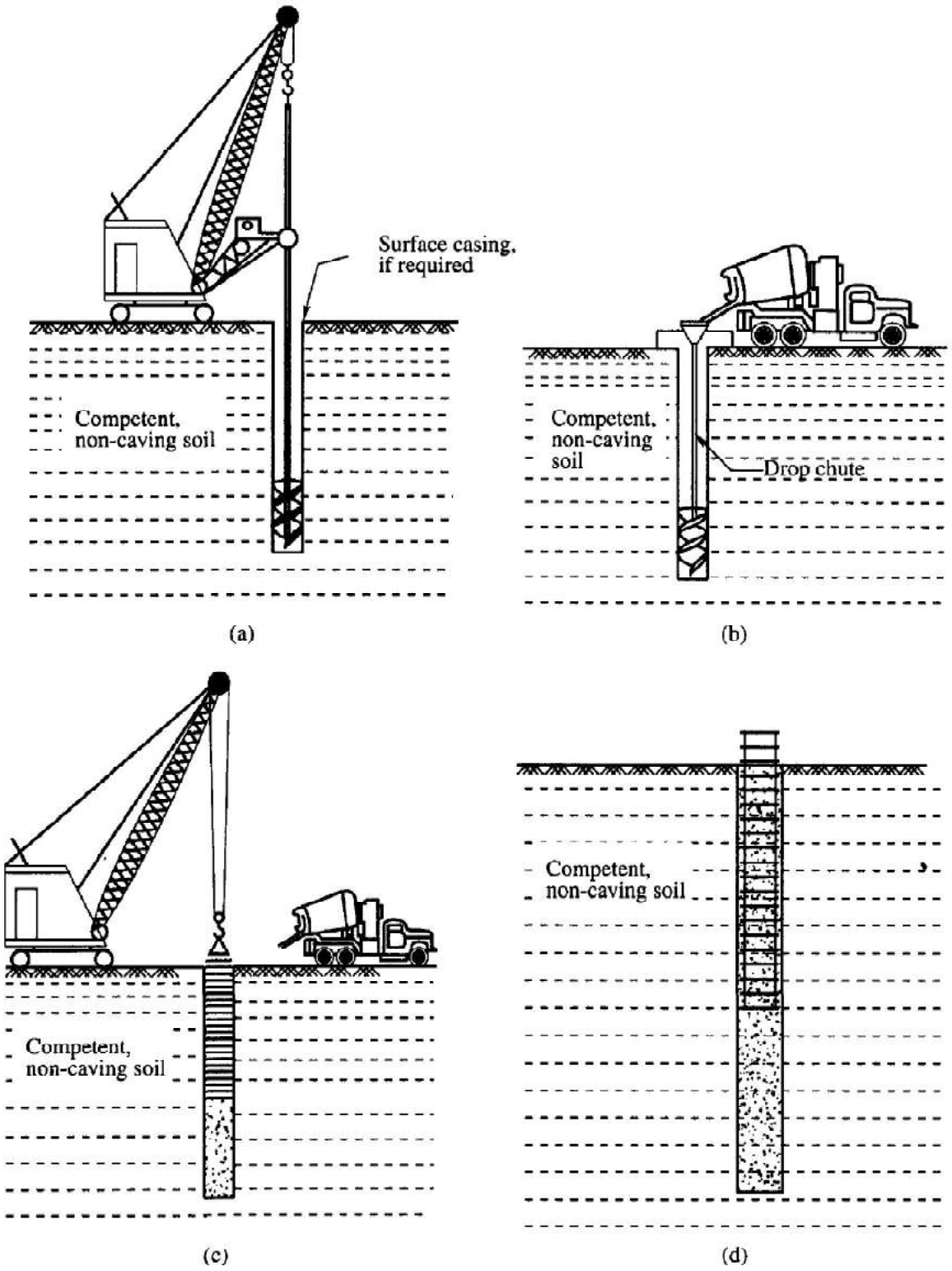

Fig. 1.2 Dry method of construction: (a) initiating drilling; (b) starting concrete pour; (c) placing rebar cage; (d) completed shaft (Based on O'Neill and Reese, 1999)

Casing Method of Construction

This method is used in soils or rocks in which caving or excessive deformation is likely to
occur when the borehole is excavated. The sequence of construction is shown in Fig. 1.3
and may be explained as follows:

Step 1. The excavation procedure is initiated as in the case of the dry method of construction. (See Fig. 1.3a.)

Step 2. When the caving soil is encountered, bentonite slurry is introduced into the borehole. (See Fig. 10.3b.) Drilling is continued until the excavation goes past the caving soil and a layer of impermeable soil or rock is encountered.

Step 3. A casing is then introduced into the hole. (See Fig. 1.3c.)

Step 4. The slurry is bailed out of the casing with a submersible pump. (See Fig. 1.3d.)

Step 5. A smaller drill that can pass through the casing is introduced into the hole, and excavation continues. (See Fig. 1.3e.)

Step 6. If needed, the base of the excavated hole can then be enlarged, using an underreamer. (See Fig. 1.3f.)

Step 7. If reinforcing steel is needed, the rebar cage needs to extend the full length of the excavation. Concrete is then poured into the excavation and the casing is gradually pulled out. (See Fig. 1.3g.)

Step 8. Fig. 1.3h shows the completed drilled shaft.

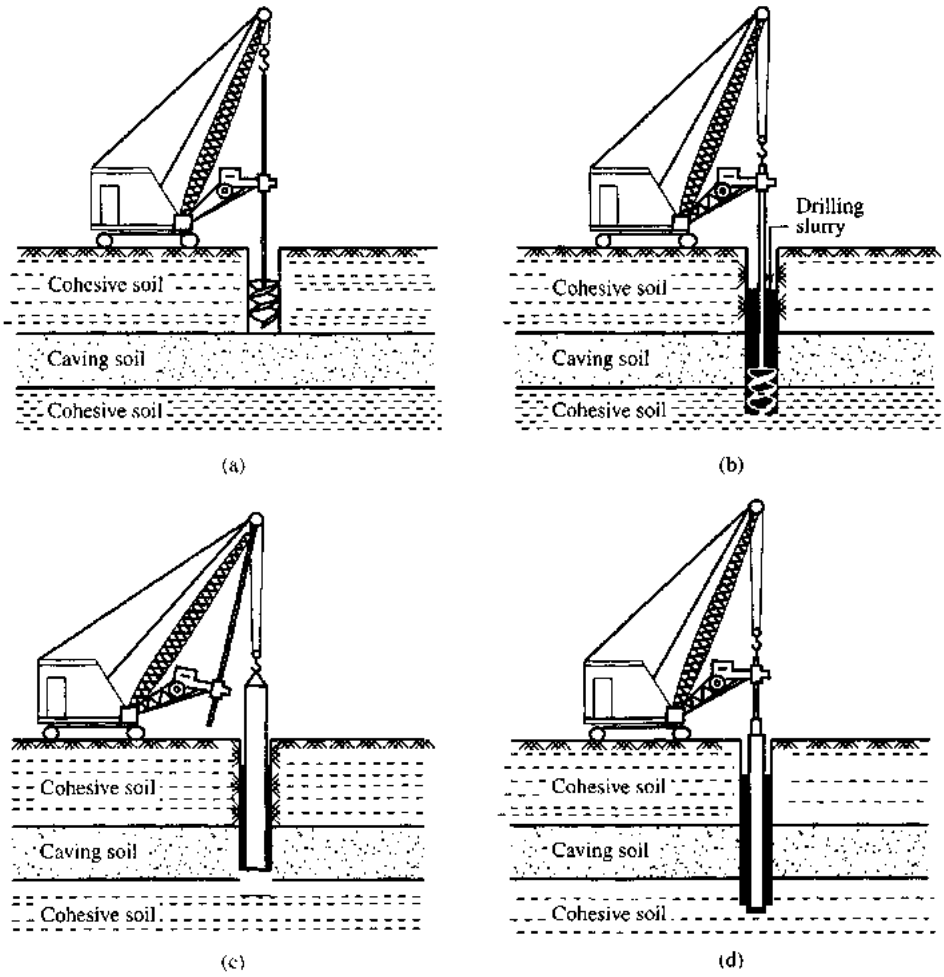

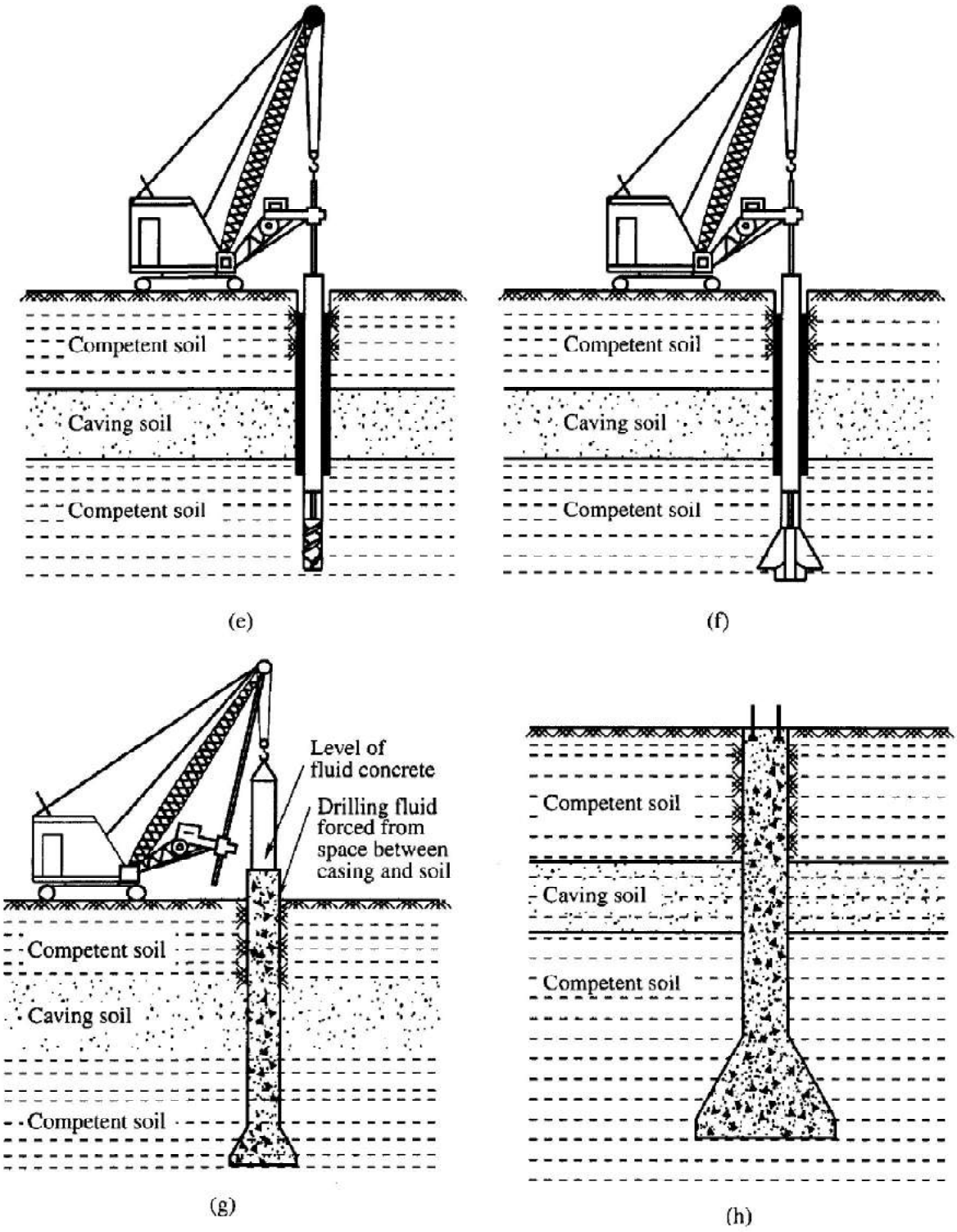

Fig. 1.3 Casing method of construction: (a) initiating drilling; (b) drilling with slurry; (c) introducing casing; (d) casing is sealed and slurry is being removed from interior of casing; (e) drilling below casing; (f) underreaming; (g) removing casing; (h) completed shaft (Based on O'Neill and Reese, 1999)

Wet Method of Construction

This method is sometimes referred to as the *slurry displacement method.* Slurry is used to keep the borehole open during the entire depth of excavation. (See Figure 1.4) Following are the steps involved in the wet method of construction:

Step 1. Excavation continues to full depth with slurry. (See Figure 1.4a.)

Step 2. If reinforcement is required, the rebar cage is placed in the slurry. (See Figure 1.4b.)

Step 3. Concrete that will displace the volume of slurry is then placed in the drill hole. (See Figure 1.4c.)

Step 4. Figure 1.4d shows the completed drilled shaft.

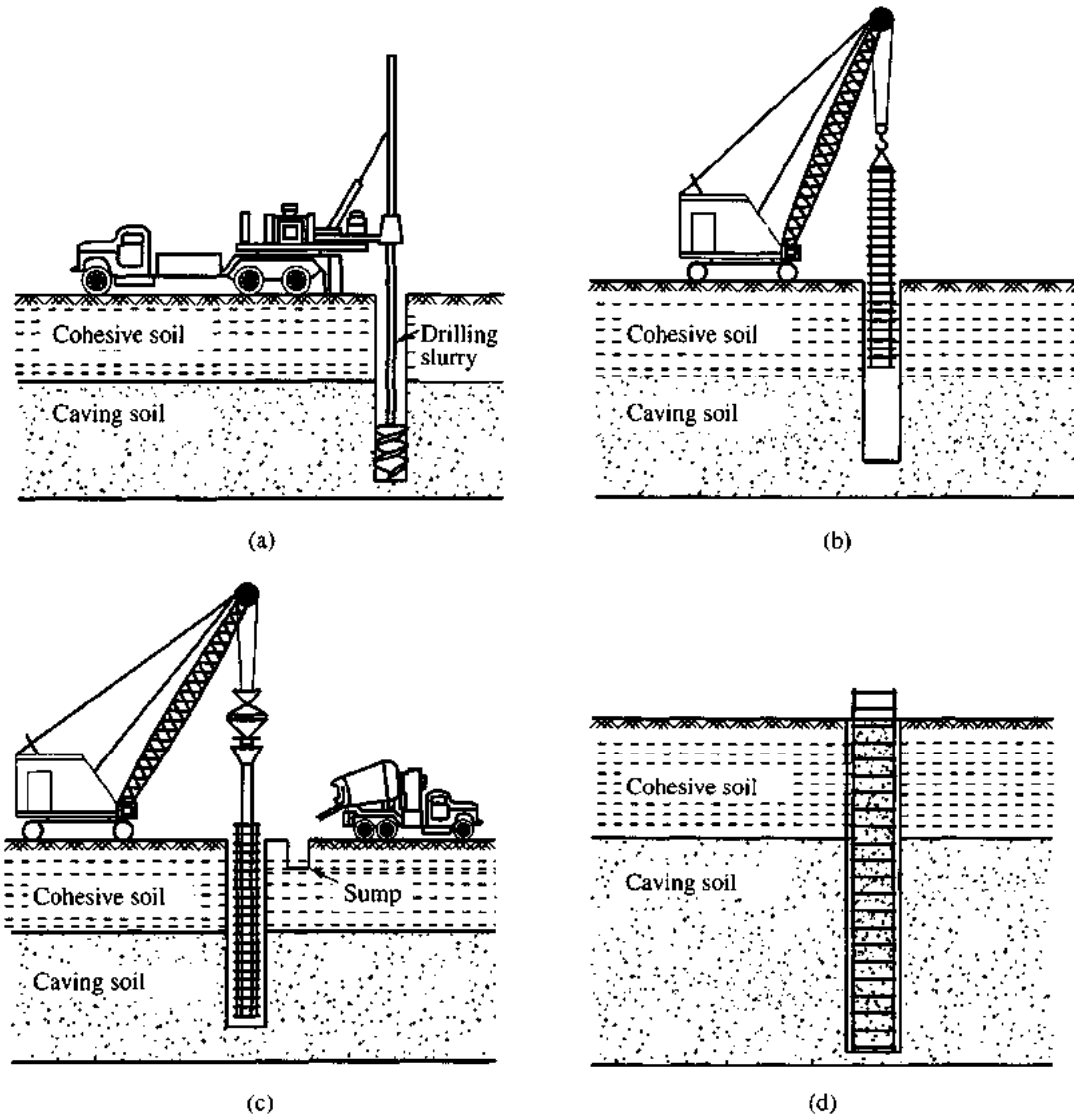

Figure 10.4 Slurry method of construction: (a) drilling to full depth with slurry; (b) placing rebar cage; (c) placing concrete; (d) completed shaft (After O'Neill and Reese, 1999)

1.5 DESIGN CONSIDERATIONS

The process of the design of a drilled pier generally involves the following:

1 . The objectives of selecting drilled pier foundations for the project.
2. Analysis of loads coming on each pier foundation element.
3. A detailed soil investigation and determining the soil parameters for the design.
4. Preparation of plans and specifications which include the methods of design, tolerable settlement, methods of construction of piers, etc.
5.The method of execution of the project.

In general the design of a drilled pier may be studied under the following headings:

1. Allowable loads on the piers based on ultimate bearing capacity theories.
2. Allowable loads based on vertical movement of the piers.
3. Allowable loads based on lateral bearing capacity of the piers.

In addition to the above, the uplift capacity of piers with or without underreams has to be evaluated. The following types of strata are considered.

1 . Piers embedded in homogeneous soils, sand or clay.
2. Piers in a layered system of soil.
3. Piers socketed in rocks.

It is better that the designer select shaft diameters that are multiples of 150 mm (6 in) since these are the commonly available drilling tool diameters.

For the design of ordinary drilled shafts without casings, a minimum amount of vertical steel reinforcement is always desirable. Minimum reinforcement is 1% of the gross cross-sectional area of the shaft. For drilled shafts with nominal reinforcement, most building codes suggest using a design concrete strength, fc , on the order of $\acute{f}c/4$. Thus, the minimum shaft diameter becomes

$$D_S = \sqrt{\frac{Q_w}{\left(\frac{\pi}{4}\right)(0.25)f_c'}} = 2.257\sqrt{\frac{Q_w}{f_c'}} \qquad (1\text{-}1)$$

where
D_s = diameter of the shaft
$\acute{f}c$ = 28-day concrete strength
Q_w = working load of the drilled shaft
A_{gs} = gross cross-sectional area of the shaft

If drilled shafts are likely to be subjected to tensile loads, reinforcement should be continued
for the entire length of the shaft.

Concrete Mix Design

The concrete mix design for drilled shafts is not much different from that for any other concrete structure. When a reinforcing cage is used, consideration should be given to the ability of the concrete to flow through the reinforcement. In most cases, a concrete slump of about 15.0 mm (6 in.) is considered satisfactory. Also, the maximum size of the aggregate should be limited to about 20 mm (0.75 in.).

1.6 Estimation of Load-Bearing Capacity - General

The load-transfer mechanism from drilled shafts to soil is similar to that of piles as last described chapter. The ultimate load-bearing capacity of a drilled shaft **(Fig. 1.5)** is

$$Q_u = Q_p + Q_s \qquad (1\text{-}2)$$

where
Q_u= ultimate load
Q_p = ultimate load-carrying capacity at the base
Q_s = frictional (skin) resistance

The equation for the ultimate base load is similar to that for shallow foundations:

$$Q_p = A_p(c'N_c^* + q'N_q^* + 0.3\gamma D_b N_\gamma^*) \qquad (1\text{-}3)$$

Where
N_c^*, N_q^*, N_γ^* = the bearing capacity factors
q'= vertical effective stress at the level of the bottom of the pier
D_b= diameter of the base (see Fig. 1.5a and b)
A_p= area of the base= $\pi/4D_b^2$

In most cases, the last term (containing N_γ^*) is neglected except for relatively short drilled shafts, so

$$Q_p = A_p(c'N_c^* + q'N_q^*) \qquad (1\text{-}4)$$

The net load-carrying capacity at the base (that is, the gross load minus the weight of the drilled shaft) may be approximated as

$$Q_{p(net)} = A_p(c'N_c^* + q'N_q^* - q' = A_p[c'N_c^* + q'(N_q^* - 1)] \qquad (1\text{-}5)$$

The expression for the frictional, or skin, resistance, Q_s, is similar to that for piles

$$Q_s = \int_0^{L_1} pf\,dz \qquad (1\text{-}6)$$

Where

p=shaft perimeter=πD_s

f=unit frictional (or skin)resistance

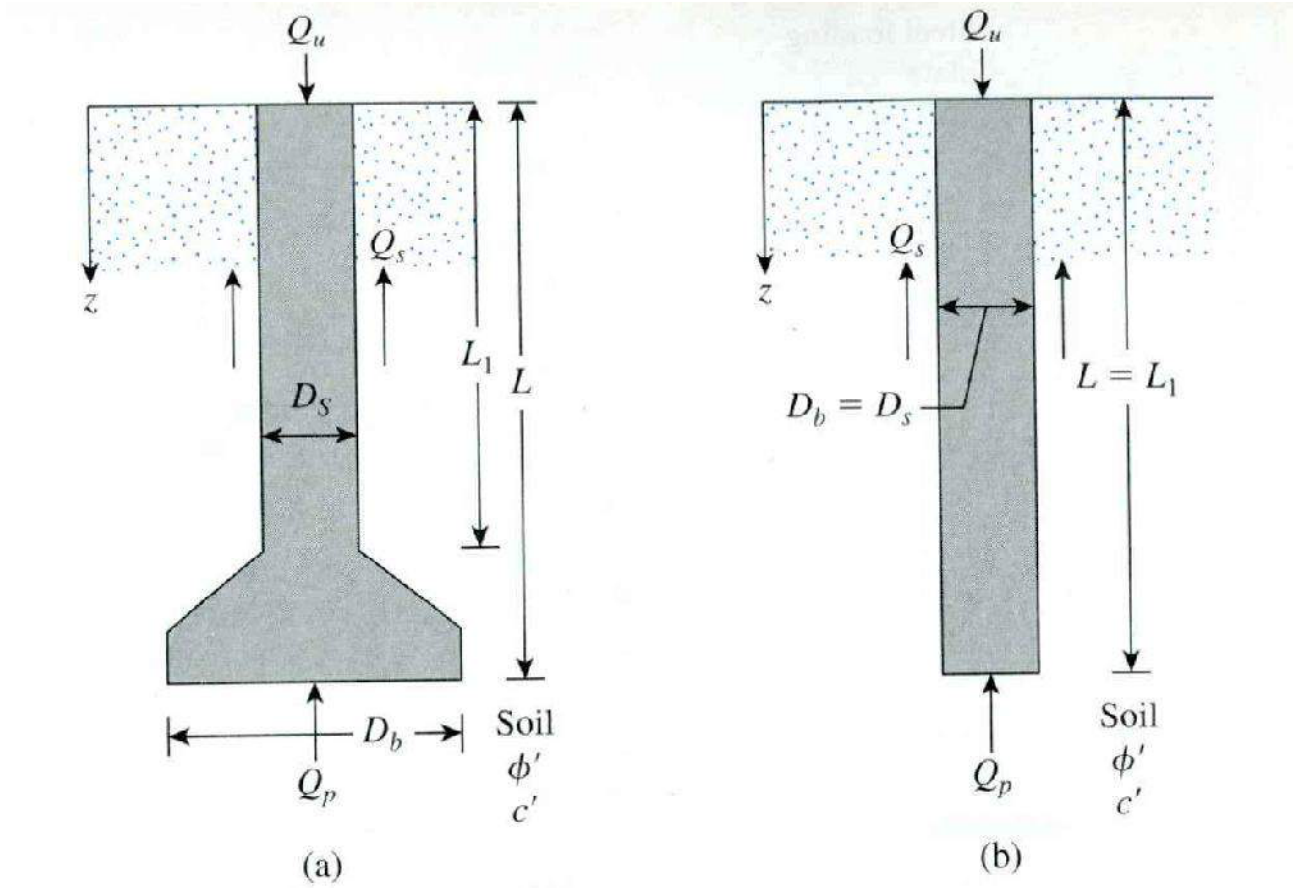

Figure 1.5 Ultimate bearing capacity of drilled shafts: (a) with bell and (b) straight shaft

The following two sections describe the procedures for obtaining the ultimate and allowable load-bearing capacities of drilled shafts in sand and clay.

1.6 Drilled Shafts in Sand: Load-Bearing Capacity

Estimation of Q_p

For drilled shafts in sand, c'=0 and , hence Eq. (1-5) simplifies to

$$Q_{p(net)} = A_p q'(N_q^* - 1) \qquad (1\text{-}7)$$

Determination of N_q^* is always a problem for deep foundation, as in the case of piles. Note, however, that all shafts are drilled, unlike the majority of piles, which are driven. The values of N_q^* given by Vesic(1963) are approximately the lower bound, and hence are used in this chapter **(Fig. 1-6)**

The frictional resistance at ultimate load, Q_s, developed in a drilled shaft may be calculated from the relation given in Eq.(1-6), in which

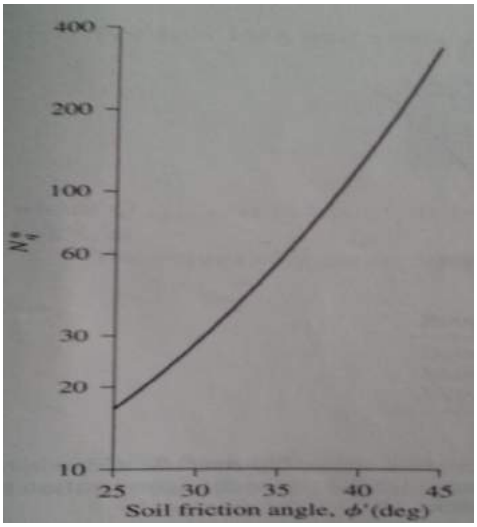

Fig. 1.6 Vesic's bearing capacity factors, N_q^*, for deep foundations

The magnitude of $Q_{p(net)}$ also can be reasonably estimated from a relationship based on the analysis of Berezantzev et al. (1961) that can be expressed as

$$Q_{p(net)} = A_p q'(\omega N_q^* - 1) \qquad (1.8)$$

where

N_q^*= bearing capacity factor = $0.21e^{0.17\phi'}$ (See Table 1.1) (1.9)

ω = correction factor = $f(L/D_b)$

In Eq. (1.9), ϕ' is in degrees. The variation of v (interpolated values) with L/D_b is given in Fig. (1.7).

Table 1.1 Variation of N_q^* with ϕ' [Eq. (1.9)]

ϕ' (deg)	N_q^*
25	14.72
26	17.45
27	20.68
28	24.52
29	29.06
30	34.44
31	40.83
32	48.39
33	57.36
34	67.99
35	80.59
36	95.52
37	113.22
38	134.20
39	159.07
40	188.55
41	223.49
42	264.90
43	313.99
44	372.17
45	441.14

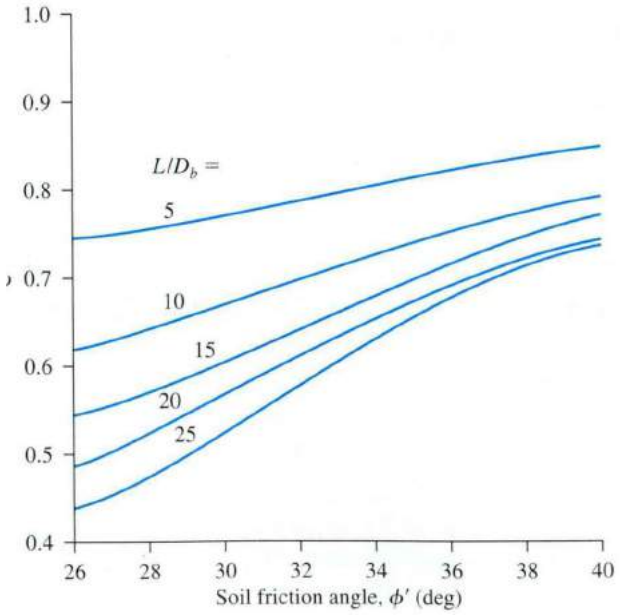

Fig. 1.7 Variation of ω with ϕ' and L/D_b

Estimation of Q_s

The frictional resistance at ultimate load, Q_s , developed in a drilled shaft may be calculated as

$$Q_s = \int_0^{L_1} pf\,dz \qquad (1\text{-}6)$$

p= shaft perimeter= πD_s

f= unit frictional (or skin) resistance= $K\sigma_o'\tan\delta'$ (1-10)

K= earth – pressure coefficient ≈ K_o= 1-sinϕ'

σ_o'= effective vertical stress at any depth z

Thus,

$$Q_s = \int_0^{L_1} pf\,dz = \pi D_s(1 - sin\emptyset') \int_0^{L_1} \sigma_o' \tan\delta'\,dz \qquad (1\text{-}11)$$

The value of σ_o' will increase to a depth of about $15D_s$ and will remain constant thereafter, as shown in Figure 1.8.

For cast-in-pile concrete and good construction techniques, a rough interface develops and, hence, δ'/ϕ' may be taken to be one. With poor slurry construction,

$\delta/\phi' < 0.7$ to 0.8.

Allowable Net Load, $Q_{all\ (net)}$

An appropriate factor of safety should be applied to the ultimate load to obtain the net allowable load, or

$$Q_{net(all)} = \frac{Q_{p(net)} + Q_s}{FS} \qquad (1\text{-}12)$$

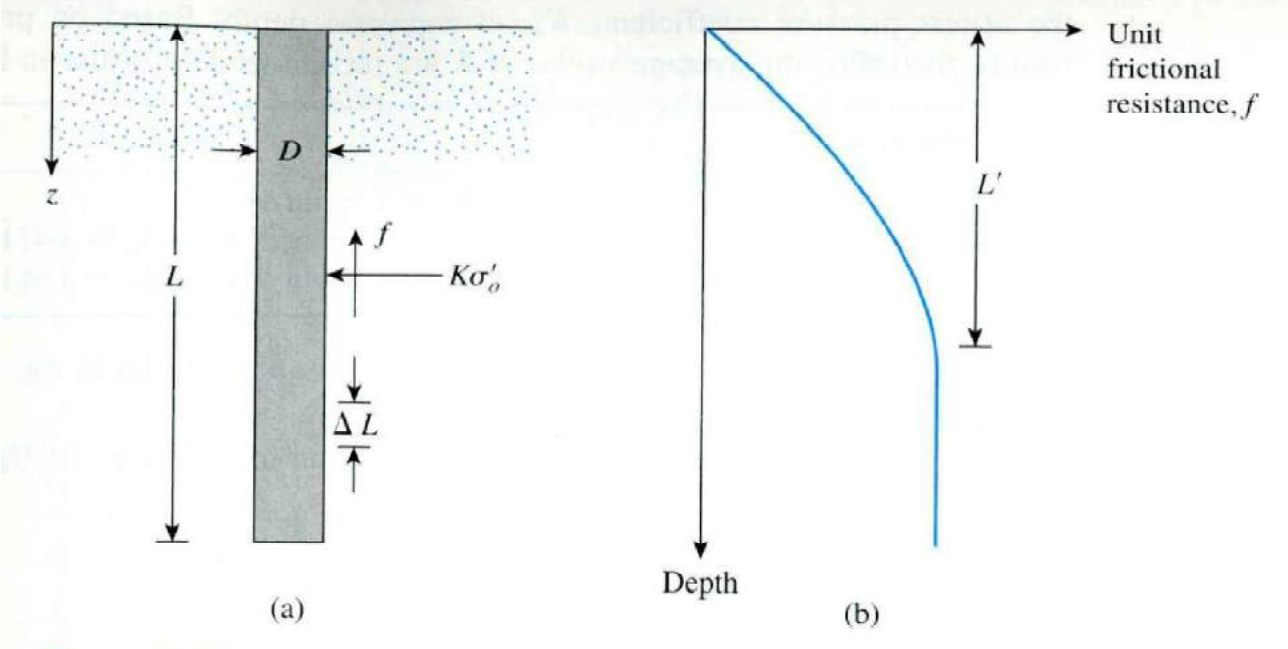

Fig. 1.8 Unit frictional resistance for piles in sand

1.7 Load Bearing Capacity Based on Settlement

On the basis of a database of 41 loading tests, Reese and O'Neill (1989) proposed a method for calculating the load-bearing capacity of drilled shafts that is based on settlement. The method is applicable to the following ranges:

1. Shaft diameter: D_s = 0.52 to 1.2 m (1.7 to 3.93 ft)
2. Bell depth: L = 4.7 to 30.5 m (15.4 to 100 ft)
3. Field standard penetration resistance: $N60$ = 5 to 60
4. Concrete slump = 100 to 225 mm (4 to 9 in.)

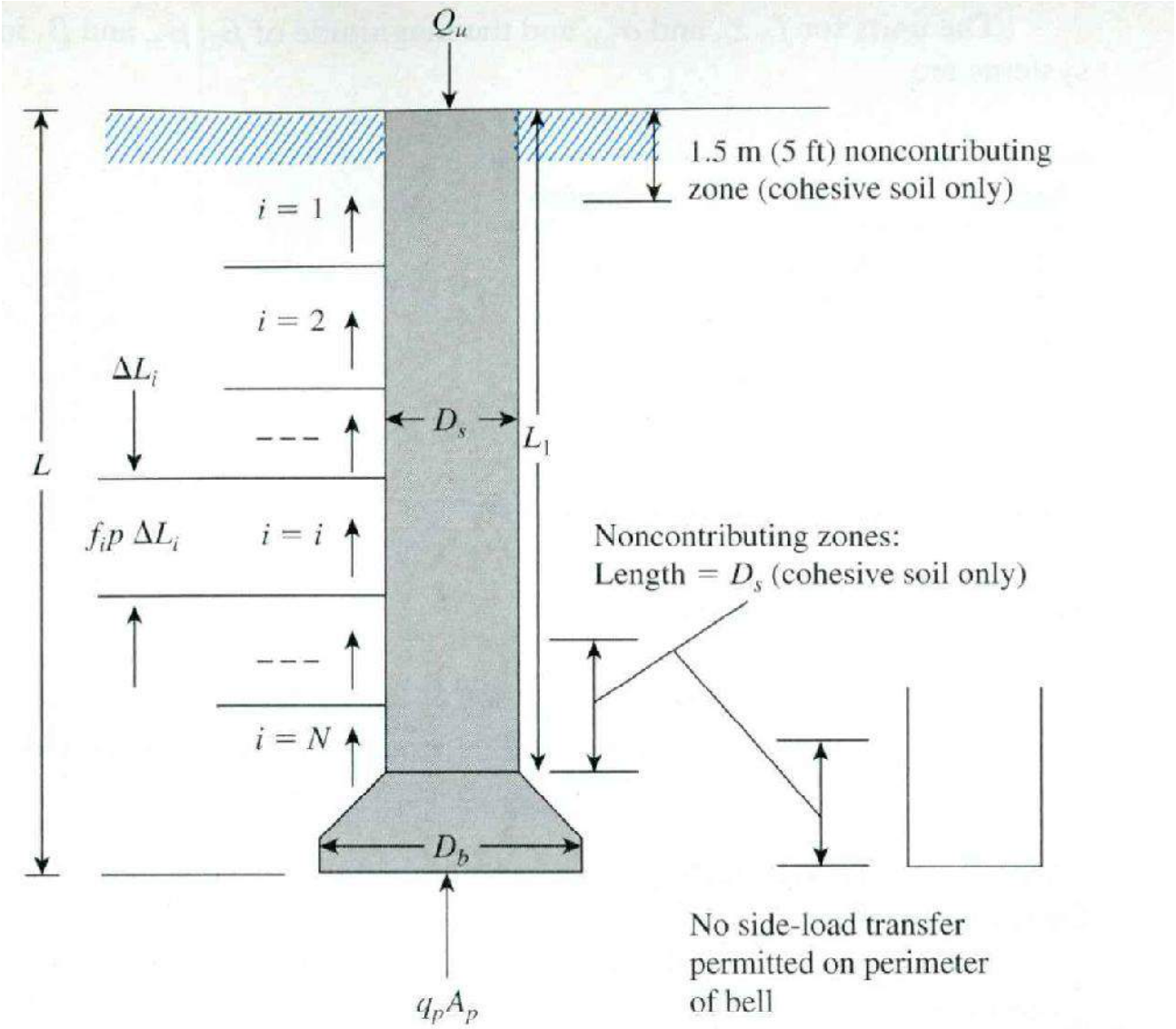

Fig. 1.9 Development of Eq.(1-13)

Reese and O'Neill's procedure (see Figure 10.10) gives

$$Q_{u(net)} = \sum_{i=1}^{N} f_i p \Delta L_i + q_p A_p \qquad (1\text{-}13)$$

where
f_i = ultimate unit shearing resistance in layer i
p = perimeter of the shaft = pD_s
qp = unit point resistance
Ap = area of the base = $(\pi/4)D^2_b$

Following are the relationships for determining $Q_{u(net)}$ in granular soils. Based on **Eq. (1-13)**

$$f_i = \beta \sigma'_{ozi} \leq 192\ kN/m^2 \qquad (1\text{-}14)$$

$$\beta = 1.5 - 0.244 z_i^{0.5} \quad (0.25 \leq \beta \leq 1.2) \qquad (1\text{-}15)$$

(where z_i is in m)

$$q_p \left(\frac{kN}{m^2}\right) = 57.5\ N_{60} \leq 4310 \frac{kN}{m^2} \qquad (for\ D_b < 1.27m) \qquad (1\text{-}16)$$

If $D_b \geq 1.27$m, excessive settlement may occur. In that case, q_p may be replaced by

$$q_{pr} = \frac{1.27}{D_b(m)} q_p \qquad (1\text{-}17)$$

Figs. 1.10 and 1.11 may now be used to calculate the allowable load $Q_{all(net)}$ based on the desired level of settlement. Example 1.2 shows the method of calculating the net allowable load.

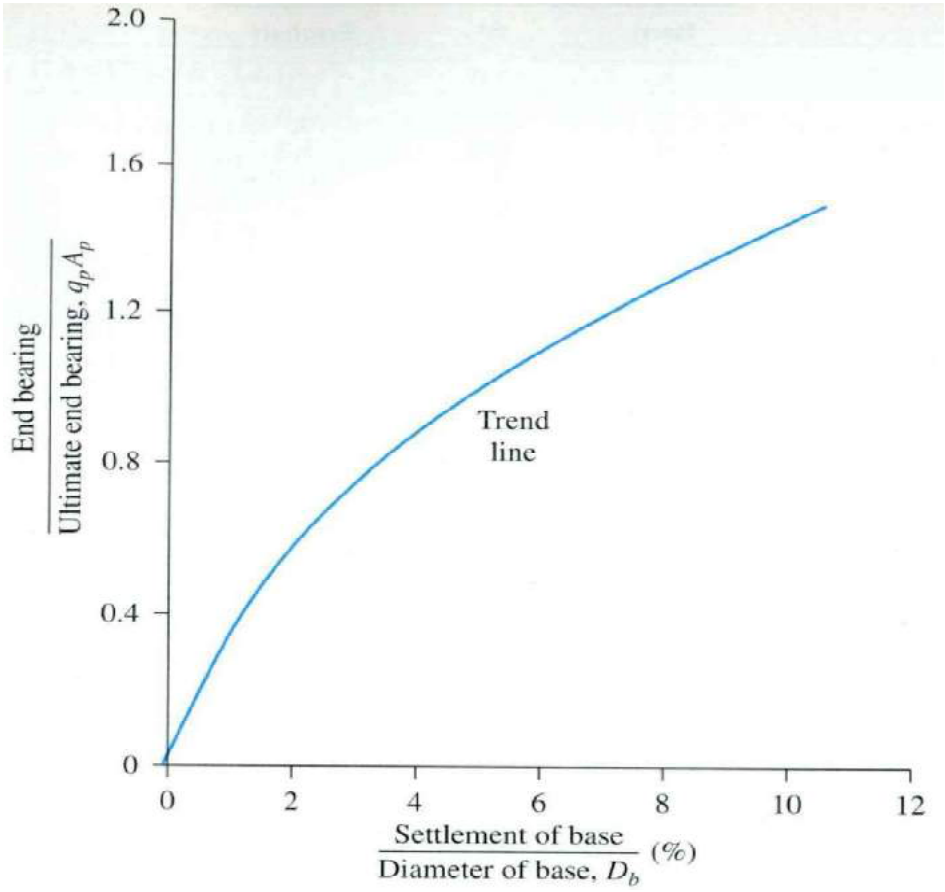

Fig. 1-10 Normalized based-load transfer versus settlement of sand

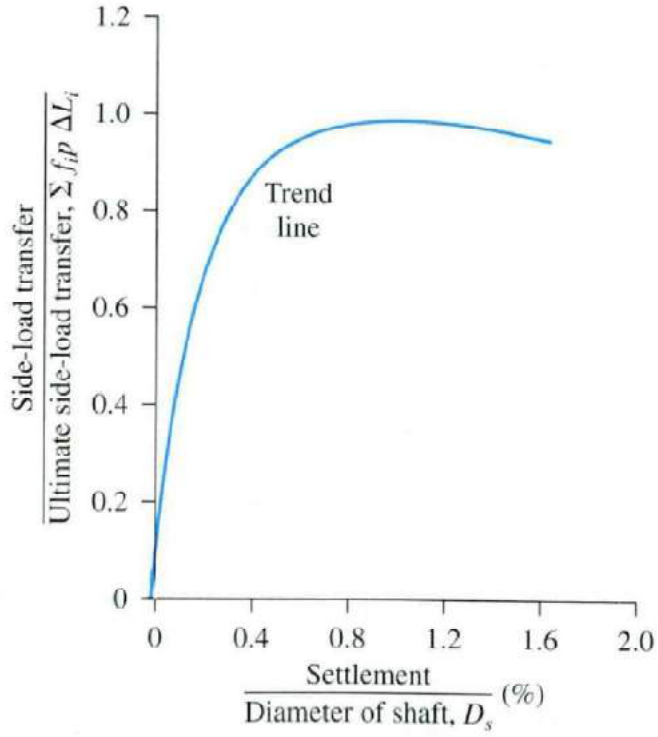

Fig. 1.11 Normalized side-load transfer versus settlement in sand

Example 1.1
Example 1.2

1.8 Drilled Shafts in Clay: Load-Bearing Capacity

From Eq.(1-5), For saturated clays with $\phi = 0$, $N_q^* = 1$; hence the net base resistance becomes

$$Q_{p(net)} = A_p c_u N_c^* \qquad (1\text{-}18)$$

Where c_u= undrained cohesion

The bearing capacity factor N_c^* is usually taken to be 9. When the $L/D_b \geq 4$, $N_c^* = 9$, which is the condition for most drilled shafts.

Experiments by **Whitaker and Cooke (1966)** showed that, for belled shafts, the full value of $N_c^* = 9$ is realized with a base movement of about 10 to 15% of D_b. Similarly, for straight shafts ($D_b = D_s$), the full value of $N_c^* = 9$ is obtained with a base movement of about 20% of D_b.

The expression for the skin resistance of drilled shafts in clay is

$$Q_s = \sum_{L=0}^{L=L_1} \alpha^* c_u p \Delta L \qquad (1\text{-}19)$$

Where p= perimeter of the shaft cross section.
the value of α^* that can be used in Eq. (1-19) has not yet been fully established however, the field test results available at this time indicate that α^* may vary between 1.0 to 0.3. **Kulhawy and Jackson (1989)** reported the field-test result of 106 straight drilled shafts—65 in uplift and 41 in compression. The best correlation obtained from the results is

$$\alpha^* = 0.21 + 0.25\left(\frac{p_a}{c_u}\right) \leq 1 \qquad (1\text{-}20)$$

Where p_a= atmospheric pressure=100 kN/m^2.

So, conservatively, we may assume that

$$\alpha^* = 0.4 \qquad (1\text{-}21)$$

Load-Bearing Capacity Based on Settlement

Reese and O'Neill (1989) suggested a procedure for estimating the ultimate and allowable (based on settlement) bearing capacities for drilled shafts in clay. According to this procedure, we can use Eq. (1-13) for the net ultimate load, or

$$Q_{u(net)} = \sum_{i=1}^{N} f_i p \Delta L_i + q_p A_p \qquad (1\text{-}13)$$

The unit skin friction resistance can be given as

$$f_i = \alpha_i^* c_{u(i)} \qquad (1\text{-}22)$$

The following values are recommended for α_i^*:

α_i^* =0 for the top 1.5m (5 ft) and bottom 1 diameter, D_s, of the drilled shaft. (*Note:* If $D_b > D_s$, then $a^* = 0$ for 1 diameter above the top of the bell and for the peripheral area of the bell itself.)

α_i^* =0.55 elsewhere.

The expression for q_p (point load per unit area) can be given as

$$q_p = 6c_{ub}\left(1 + 0.2\frac{L}{D_b}\right) \leq 9c_{ub} \leq 40p_a \qquad (1\text{-}23)$$

where
c_{ub} = average undrained cohesion within a vertical distance of $2D_b$ below the base
p_a = atmospheric pressure

If D_b is large, excessive settlement will occur at the ultimate load per unit area, q_p, as given by Eq. (1.23). Thus, for D_b >1.91 m (75 in.), q_p may be replaced by

$$q_{pr} = F_r q_p \qquad (1\text{-}24)$$

Where

$$F_r = \frac{2.5}{\varphi_1 D_b(mm) + \varphi_2} \leq 1 \qquad (1\text{-}25)$$

$$\varphi_1 = 2.78 \times 10^{-4} + 8.26 \times 10^{-5}\left(\frac{L}{D_b}\right) \leq 5.9 \times 10^{-4} \qquad (1\text{-}26)$$

and

$$\varphi_2 = 0.065\left[c_{ub}\left(\frac{kN}{m^2}\right)\right]^{0.5} \qquad (1\text{-}27)$$

Figures (1-12) and (1-13) may now be used to evaluate the allowable load-bearing capacity, based on settlement. (Note that the ultimate bearing capacity in **Figure (1-13)** is q_b, not q_{br}). To do so

Step 1. Select a value of settlement, *s*.

Step 2. Calculate $\sum_{i=1}^{N} f_i p \Delta L_i \; and \; q_b A_p$

Step 3. Using **Figures 1.12 and 1.13** and the calculated values in Step 2, determine the *side load* and the *end bearing load.*

Step 4. The sum of the side load and the end bearing load gives the total allowable load.

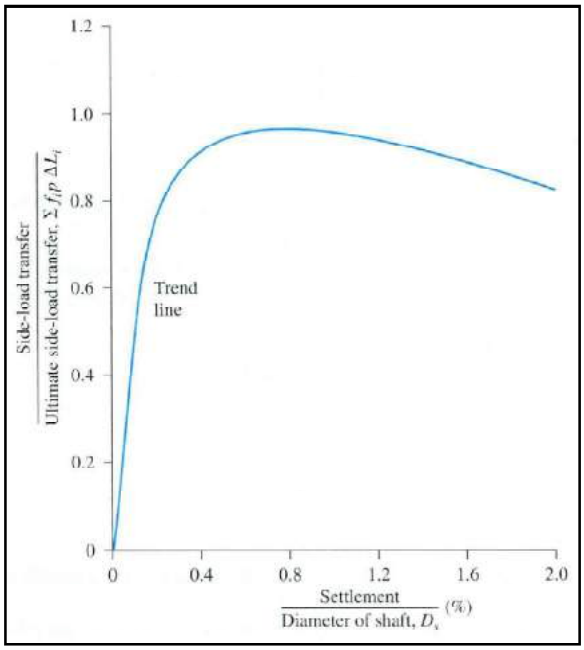

Fig 1.12 Normalized side-load transfer versus settlement in cohesive soil

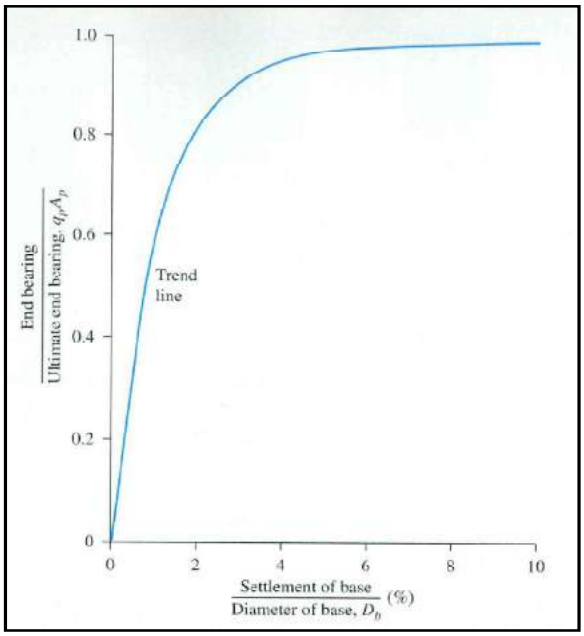

Fig. 1.13 Normalized base-load transfer versus settlement in cohesive soil

Example 1.3
Example 1.4

1.9 Lateral Load- Carrying Capacity

The lateral load-carrying capacity of piers can be analyzed in a manner similar to that presented in last section for piles. Therefore, it will not be repeated here.

1.10 Caissons

1.10.1 Types of Caissons

Caissons are divided into three major types:
(1) open caissons,
(2) box caissons (or closed caissons), and
(3) pneumatic caissons.

Open caissons (**Figure 1.14**) are concrete shafts that remain open at the top and bottom during construction. The bottom of the caisson of the caisson has a cutting edge. The caisson is sunk into place, and soil from the inside of the shaft is removed by grab buckets until the bearing stratum is reached. The shafts may be circular, square, rectangular, or oval. Once the bearing stratum is reached, concrete is poured into the shaft (under water) to form a seal at its bottom. When the concrete seal hardens, the water inside the caisson shaft is pumped out. Concrete is then poured into the shaft to fill it. Open caissons can be extended to great depths, and the cost of construction is relatively low. However, one of their major of disadvantages is the lack of quality control over the concrete poured into the shaft for the seal. Also, the bottom of the caisson cannot be thoroughly cleaned out. An alternative method of open-caisson construction is to drive some sheet piles to form an enclosed area, which is filled with sand and is generally referred to as a *sand island*. The caisson is then sunk through the sand to the desired bearing stratum. This procedure is somewhat analogous to sinking a caisson when the ground surface is above the water table.

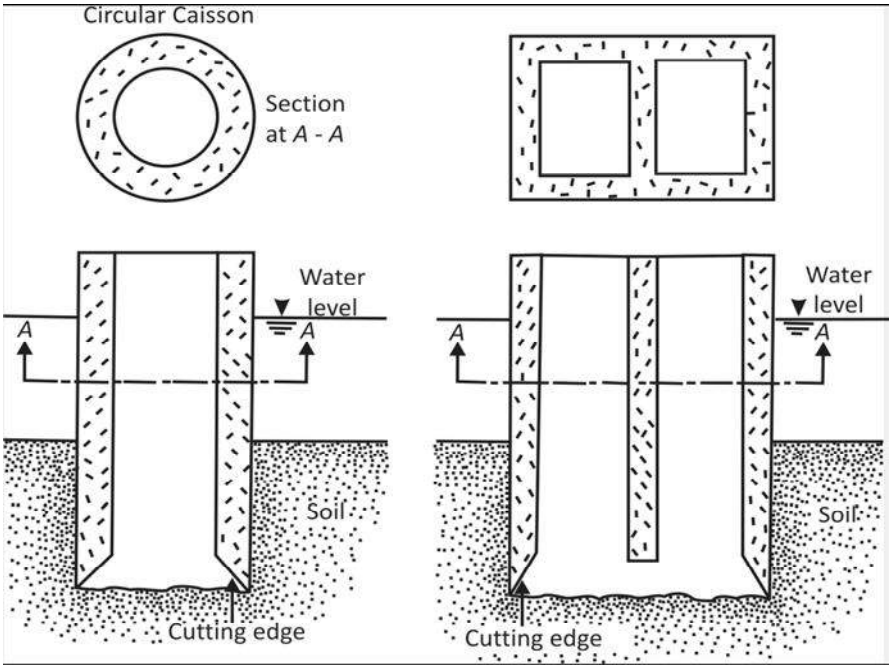

Fig. 1.14 Open caisson

Box caissons **(Figure 1. 15)** are caissons with closed bottoms. They are constructed on land and then transported to the construction site. They are gradually sunk at the site by filling the inside with sand, ballast, water, or concrete. The cost for this type of construction is low. The bearing surface must be level, and if it is not, it must be leveled by excavation.

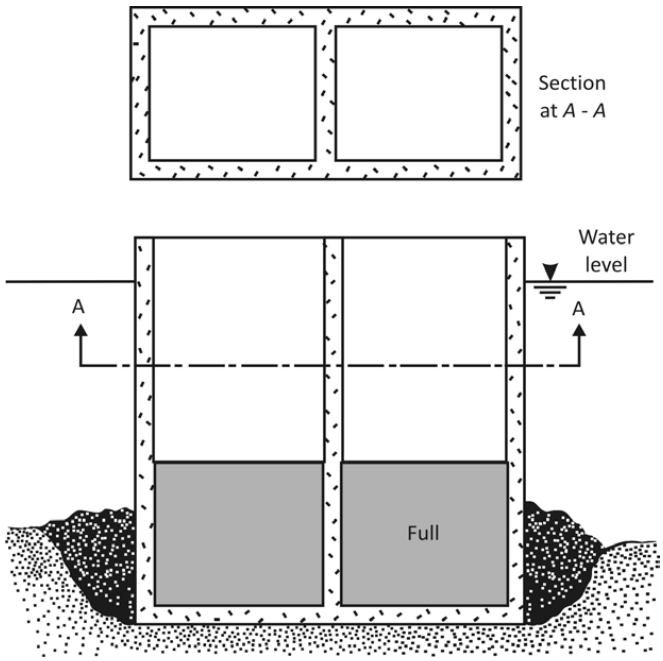

Fig. 1.15 Box caisson

Pneumatic caissons **(Figure 1.16)** are generally used for depths of about (15-40 m). This type of caisson is required when an excavation cannot be kept open because the soil flows into the excavated area faster than it can be removed. A pneumatic caisson has a work chamber at the bottom that is at least (*3* m) high. In this chamber, the workers excavate the soil and place the concrete. The air pressure in the chamber is kept high enough to prevent water and soil from entering. Workers usually do not counter severe discomfort when the chamber pressure is raised to about *15* lb/in2(.100 kN/m^2) above atmospheric pressure. Beyond this pressure, decompression periods are required when the workers leave the chamber. When chamber pressures of about (300 kN/m^2) above atmospheric pressure are required, workers should not be kept inside the chamber for more than *1122* hours at a time. Workers enter and leave the chamber through a steel shaft by means of a ladder. This shaft is also used for the removal of excavated soil and the placement of concrete. For large caisson construction, more than one shaft may be necessary, an airlock is provided for each one. Pneumatic caissons gradually sink as excavation proceeds. When the bearing stratum is reached, the work chamber is filled with concrete. Calculation of the load-bearing capacity of caissons is similar to that for drilled shafts. Therefore, it will not be further discussed in this section.

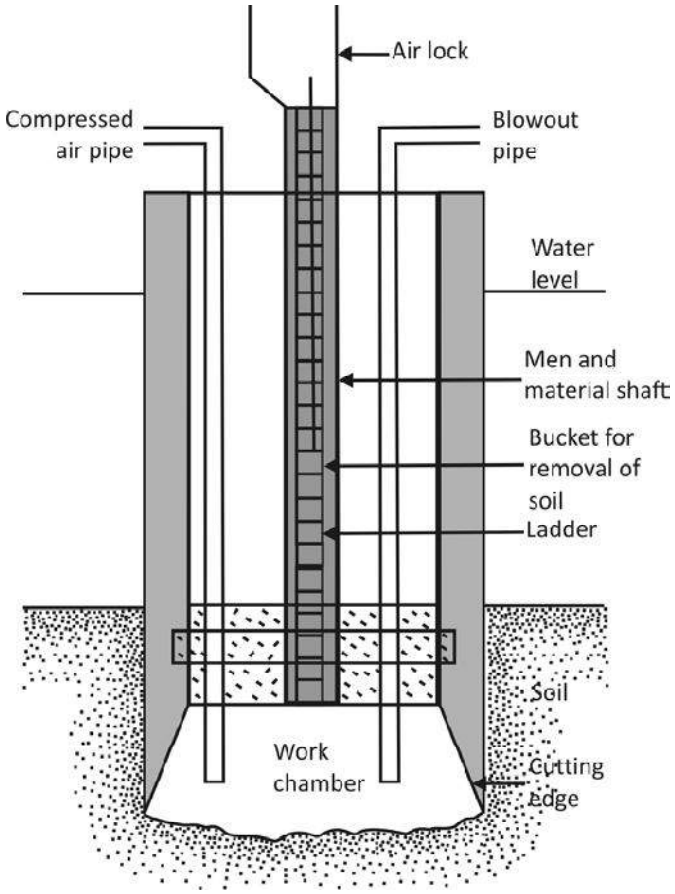

Fig 1.16 Pneumatic caisson

1.11 Thickness of Concrete Seal in Open Caissons

we mentioned that, before dewatering the caisson, a concrete seal is placed at the bottom of the shaft (**Figure 1.17**) and allowed to cure for some time. The concrete seal should be thick enough to withstand an upward hydrostatic force from it bottom after dewatering is complete and before concrete fills the shaft. Based on the theory of elasticity the thickness, *t,* according to Teng (1962) is

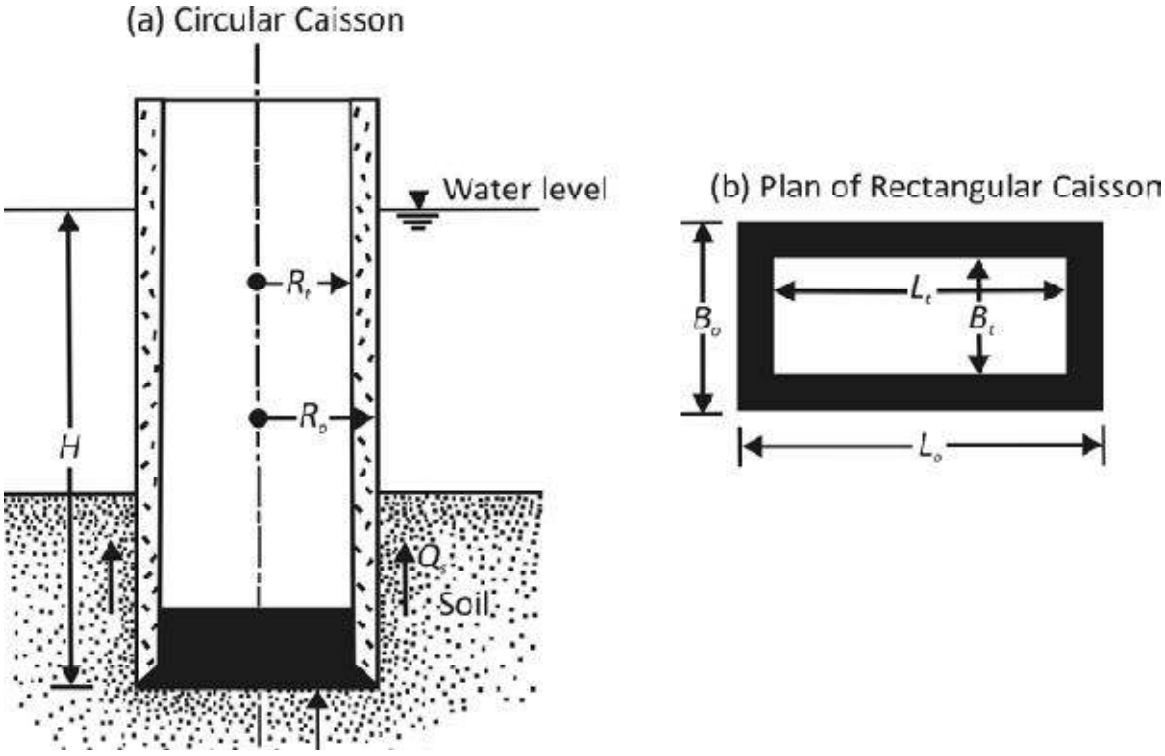

Fig. 1.17 Calculation of the thickness of seal for an open caisson

$$t = 1.18R_i\sqrt{\frac{q}{f_c}} \qquad \text{(circular caisson)} \qquad (1\text{-}28)$$

and

$$t = 0.866B_i\sqrt{\frac{q}{fc\left[1+1.61\left(\frac{L_i}{B_i}\right)\right]}} \qquad \text{(rectangular caisson)} \qquad (1\text{-}29)$$

Where

R_i =inside radius of a circular caisson

q =unit bearing pressure at the base of the caisson

f_c=allowable concrete flexural stress (≈*0.1-0.2* of f_c' where f_c' is than 28day compressive strength of concrete)

B_i, L_i = inside with and length, respectively, of rectangular caisson

According to **Figure 1.17**, the value of q in **Equations (1-28 and 1-29)** can be approximated as

$q \approx H\gamma_w - t\gamma_c$ (1-30)

Where
γ_c=unit weight of concrete

The thickness of the seal calculated by **Equations (1-28 and 1-29)** will be sufficient to protect it from cracking immediately after dewatering. However, two other conditions should also be checked for safety.

1. Check for Perimeter Shear an Contact Face of Seal and Shaft

According to **Figure 1-17**, the net upward hydrostatic force from the bottom of the seal is $A_i H\gamma_w - A_i t\gamma_c$(where$A_i = \pi R_i^2$ for circular caissons and $A_i = B_i L_i$ for rectangular caissons). So the perimeter shear developed is

$$\upsilon = \frac{A_i H\gamma_w - A_i t\gamma_c}{p_i t} \quad (1\text{-}31)$$

Where
p_i= inside perimeter of the caisson

Note that
$p_i = 2\pi R_i$ (for circular caissons) (1-32)

And that
$p_i = 2(B_i + L_i)$ (for rectangular caisson) (1-33)

The perimeter shear given by **Eq. (1-31)** should be less than the permissible shear stress, υ_u, or

$$\nu\left(\frac{MN}{m^2}\right) \leq \nu_u\left(\frac{MN}{m^2}\right) = 0.17\phi\sqrt{f_c'\left(\frac{MN}{m^2}\right)} \quad (1\text{-}34)$$

Where
ϕ=0.85

2. Check for Buoyancy
If the shaft is completely dewatered, the buoyant upward force,F_u, is

$$F_u = (\pi R_o^2)H\gamma_w \quad \text{(for circular caissons)} \quad (1\text{-}35)$$

$F_u = (B_o L_o) H \gamma_w$ (for rectangular caissons) (1-36)

The downward force, F_d , is caused by the weight of the caisson and the seal and by the skin friction at the caisson-soil interface, or

$$F_d = W_c + W_s + Q_s \quad (1\text{-}37)$$

Where
W_c=weight of caisson
W_s=weight of seal
Q_s=skin friction

If $F_d > F_u$, the caisson is safe from buoyancy. However, if $F_d < F_u$ dewatering the shaft completely will be unsafe. For that reason, the thickness of the seal should be increased by Δt [over the thickness calculated by using **Equation (1-28) or (1-29)]** or

$$\Delta t = \frac{F_u - F_d}{A_t \gamma_c} \quad (1\text{-}38)$$

Example 1-5

University of Anbar
Engineering College
Civil Engineering Department

CHAPTER TWO

LATERAL EARTH PRESSURE AND RETAINING WALLS

LECTURE
DR. AHMED H. ABDULKAREEM
2017

2.1 Introduction

A retaining wall is a wall that provides lateral support for a vertical or near-vertical slope of soil. It is a common structure used in many construction projects. The most common types of retaining wall may be classified as follows:

1. Gravity retaining walls
2. Semigravity retaining walls
3. Cantilever retaining walls
4. Counterfort retaining walls

Gravity retaining walls **(Figure 1.1a)** are constructed with plain concrete or stone masonry. They depend for stability on their own weight and any soil resting on the masonry. This type of construction is not economical for high walls.

In many cases, a small amount of steel may be used for the construction of gravity walls, thereby minimizing the size of wall sections. Such walls are generally referred to as ***semigravity walls*** **(Figure 1.1b)**.

Cantilever retaining walls **(Figure 1.1c)** are made of reinforced concrete that consists of a thin stem and a base slab. This type of wall is economical to a height of about 8 m.

Counterfort retaining walls **(Figure 1.1d)** are similar to cantilever walls. At regular intervals, however, they have thin vertical concrete slabs known as *counterforts* that tie the wall and the base slab together. The purpose of the counterforts is to reduce the shear and the bending moments.

To design retaining walls properly, an engineer must know the basic parameters—the *unit weight, angle of friction,* and *cohesion*—of the soil retained behind the wall and the soil below the base slab. Knowing the properties of the soil behind the wall enables the engineer to determine the lateral pressure distribution that has to be designed for.

There are two phases in the design of a conventional retaining wall. First, with the lateral earth pressure known, the structure as a whole is checked for *stability*. The structure is examined for possible *overturning, sliding,* and *bearing capacity* failures. Second, each component of the structure is checked for *strength,* and the *steel reinforcement* of each component is determined.

This chapter presents the procedures for determination of lateral earth pressure and retaining-wall stability.

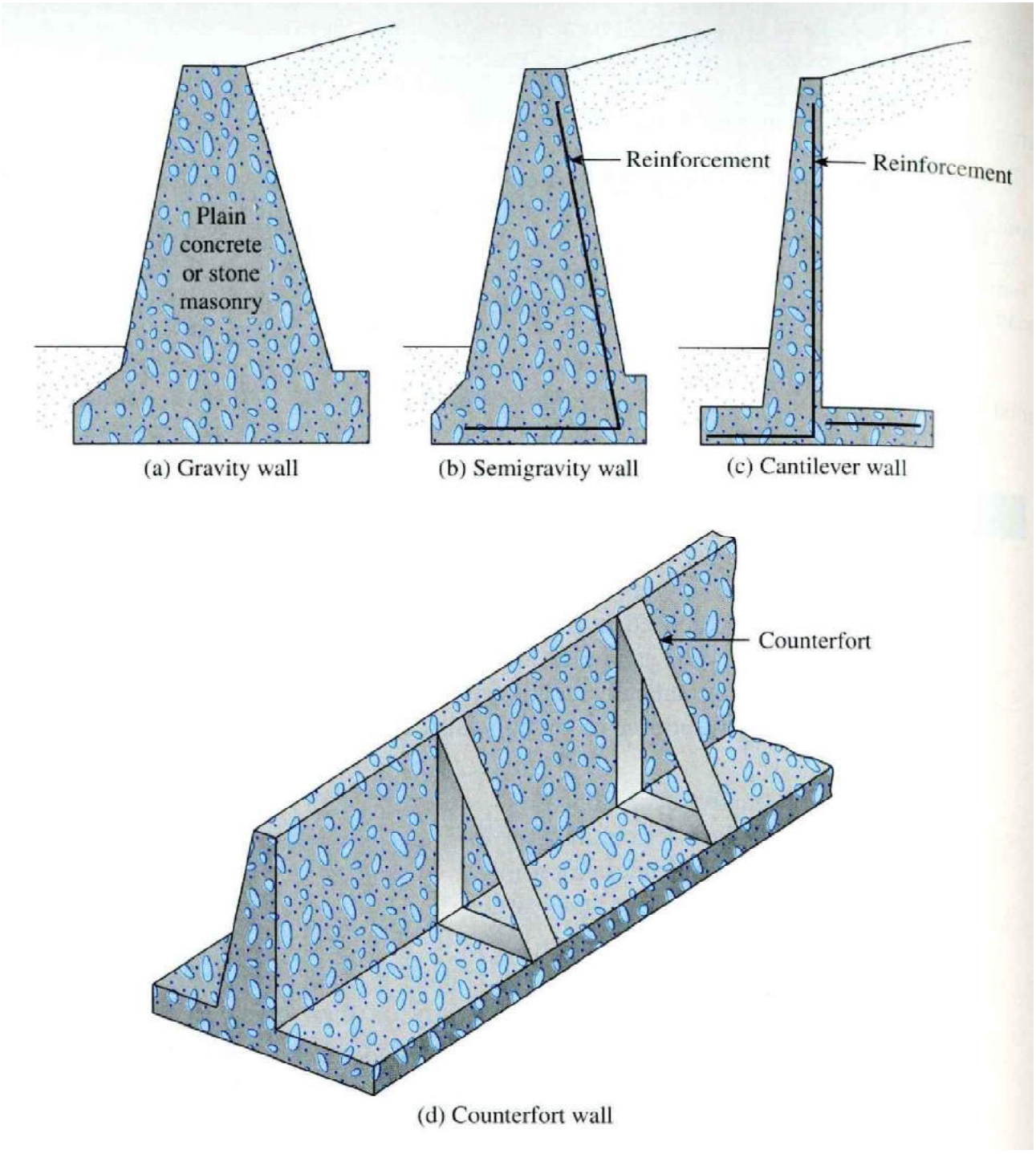

Figure 2.1 Types of retaining wall

2.2 Lateral Earth Pressure at Rest

Consider a vertical wall of height *H,* as shown in Figure 2.2, retaining a soil having a unit weight of γ. A uniformly distributed load, q/unit area, is also applied at the ground surface. The shear strength of the soil is

$$s = c' + \sigma' \tan \emptyset'$$

Where
c' = cohesion
$\emptyset'$ = effective angle of friction
σ' = effective normal stress

At any depth z below the ground surface, the vertical subsurface stress is

$$\sigma_o' = q + \gamma z \qquad (2.1)$$

If the *wall is at rest and is not allowed to move at all,* either away from the soil mass or into the soil mass (i.e., there is zero horizontal strain), the lateral pressure at a depth *z* is

$$\sigma_h = K_o \sigma_o' + u \qquad (2.2)$$

Where
u= pore water pressure
K_o = coefficient of at-rest earth pressure

For normally consolidated soil, the relation for K_o (Jaky, 1944) is

$$K_o \approx 1 - sin\emptyset' \qquad (2.3)$$

Equation (2.3) is an empirical approximation.

For overconsolidated soil, the at-rest earth pressure coefficient may be expressed as (Mayne and Kulhawy, 1982)

$$K_o = (1 - sin\emptyset')OCR^{sin\emptyset'} \qquad (2.4)$$

where OCR = overconsolidation ratio.

With a properly selected value of the at-rest earth pressure coefficient, Eq. (2.2) can be used to determine the variation of lateral earth pressure with depth *z*. Figure 2.2b shows the variation of σ_h' with depth for the wall depicted in Figure 2.2a. Note that if

the surcharge q=0 and the pore water pressure the pressure u=0, diagram will be a triangle. The total force, P_o , *per unit length* of the wall given in Figure 2.2a can now be obtained from the area of the pressure diagram given in Figure 2.2b and is

$$P_o = P_1 + P_2 = qK_0H + \frac{1}{2}\gamma H^2 K_o \qquad (2.5)$$

where
P_1= area of rectangle 1
P_2= area of triangle 2

The location of the line of action of the resultant force, P_o, can be obtained by taking the moment about the bottom of the wall. Thus,

$$\bar{z} = \frac{P_1\left(\frac{H}{2}\right)+P_2\left(\frac{H}{3}\right)}{P_o} \qquad (2.6)$$

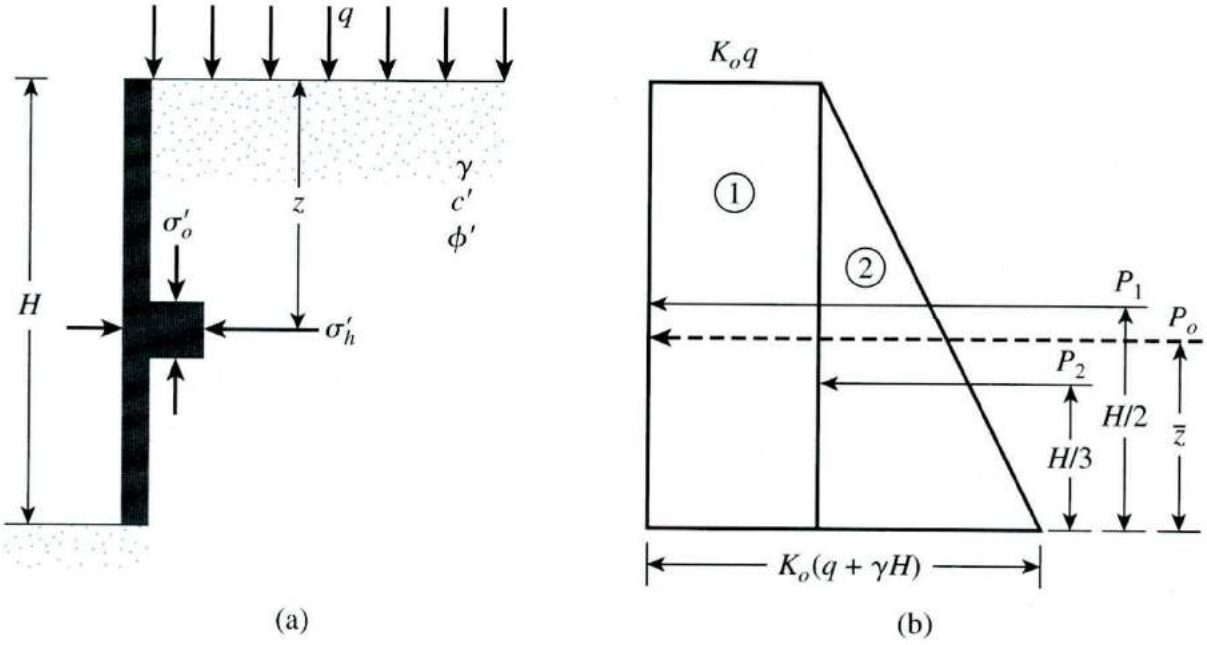

Figure 2.2 At-rest earth pressure

If the water table is located at a depth z< H, the at-rest pressure diagram shown in Figure 2.2b will have to be somewhat modified, as shown in Figure 2.3. If the effective unit weight of soil below the water table equals γ (i.e., γ_{sat} - γ_w), then

At z = 0 : $\sigma_h' = K_o\sigma_o' = K_o q$
At z= H_1 : $\sigma_h' = K_o\sigma_o' = K_o(q + \gamma H_1\ )$

And
At z =H_2 , $\sigma_h' = K_o\sigma_o' = K_o(q + \gamma H_1\ + \gamma' H_2)$

Note that in the preceding equations, σ_o' and $\sigma_h'$are effective vertical and horizontal pressures, respectively. Determining the total pressure distribution on the wall requires adding the hydrostatic pressure, *u,* which is zero from z=0 to z= H_1 and is $\gamma_w H_2$ at z= H_2. The variation of σ_h' and *u* with depth is shown in Figure 2.3b. Hence, the total force per unit length of the wall can be determined from the area of the pressure diagram. Specifically,

$$P_o = A_1 + A_2 + A_3 + A_4 + A_5$$

where A= area of the pressure diagram.
So,

$$P_o = K_o q H_1 + \frac{1}{2}K_o\gamma H_1^2 + K_o(q + \gamma H_1)H_2 + \frac{1}{2}K_o\gamma' H_2^2 + \frac{1}{2}\gamma_w H_2^2$$

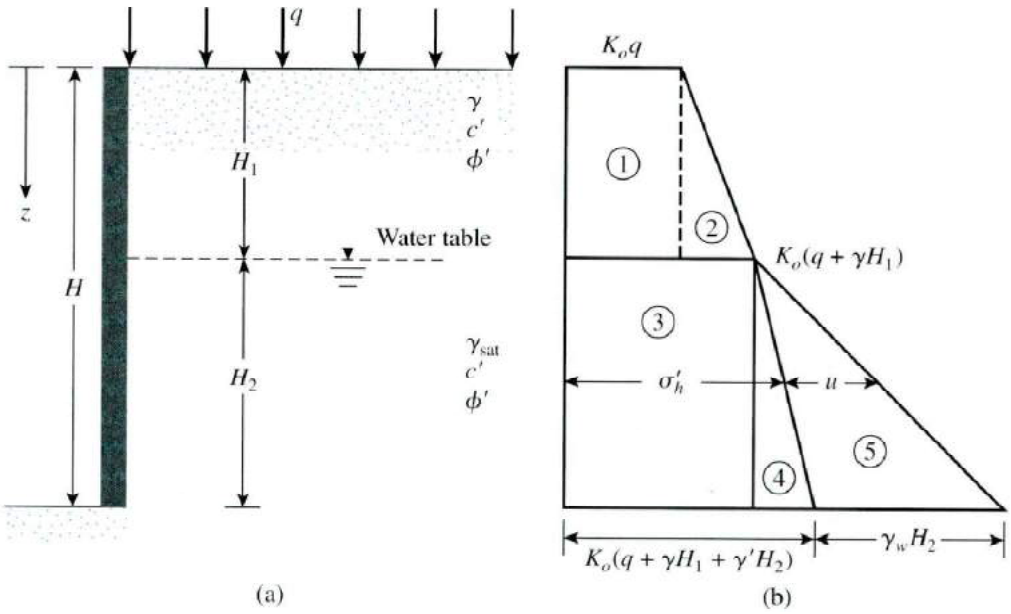

Figure 2.3 At-rest earth pressure with water table located at a depth z< H

2.3 Active Pressure

2.3.1 Rankine Active Earth Pressure

The lateral earth pressure described in Section 2.2 involves walls that do not yield at all. However, if a wall tends to move away from the soil a distance Δx as shown in Figure 1.4a, the soil pressure on the wall at any depth will decrease. For a wall that is *frictionless,* the horizontal stress, σ_h' , at depth *z* will equal $K_o\sigma_o'(= K_o\gamma z)$ when Δx is zero. However, with Δx > 0, σ_h' will be less than $K_o\sigma_o'$.

The Mohr's circles corresponding to wall displacements of Δx =0 and Δx > 0 are shown as circles *a* and *b,* respectively, in Figure 2.4b. If the displacement of the wall, Δx , continues to increase, the corresponding Mohr's circle eventually will just touch the Mohr–Coulomb failure envelope defined by the equation

$$S = c' + \sigma' tan\emptyset'$$

This circle, marked *c* in the figure, represents the failure condition in the soil mass; the horizontal stress then equals σ_a' , referred to as the ***Rankine active pressure***. The *slip lines* (failure planes) in the soil mass will then make angles of $\pm\left(45 + \frac{\emptyset'}{2}\right)$ with the horizontal, as shown in Figure 2.4a.

Equation (2.7) relates the principal stresses for a Mohr's circle that touches the Mohr–Coulomb failure envelope:

$$\sigma_1' = \sigma_3' tan^2\left(45 + \frac{\emptyset'}{2}\right) + 2c'\tan\,(45 + \frac{\emptyset'}{2}) \qquad (2.7)$$

For the Mohr's circle *c* in Figure 2.4b,

Major principle stress: $\sigma_1' = \sigma_o'$
and

Minor principle stress: $\sigma_3' = \sigma_a'$
Thus,

$$\sigma_o' = \sigma_a' tan^2\left(45 + \frac{\emptyset'}{2}\right) + 2c'\tan\,(45 + \frac{\emptyset'}{2})$$

$$\sigma_a' = \frac{\sigma_o'}{tan^2\left(45+\frac{\emptyset'}{2}\right)} - \frac{2c'}{\tan\,(45+\frac{\emptyset'}{2})}$$

or

$$\sigma'_a = \sigma'_o tan^2\left(45 - \frac{\emptyset'}{2}\right) - 2c'\tan\left(45 - \frac{\emptyset'}{2}\right)$$

$$= \sigma'_o K_a - 2c'\sqrt{K_a} \qquad (2.8)$$

where $K_a = tan^2\left(45 - \frac{\emptyset'}{2}\right)$ = Rankine active pressure coefficient.

The variation of the active pressure with depth for the wall shown in Figure 2.4a is given in Figure 2.4c. Note that $\sigma'_o = 0$ at z= 0 and $\sigma'_o = \gamma H$ at z=H. the pressure distribution shows that at z=0 the active pressure equals $-2c'\sqrt{K_a}$, indicating a tensile stress that decreases with depth and becomes zero at a depth z= z_c , or

$$\gamma z_c K_a - 2c'\sqrt{K_a} = 0$$

And

$$z_c = \frac{2c'}{\gamma\sqrt{K_a}} \qquad (2.9)$$

The depth z_c is usually referred to as the depth of tensile crack, because the tensile stress in the soil will eventually cause a crak along the soil-wall interface.

Thus, the total Rankine active force per unit length of the wall before the tensile crack occurs is

$$P_a = \int_0^H \sigma'_a dz = \int_0^H \gamma z\, K_a dz - \int_0^H 2c'\sqrt{K_a} dz$$

$$= \frac{1}{2}\gamma H^2 K_a - 2c'H\sqrt{K_a} \qquad (2.10)$$

After the tensile crack appears, the force per unit length on the wall will be caused only by the pressure distribution between depths z= z_c and z= H as shown by the hatched area in Figure 2.4c. This force may be expressed as

$$P_a = \frac{1}{2}(H - z_c)(\gamma H K_a - 2c'\sqrt{K_a}) \qquad (2.11)$$

$$P_a = \frac{1}{2}\left(H - \frac{2c'}{\gamma\sqrt{K_a}}\right)(\gamma H K_a - 2c'\sqrt{K_a}) \qquad (2.12)$$

However, it is important to realize that the active earth pressure condition will be reached only if the wall is allowed to "yield" sufficiently. The necessary amount of outward displacement of the wall is about $0.001H$ to $0.004H$ for granular soil backfills and about $0.01H$ to $0.04H$ for cohesive soil backfills.

Note further that if the *total stress* shear strength parameters (c, ϕ) were used, an equation similar to Eq. (2.9) could have been derived, namely

$$\sigma_a = \sigma_o \tan^2\left(45 - \frac{\emptyset'}{2}\right) - 2c \tan\left(45 - \frac{\emptyset'}{2}\right)$$

Example 2.1
Example 2.2
Example 2.3

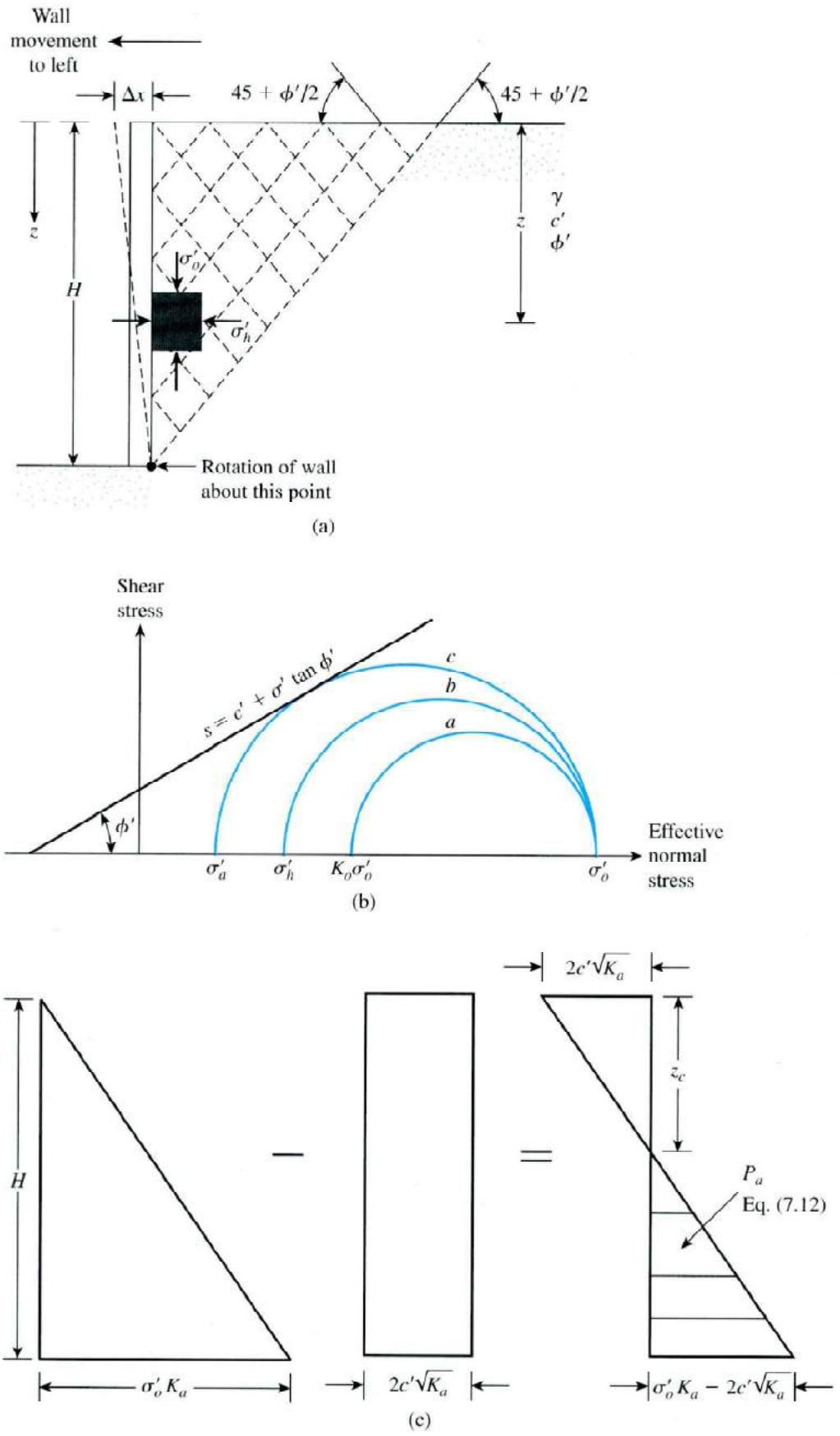

Figure 2.4 Rankine active pressure

2.3.2 Rankine Active Earth Pressure for Inclined Backfill

If the backfill of a frictionless retaining wall is a granular soil ($c' = 0$) and rises at an angle α with respect to the horizontal (see Figure 2.5), the active earth-pressure coefficient may be expressed in the form

$$K_a = cos\alpha \frac{cos\alpha - \sqrt{cos^2\alpha - cos^2\phi'}}{cos\alpha + \sqrt{cos^2\alpha - cos^2\phi'}} \qquad (2.13)$$

where ϕ'=angle of friction of soil.

At any depth z, the Rankine active pressure may be expressed as

$$\sigma'_a = \gamma H^2 K_a \qquad (2.14)$$

Also, the total force per unit length of the wall is

$$P_a = 1/2\, \gamma H^2 K_a \qquad (2.15)$$

Note that, in this case, the direction of the resultant force P_a is *inclined at an angle with the horizontal* and intersects the wall at a distance H/3 from the base of the wall. **Table 2.1** presents the values of K_a (active earth pressure) for various values of α and ϕ'.

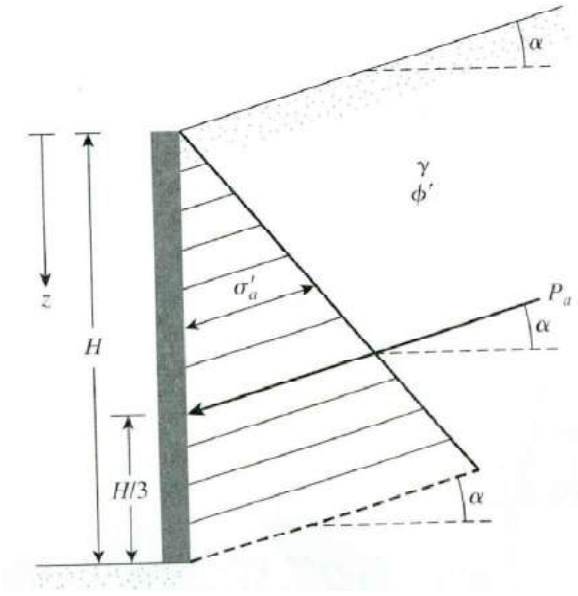

Figure 2.5 Notations for active pressure—Eqs. (2.13), (2.14), (2.15)

Table 2.1 Values of K_a [Eq. (2.13)]

α (deg) ↓	ϕ' (deg) → 28	29	30	31	32	33	34	35	36	37	38	39	40
0	0.3610	0.3470	0.3333	0.3201	0.3073	0.2948	0.2827	0.2710	0.2596	0.2486	0.2379	0.2275	0.2174
1	0.3612	0.3471	0.3335	0.3202	0.3074	0.2949	0.2828	0.2711	0.2597	0.2487	0.2380	0.2276	0.2175
2	0.3618	0.3476	0.3339	0.3207	0.3078	0.2953	0.2832	0.2714	0.2600	0.2489	0.2382	0.2278	0.2177
3	0.3627	0.3485	0.3347	0.3214	0.3084	0.2959	0.2837	0.2719	0.2605	0.2494	0.2386	0.2282	0.2181
4	0.3639	0.3496	0.3358	0.3224	0.3094	0.2967	0.2845	0.2726	0.2611	0.2500	0.2392	0.2287	0.2186
5	0.3656	0.3512	0.3372	0.3237	0.3105	0.2978	0.2855	0.2736	0.2620	0.2508	0.2399	0.2294	0.2192
6	0.3676	0.3531	0.3389	0.3253	0.3120	0.2992	0.2868	0.2747	0.2631	0.2518	0.2409	0.2303	0.2200
7	0.3701	0.3553	0.3410	0.3272	0.3138	0.3008	0.2883	0.2761	0.2644	0.2530	0.2420	0.2313	0.2209
8	0.3730	0.3580	0.3435	0.3294	0.3159	0.3027	0.2900	0.2778	0.2659	0.2544	0.2432	0.2325	0.2220
9	0.3764	0.3611	0.3463	0.3320	0.3182	0.3049	0.2921	0.2796	0.2676	0.2560	0.2447	0.2338	0.2233
10	0.3802	0.3646	0.3495	0.3350	0.3210	0.3074	0.2944	0.2818	0.2696	0.2578	0.2464	0.2354	0.2247
11	0.3846	0.3686	0.3532	0.3383	0.3241	0.3103	0.2970	0.2841	0.2718	0.2598	0.2482	0.2371	0.2263
12	0.3896	0.3731	0.3573	0.3421	0.3275	0.3134	0.2999	0.2868	0.2742	0.2621	0.2503	0.2390	0.2281
13	0.3952	0.3782	0.3620	0.3464	0.3314	0.3170	0.3031	0.2898	0.2770	0.2646	0.2527	0.2412	0.2301
14	0.4015	0.3839	0.3671	0.3511	0.3357	0.3209	0.3068	0.2931	0.2800	0.2674	0.2552	0.2435	0.2322
15	0.4086	0.3903	0.3729	0.3564	0.3405	0.3253	0.3108	0.2968	0.2834	0.2705	0.2581	0.2461	0.2346
16	0.4165	0.3975	0.3794	0.3622	0.3458	0.3302	0.3152	0.3008	0.2871	0.2739	0.2612	0.2490	0.2373
17	0.4255	0.4056	0.3867	0.3688	0.3518	0.3356	0.3201	0.3053	0.2911	0.2776	0.2646	0.2521	0.2401
18	0.4357	0.4146	0.3948	0.3761	0.3584	0.3415	0.3255	0.3102	0.2956	0.2817	0.2683	0.2555	0.2433
19	0.4473	0.4249	0.4039	0.3842	0.3657	0.3481	0.3315	0.3156	0.3006	0.2862	0.2724	0.2593	0.2467
20	0.4605	0.4365	0.4142	0.3934	0.3739	0.3555	0.3381	0.3216	0.3060	0.2911	0.2769	0.2634	0.2504
21	0.4758	0.4498	0.4259	0.4037	0.3830	0.3637	0.3455	0.3283	0.3120	0.2965	0.2818	0.2678	0.2545
22	0.4936	0.4651	0.4392	0.4154	0.3934	0.3729	0.3537	0.3356	0.3186	0.3025	0.2872	0.2727	0.2590
23	0.5147	0.4829	0.4545	0.4287	0.4050	0.3832	0.3628	0.3438	0.3259	0.3091	0.2932	0.2781	0.2638
24	0.5404	0.5041	0.4724	0.4440	0.4183	0.3948	0.3731	0.3529	0.3341	0.3164	0.2997	0.2840	0.2692
25	0.5727	0.5299	0.4936	0.4619	0.4336	0.4081	0.3847	0.3631	0.3431	0.3245	0.3070	0.2905	0.2750

2.3.3 Coulomb's Active Earth Pressure

The Rankine active earth pressure calculations discussed in the preceding sections were based on the assumption that the wall is frictionless. In 1776, Coulomb proposed a theory for calculating the lateral earth pressure on a retaining wall with granular soil backfill. This theory takes wall friction into consideration.

To apply Coulomb's active earth pressure theory, let us consider a retaining wall with its back face inclined at an angle βwith the horizontal, as shown in Figure 2.6a. The backfill is a granular soil that slopes at an angle α a with the horizontal. Also, let δ' be the angle of friction between the soil and the wall (i.e., the angle of wall friction).

Under active pressure, the wall will move away from the soil mass (to the left in the figure). Coulomb assumed that, in such a case, the failure surface in the soil mass would be a plane (e.g., BC_1, BC_2, …). So, to find the active force, consider a possible soil failure wedge ABC_1. The forces acting on this wedge (per unit length at right angles to the cross section shown) are as follows:

1. The weight of the wedge, *W*.
2. The resultant, *R,* of the normal and resisting shear forces along the surface,BC_1.

The force *R* will be inclined at an angle to the normal drawn to BC_1.

3. The active force per unit length of the wall, P_a, which will be inclined at an angle δ' to the normal drawn to the back face of the wall.

For equilibrium purposes, a force triangle can be drawn, as shown in Figure 2.6b. Note that θ_1 is the angle that BC_1 makes with the horizontal. Because the magnitude of *W,*as well as the directions of all three forces, are known, the value of P_a can now be determined. Similarly, the active forces of other trial wedges, such as ABC_2, ABC_3, …, can be determined. The maximum value of P_a thus determined is Coulomb's active force (see top part of Figure 2.7), which may be expressed as

$$P_a = 1/2\,\gamma H^2 K_a \qquad (2.16)$$

Where

K_a= Coulomb's active earth-pressure coefficient

$$= \frac{sin^2(\beta-\emptyset')}{sin^2\beta\,\sin(\beta-\delta')\left[1+\sqrt{\frac{\sin(\emptyset'+\delta')\sin(\emptyset'-\alpha)}{\sin(\beta+\delta')\sin(\alpha+\beta)}}\right]^2} \qquad (2.17)$$

and H= height of the wall.

The values of the active earth pressure coefficient, K_a ,for a vertical retaining wall ($\beta = 90^o$) with horizontal backfill ($\alpha = 0^o$) are given in Table 2.2. Note that the line of action of the resultant force (P_a) will act at a distance H/3 above the base of the wall and will be inclined at an angle δ' to the normal drawn to the back of the wall.

In the actual design of retaining walls, the value of the wall friction angle δ' is assumed to be between $\emptyset'/2$ and $2/3\emptyset'$. The active earth pressure coefficients for various values of $\emptyset', \alpha,$ and β with $\emptyset'/2$ and $2/3\emptyset'$ are respectively given in Tables 2.3 and 2.4. These coefficients are very useful design considerations.

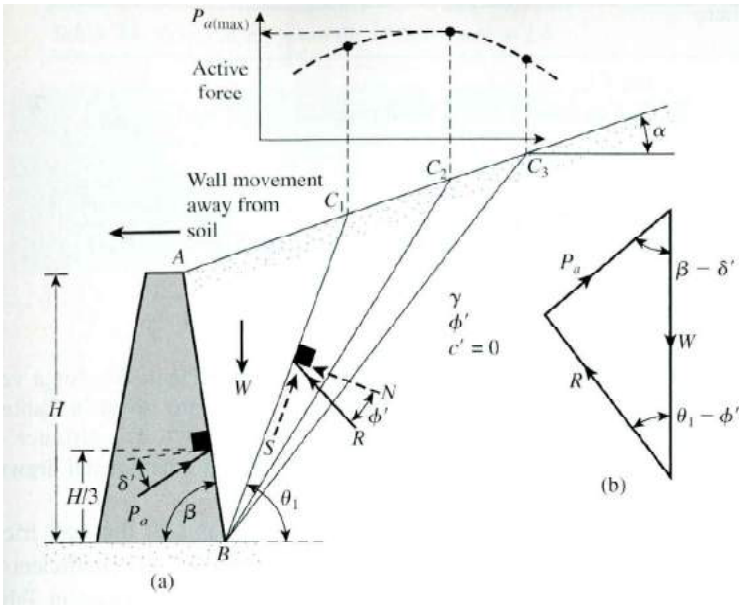

Figure 2.6 Coulomb's active pressure

Table 2.2 Values of K_a Eq(2.17) for $\beta=90^o$ and $\alpha=0^o$

	δ' (deg)					
ϕ' (deg)	0	5	10	15	20	25
28	0.3610	0.3448	0.3330	0.3251	0.3203	0.3186
30	0.3333	0.3189	0.3085	0.3014	0.2973	0.2956
32	0.3073	0.2945	0.2853	0.2791	0.2755	0.2745
34	0.2827	0.2714	0.2633	0.2579	0.2549	0.2542
36	0.2596	0.2497	0.2426	0.2379	0.2354	0.2350
38	0.2379	0.2292	0.2230	0.2190	0.2169	0.2167
40	0.2174	0.2098	0.2045	0.2011	0.1994	0.1995
42	0.1982	0.1916	0.1870	0.1841	0.1828	0.1831

Table 2.3 Values of K_a Eq(2.17) for $\delta' = 2/3\ \phi'$

		β (deg)					
α (deg)	φ' (deg)	90	85	80	75	70	65
0	28	0.3213	0.3588	0.4007	0.4481	0.5026	0.5662
	29	0.3091	0.3467	0.3886	0.4362	0.4908	0.5547
	30	0.2973	0.3349	0.3769	0.4245	0.4794	0.5435
	31	0.2860	0.3235	0.3655	0.4133	0.4682	0.5326
	32	0.2750	0.3125	0.3545	0.4023	0.4574	0.5220
	33	0.2645	0.3019	0.3439	0.3917	0.4469	0.5117
	34	0.2543	0.2916	0.3335	0.3813	0.4367	0.5017
	35	0.2444	0.2816	0.3235	0.3713	0.4267	0.4919
	36	0.2349	0.2719	0.3137	0.3615	0.4170	0.4824
	37	0.2257	0.2626	0.3042	0.3520	0.4075	0.4732
	38	0.2168	0.2535	0.2950	0.3427	0.3983	0.4641
	39	0.2082	0.2447	0.2861	0.3337	0.3894	0.4553
	40	0.1998	0.2361	0.2774	0.3249	0.3806	0.4468
	41	0.1918	0.2278	0.2689	0.3164	0.3721	0.4384
	42	0.1840	0.2197	0.2606	0.3080	0.3637	0.4302
5	28	0.3431	0.3845	0.4311	0.4843	0.5461	0.6190
	29	0.3295	0.3709	0.4175	0.4707	0.5325	0.6056
	30	0.3165	0.3578	0.4043	0.4575	0.5194	0.5926
	31	0.3039	0.3451	0.3916	0.4447	0.5067	0.5800
	32	0.2919	0.3329	0.3792	0.4324	0.4943	0.5677
	33	0.2803	0.3211	0.3673	0.4204	0.4823	0.5558
	34	0.2691	0.3097	0.3558	0.4088	0.4707	0.5443
	35	0.2583	0.2987	0.3446	0.3975	0.4594	0.5330
	36	0.2479	0.2881	0.3338	0.3866	0.4484	0.5221
	37	0.2379	0.2778	0.3233	0.3759	0.4377	0.5115
	38	0.2282	0.2679	0.3131	0.3656	0.4273	0.5012
	39	0.2188	0.2582	0.3033	0.3556	0.4172	0.4911
	40	0.2098	0.2489	0.2937	0.3458	0.4074	0.4813
	41	0.2011	0.2398	0.2844	0.3363	0.3978	0.4718
	42	0.1927	0.2311	0.2753	0.3271	0.3884	0.4625
10	28	0.3702	0.4164	0.4686	0.5287	0.5992	0.6834
	29	0.3548	0.4007	0.4528	0.5128	0.5831	0.6672
	30	0.3400	0.3857	0.4376	0.4974	0.5676	0.6516
	31	0.3259	0.3713	0.4230	0.4826	0.5526	0.6365
	32	0.3123	0.3575	0.4089	0.4683	0.5382	0.6219
	33	0.2993	0.3442	0.3953	0.4545	0.5242	0.6078
	34	0.2868	0.3314	0.3822	0.4412	0.5107	0.5942
	35	0.2748	0.3190	0.3696	0.4283	0.4976	0.5810
	36	0.2633	0.3072	0.3574	0.4158	0.4849	0.5682
	37	0.2522	0.2957	0.3456	0.4037	0.4726	0.5558
	38	0.2415	0.2846	0.3342	0.3920	0.4607	0.5437
	39	0.2313	0.2740	0.3231	0.3807	0.4491	0.5321
	40	0.2214	0.2636	0.3125	0.3697	0.4379	0.5207
	41	0.2119	0.2537	0.3021	0.3590	0.4270	0.5097
	42	0.2027	0.2441	0.2921	0.3487	0.4164	0.4990
15	28	0.4065	0.4585	0.5179	0.5868	0.6685	0.7670

(continued)

Table 2.3 Values of K_a Eq(2.17) for $\delta' = 2/3\ \phi'$

		β (deg)					
α (deg)	φ′ (deg)	90	85	80	75	70	65
	29	0.3881	0.4397	0.4987	0.5672	0.6483	0.7463
	30	0.3707	0.4219	0.4804	0.5484	0.6291	0.7265
	31	0.3541	0.4049	0.4629	0.5305	0.6106	0.7076
	32	0.3384	0.3887	0.4462	0.5133	0.5930	0.6895
	33	0.3234	0.3732	0.4303	0.4969	0.5761	0.6721
	34	0.3091	0.3583	0.4150	0.4811	0.5598	0.6554
	35	0.2954	0.3442	0.4003	0.4659	0.5442	0.6393
	36	0.2823	0.3306	0.3862	0.4513	0.5291	0.6238
	37	0.2698	0.3175	0.3726	0.4373	0.5146	0.6089
	38	0.2578	0.3050	0.3595	0.4237	0.5006	0.5945
	39	0.2463	0.2929	0.3470	0.4106	0.4871	0.5805
	40	0.2353	0.2813	0.3348	0.3980	0.4740	0.5671
	41	0.2247	0.2702	0.3231	0.3858	0.4613	0.5541
	42	0.2146	0.2594	0.3118	0.3740	0.4491	0.5415
20	28	0.4602	0.5205	0.5900	0.6714	0.7689	0.8880
	29	0.4364	0.4958	0.5642	0.6445	0.7406	0.8581
	30	0.4142	0.4728	0.5403	0.6195	0.7144	0.8303
	31	0.3935	0.4513	0.5179	0.5961	0.6898	0.8043
	32	0.3742	0.4311	0.4968	0.5741	0.6666	0.7799
	33	0.3559	0.4121	0.4769	0.5532	0.6448	0.7569
	34	0.3388	0.3941	0.4581	0.5335	0.6241	0.7351
	35	0.3225	0.3771	0.4402	0.5148	0.6044	0.7144
	36	0.3071	0.3609	0.4233	0.4969	0.5856	0.6947
	37	0.2925	0.3455	0.4071	0.4799	0.5677	0.6759
	38	0.2787	0.3308	0.3916	0.4636	0.5506	0.6579
	39	0.2654	0.3168	0.3768	0.4480	0.5342	0.6407
	40	0.2529	0.3034	0.3626	0.4331	0.5185	0.6242
	41	0.2408	0.2906	0.3490	0.4187	0.5033	0.6083
	42	0.2294	0.2784	0.3360	0.4049	0.4888	0.5930

Table 2.4 Values of K_a Eq(2.17) for $\delta' = 1/2\ \phi'$

α (deg)	φ′ (deg)	90	85	80	75	70	65
0	28	0.3264	0.3629	0.4034	0.4490	0.5011	0.5616
	29	0.3137	0.3502	0.3907	0.4363	0.4886	0.5492
	30	0.3014	0.3379	0.3784	0.4241	0.4764	0.5371
	31	0.2896	0.3260	0.3665	0.4121	0.4645	0.5253
	32	0.2782	0.3145	0.3549	0.4005	0.4529	0.5137
	33	0.2671	0.3033	0.3436	0.3892	0.4415	0.5025
	34	0.2564	0.2925	0.3327	0.3782	0.4305	0.4915
	35	0.2461	0.2820	0.3221	0.3675	0.4197	0.4807
	36	0.2362	0.2718	0.3118	0.3571	0.4092	0.4702

Table 2.4 Values of K_a Eq(2.17) for $\delta' = 1/2\ \phi'$

		β (deg)					
α (deg)	φ′ (deg)	90	85	80	75	70	65
	37	0.2265	0.2620	0.3017	0.3469	0.3990	0.4599
	38	0.2172	0.2524	0.2920	0.3370	0.3890	0.4498
	39	0.2081	0.2431	0.2825	0.3273	0.3792	0.4400
	40	0.1994	0.2341	0.2732	0.3179	0.3696	0.4304
	41	0.1909	0.2253	0.2642	0.3087	0.3602	0.4209
	42	0.1828	0.2168	0.2554	0.2997	0.3511	0.4177
5	28	0.3477	0.3879	0.4327	0.4837	0.5425	0.6115
	29	0.3337	0.3737	0.4185	0.4694	0.5282	0.5972
	30	0.3202	0.3601	0.4048	0.4556	0.5144	0.5833
	31	0.3072	0.3470	0.3915	0.4422	0.5009	0.5698
	32	0.2946	0.3342	0.3787	0.4292	0.4878	0.5566
	33	0.2825	0.3219	0.3662	0.4166	0.4750	0.5437
	34	0.2709	0.3101	0.3541	0.4043	0.4626	0.5312
	35	0.2596	0.2986	0.3424	0.3924	0.4505	0.5190
	36	0.2488	0.2874	0.3310	0.3808	0.4387	0.5070
	37	0.2383	0.2767	0.3199	0.3695	0.4272	0.4954
	38	0.2282	0.2662	0.3092	0.3585	0.4160	0.4840
	39	0.2185	0.2561	0.2988	0.3478	0.4050	0.4729
	40	0.2090	0.2463	0.2887	0.3374	0.3944	0.4620
	41	0.1999	0.2368	0.2788	0.3273	0.3840	0.4514
	42	0.1911	0.2276	0.2693	0.3174	0.3738	0.4410
10	28	0.3743	0.4187	0.4688	0.5261	0.5928	0.6719
	29	0.3584	0.4026	0.4525	0.5096	0.5761	0.6549
	30	0.3432	0.3872	0.4368	0.4936	0.5599	0.6385
	31	0.3286	0.3723	0.4217	0.4782	0.5442	0.6225
	32	0.3145	0.3580	0.4071	0.4633	0.5290	0.6071
	33	0.3011	0.3442	0.3930	0.4489	0.5143	0.5920
	34	0.2881	0.3309	0.3793	0.4350	0.5000	0.5775
	35	0.2757	0.3181	0.3662	0.4215	0.4862	0.5633
	36	0.2637	0.3058	0.3534	0.4084	0.4727	0.5495
	37	0.2522	0.2938	0.3411	0.3957	0.4597	0.5361
	38	0.2412	0.2823	0.3292	0.3833	0.4470	0.5230
	39	0.2305	0.2712	0.3176	0.3714	0.4346	0.5103
	40	0.2202	0.2604	0.3064	0.3597	0.4226	0.4979
	41	0.2103	0.2500	0.2956	0.3484	0.4109	0.4858
	42	0.2007	0.2400	0.2850	0.3375	0.3995	0.4740
15	28	0.4095	0.4594	0.5159	0.5812	0.6579	0.7498
	29	0.3908	0.4402	0.4964	0.5611	0.6373	0.7284
	30	0.3730	0.4220	0.4777	0.5419	0.6175	0.7080
	31	0.3560	0.4046	0.4598	0.5235	0.5985	0.6884
	32	0.3398	0.3880	0.4427	0.5059	0.5803	0.6695
	33	0.3244	0.3721	0.4262	0.4889	0.5627	0.6513
	34	0.3097	0.3568	0.4105	0.4726	0.5458	0.6338
	35	0.2956	0.3422	0.3953	0.4569	0.5295	0.6168

(continued)

2.4 Passive Pressure

2.4.1 Rankine Passive Earth Pressure

Figure 2.8a shows a vertical frictionless retaining wall with a horizontal backfill. At depth *z,* the effective vertical pressure on a soil element is $\sigma'_o=\gamma z$ Initially, if the wall does not yield at all, the lateral stress at that depth will be $\sigma'_h=K_o\sigma'_o$. This state of stress is illustrated by the Mohr's circle *a* in Figure 2.8b. Now, if the wall is pushed into the soil mass by an amount Δx as shown in Figure 2.8a, the vertical stress at depth *z* will stay the same; however, the horizontal stress will increase. Thus, σ'_h will be greater than $K_o\sigma'_o$. The state of stress can now be represented by the Mohr's circle *b* in Figure 2.8b. If the wall moves farther inward (i.e., is increased still more), the stresses at depth *z* will ultimately reach the state represented by Mohr's circle *c.* Note that this Mohr's circle touches the Mohr–Coulomb failure envelope, which implies that the soil behind the wall will fail by being pushed upward. The horizontal stress, σ'_h , at this point is referred to as the ***Rankine passive pressure,*** or $\sigma'_h = \sigma'_p$.

For Mohr's circle *c* in Figure 2.8b, the major principal stress is σ'_p and the minor principal stress is σ'_o .Substituting these quantities into Eq. (2.8) yields

$$\sigma'_p = \sigma'_o tan^2\left(45+\frac{\emptyset'}{2}\right)+2c'\tan\left(45+\frac{\emptyset'}{2}\right) \qquad (2.18)$$

K_p= Rankine passive earth-pressure coefficient

$$K_p = tan^2\left(45+\frac{\emptyset'}{2}\right) \qquad (2.19)$$

$$\sigma'_p = \sigma'_o K_p + 2c'\sqrt{K_p} \qquad (2.20)$$

Equation (2.20) produces (Figure 2.18c), the passive pressure diagram for the wall shown in Figure 2.18a. Note that at z=0

$$\sigma'_o = 0 \ \ and \ \ \sigma'_p = 2c'\sqrt{K_p}$$

and at z= H

$$\sigma'_o = \gamma H \ \ and \ \ \sigma'_p = \gamma H K_p + 2c'\sqrt{K_p}$$

The passive force per unit length of the wall can be determined from the area of the pressure diagram, or

$$P_p = \frac{1}{2}\gamma H^2 K_p + 2c'H\sqrt{K_p} \qquad (2.21)$$

The approximate magnitudes of the wall movements, Δx , required to develop failure under passive conditions are as follows:

Soil type	Wall movement for passive condition, Δx
Dense sand	$0.005H$
Loose sand	$0.01H$
Stiff clay	$0.01H$
Soft clay	$0.05H$

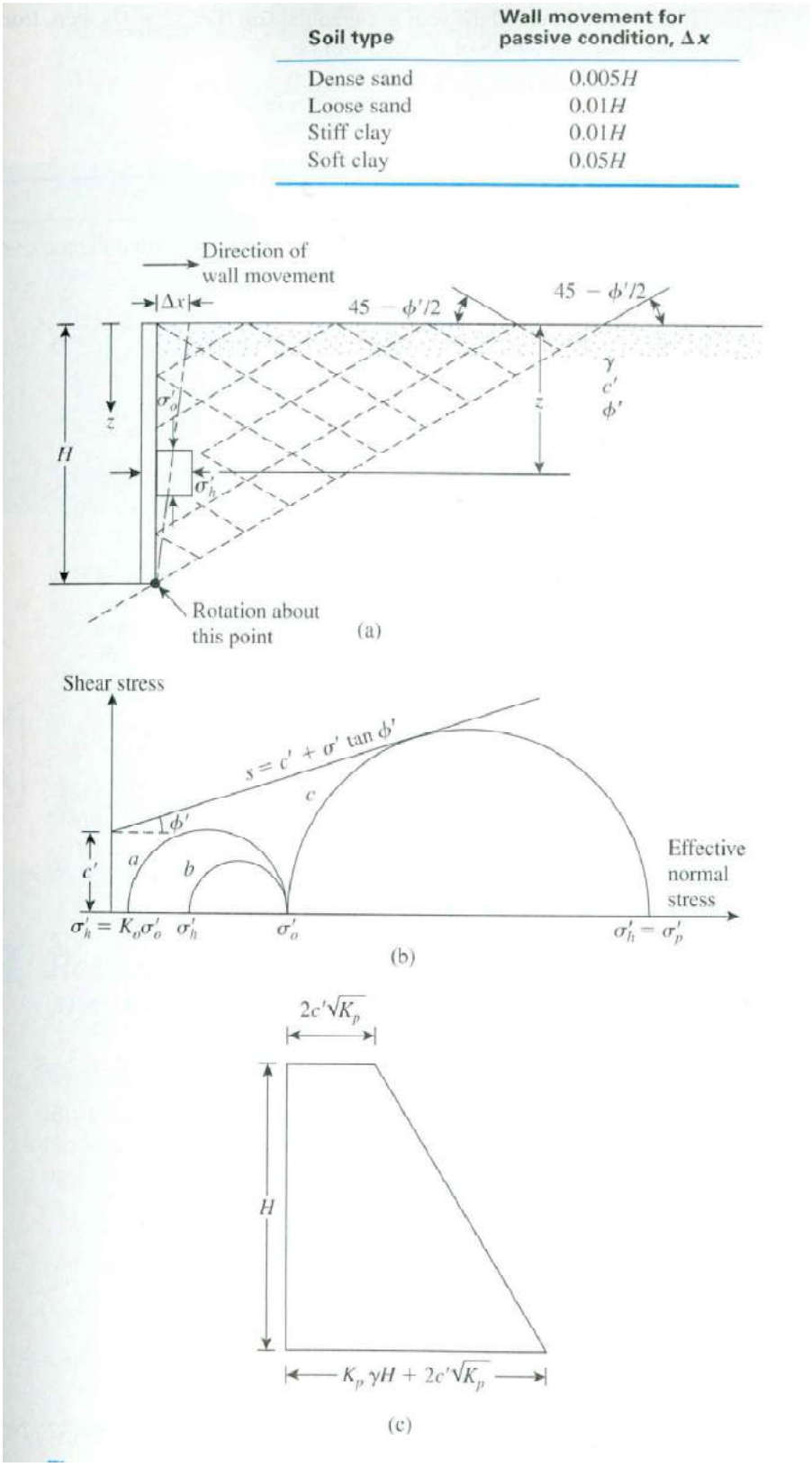

Figure 2.8 Rankine passive pressure

If the backfill behind the wall is a granular soil (i.e., c'=0), then, from Eq. (2.21), the passive force per unit length of the wall will be

$$P_p = \frac{1}{2}\gamma H^2 K_p \qquad (2.22)$$

2.4.2 Rankine Passive Earth Pressure for Inclined Backfill

For a frictionless vertical retaining wall (Figure 2.5) with a *granular backfill* (c'=0), the Rankine passive pressure at any depth can be determined in a manner similar to that done in the case of active pressure in Section 2.3.2. The pressure is

$$\sigma_p' = \gamma z K_p \qquad (2.23)$$

And the passive force is

$$P_p = 1/2\,\gamma H^2 K_p \qquad (2.24)$$

where

$$K_p = cos\alpha \frac{cos\alpha+\sqrt{cos^2\alpha-cos^2\emptyset'}}{cos\alpha-\sqrt{cos^2\alpha-cos^2\emptyset'}} \qquad (2.25)$$

As in the case of the active force, the resultant force, P_p, is inclined at an angle α with the horizontal and intersects the wall at a distance H/3 from the bottom of the wall. The values of K_p (the passive earth pressure coefficient) for various values of α and ϕ' are given in **Table 2.6**.

Table 2.6 Passive Earth Pressure Coefficient [from Eq. (2.25)]

	ϕ' (deg)→						
↓α (deg)	28	30	32	34	36	38	40
0	2.770	3.000	3.255	3.537	3.852	4.204	4.599
5	2.715	2.943	3.196	3.476	3.788	4.136	4.527
10	2.551	2.775	3.022	3.295	3.598	3.937	4.316
15	2.284	2.502	2.740	3.003	3.293	3.615	3.977
20	1.918	2.132	2.362	2.612	2.886	3.189	3.526
25	1.434	1.664	1.894	2.135	2.394	2.676	2.987

2.4.3 Coulomb's Passive Earth Pressure

Coulomb (1776) also presented an analysis for determining the passive earth pressure (i.e., when the wall moves *into* the soil mass) for walls possessing friction (δ'=angle of wall friction) and retaining a granular backfill material similar to that discussed in Section 2.3.3.

To understand the determination of Coulomb's passive force, P_p , consider the wall shown in Figure 2.9a. As in the case of active pressure, Coulomb assumed that the potential failure surface in soil is a plane. For a trial failure wedge of soil, such as ABC_1, the forces per unit length of the wall acting on the wedge are

1. The weight of the wedge, W
2. The resultant, R, of the normal and shear forces on the plane and
3. The passive force, P_p

Figure 2.9b shows the force triangle at equilibrium for the trial wedge ABC_1. From this force triangle, the value of P_p can be determined, because the direction of all three forces and the magnitude of one force are known.

Similar force triangles for several trial wedges, such as ABC_1, ABC_2, ABC_3, … can be constructed, and the corresponding values of P_p can be determined. The top part of Figure 2.9a shows the nature of variation of P_p the values for different wedges. The *minimum value of* P_p in this diagram is *Coulomb's passive force,* mathematically expressed as

$$P_a = 1/2\,\gamma H^2 K_p \qquad (2.26)$$

Where

K_a= Coulomb's passive earth-pressure coefficient

$$= \frac{sin^2(\beta - \emptyset')}{sin^2\beta \sin(\beta+\delta')\left[1-\sqrt{\frac{\sin(\emptyset'+\delta')\sin(\emptyset'+\alpha)}{\sin(\beta+\delta')\sin(\alpha+\beta)}}\right]^2} \qquad (2.27)$$

and H= height of the wall.

The values of the passive pressure coefficient, K_p, for various values of $\emptyset'$ and δ' are given in Table 2.7 ($\beta = 90^o$, $\alpha = 0^o$).

Note that the resultant passive force, P_p , will act at a distance H/3 from the bottom of the wall and will be inclined at an angle δ' to the normal drawn to the back face of the wall.

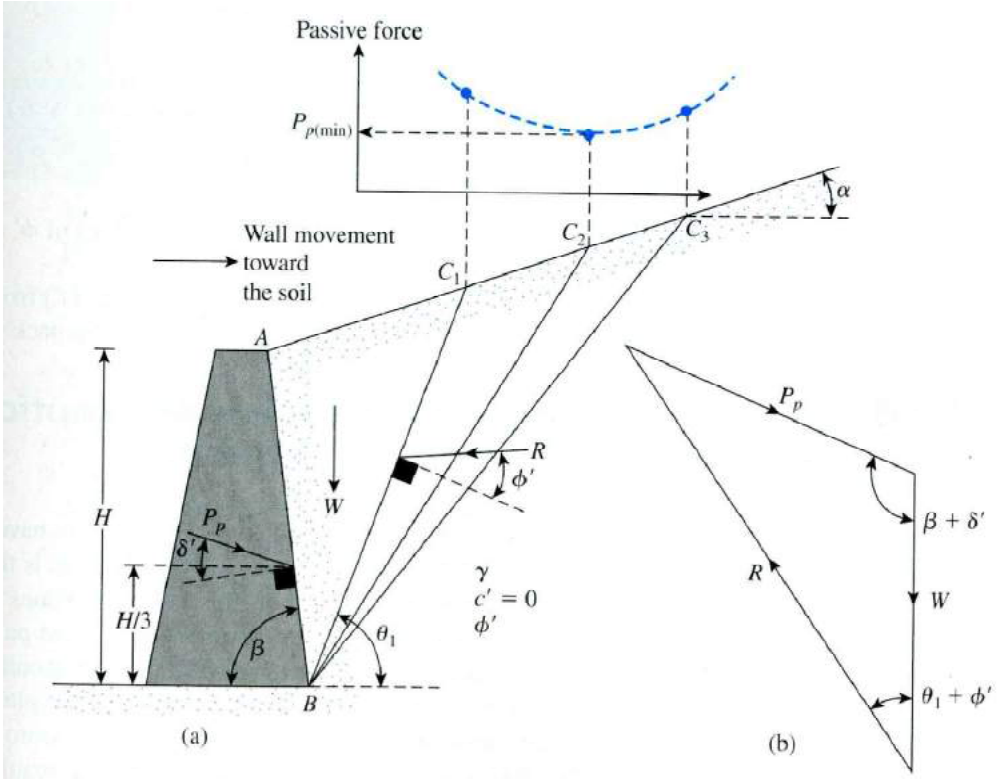

Figure 2.9 Coulomb's passive pressure

Table 7.10 Values of [from Eq. (2.27)] for $\beta=90^o$ and $\alpha=0^o$

ϕ' (deg)	δ' (deg)				
	0	5	10	15	20
15	1.698	1.900	2.130	2.405	2.735
20	2.040	2.313	2.636	3.030	3.525
25	2.464	2.830	3.286	3.855	4.597
30	3.000	3.506	4.143	4.977	6.105
35	3.690	4.390	5.310	6.854	8.324
40	4.600	5.590	6.946	8.870	11.772

University of Anbar
Engineering College
Civil Engineering Department

CHAPTER THREE

RETAINING WALLS

LECTURE
DR. AHMED H. ABDULKAREEM
2017

1. Introduction

A retaining wall is a wall that provides lateral support for a vertical or near-vertical slope of soil. It is a common structure used in many construction projects. The most common types of retaining wall may be classified as follows:

1. Gravity retaining walls
2. Semigravity retaining walls
3. Cantilever retaining walls
4. Counterfort retaining walls

Gravity retaining walls **(Figure 3.1a)** are constructed with plain concrete or stone masonry. They depend for stability on their own weight and any soil resting on the masonry. This type of construction is not economical for high walls.

In many cases, a small amount of steel may be used for the construction of gravity walls, thereby minimizing the size of wall sections. Such walls are generally referred to as ***semigravity walls*** **(Figure 3.1b)**.

Cantilever retaining walls **(Figure 3.1c)** are made of reinforced concrete that consists of a thin stem and a base slab. This type of wall is economical to a height of about 8 m as Figure (3.2).

Counterfort retaining walls **(Figure 3.1d)** are similar to cantilever walls. At regular intervals, however, they have thin vertical concrete slabs known as *counterforts* that tie the wall and the base slab together. The purpose of the counterforts is to reduce the shear and the bending moments.

To design retaining walls properly, an engineer must know the basic parameters—the *unit weight, angle of friction,* and *cohesion*—of the soil retained behind the wall and the soil below the base slab. Knowing the properties of the soil behind the wall enables the engineer to determine the lateral pressure distribution that has to be designed for.

There are two phases in the design of a conventional retaining wall. First, with the lateral earth pressure known, the structure as a whole is checked for *stability*. The structure is examined for possible *overturning, sliding,* and *bearing capacity* failures. Second, each component of the structure is checked for *strength,* and the *steel reinforcement* of each component is determined.

This chapter presents the procedures for determination of lateral earth pressure and retaining-wall stability.

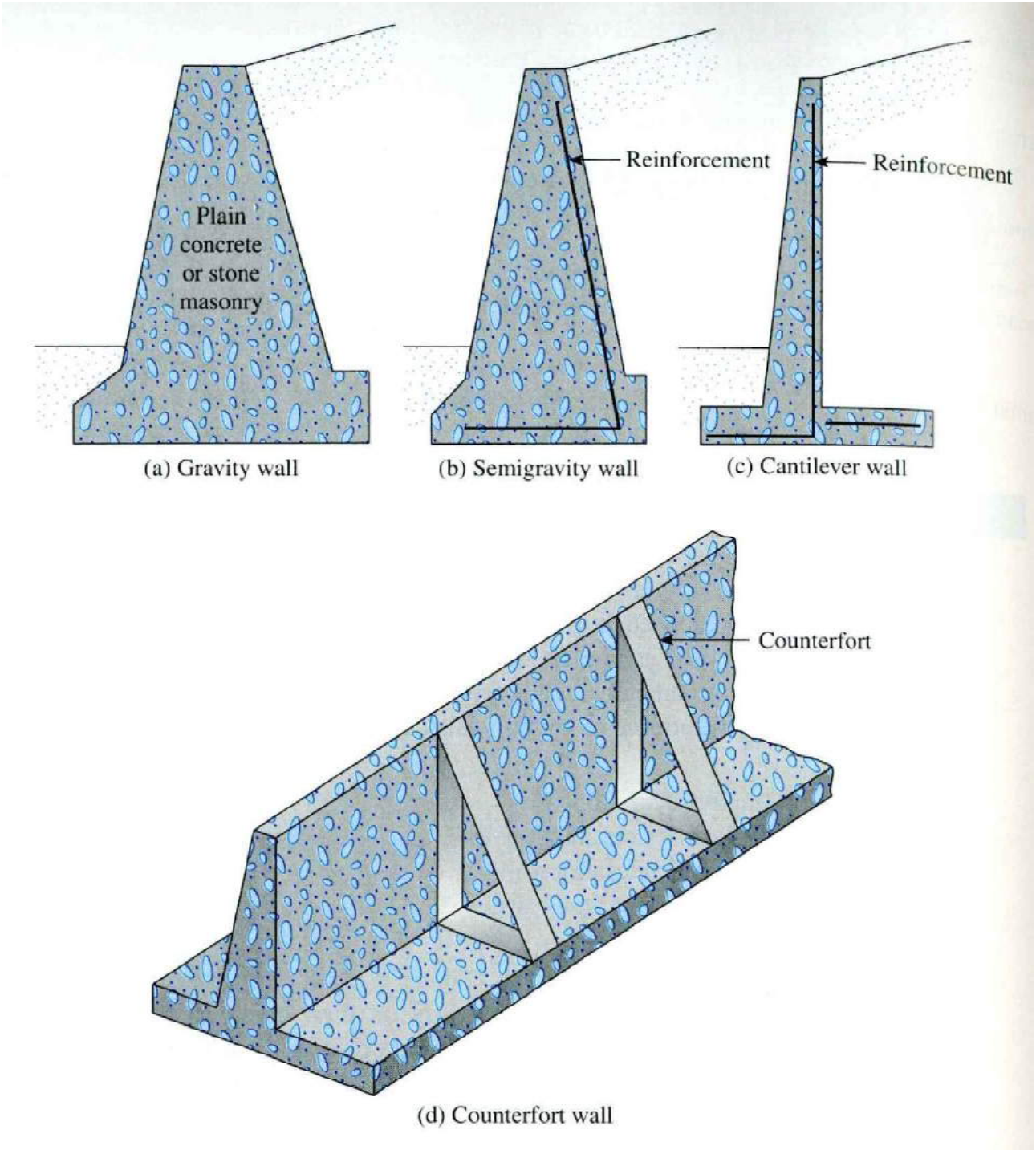

Figure 3.1 Types of retaining wall

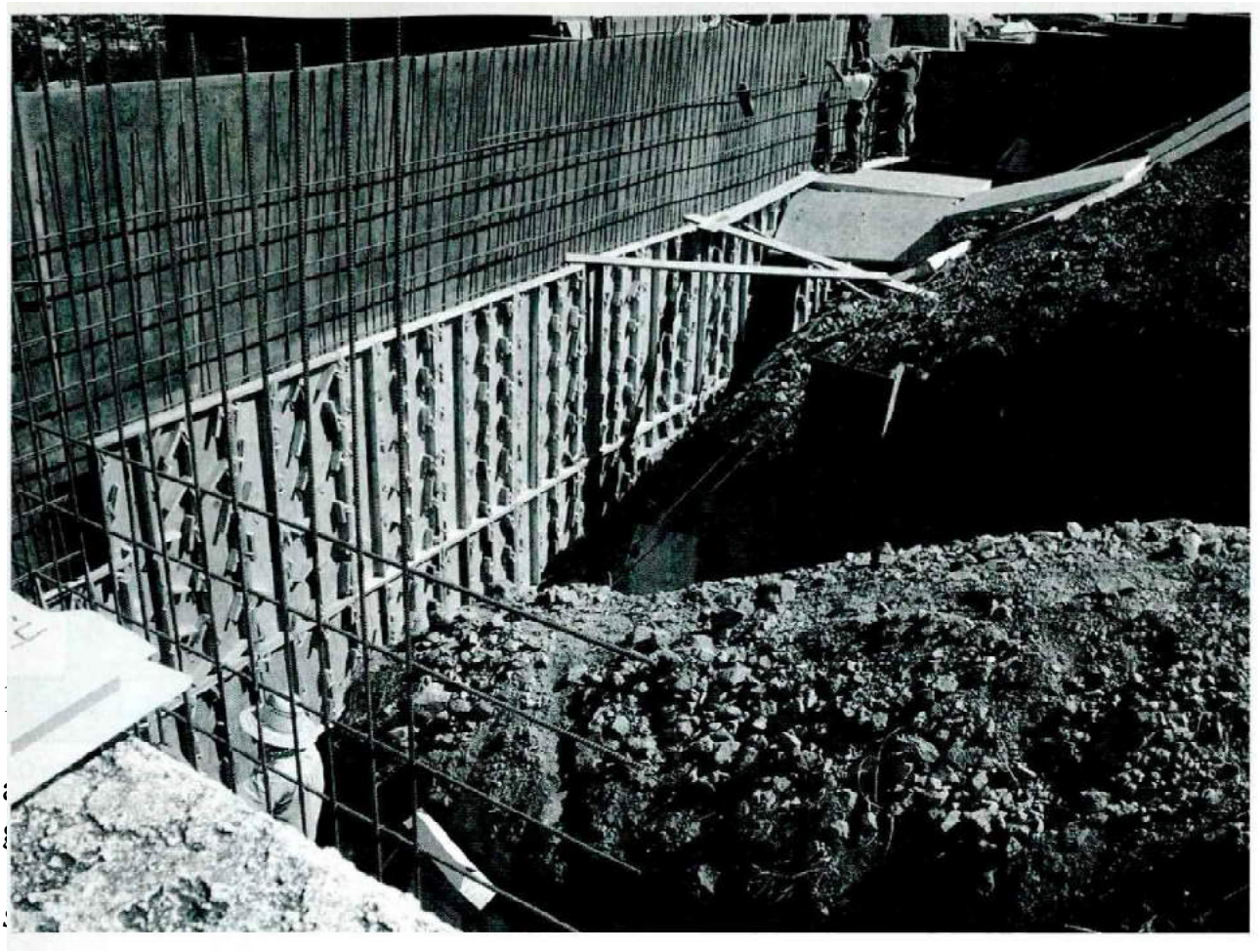

Figure 3.2 A cantilever retaining wall under construction

3.2 Gravity and Cantilever Walls

3.2.1 Proportioning Retaining Walls

In designing retaining walls, an engineer must assume some of their dimensions. Called *proportioning,* such assumptions allow the engineer to check trial sections of the walls for stability. If the stability checks yield undesirable results, the sections can be changed and rechecked. Figure 3.3 shows the general proportions of various retaining-wall components that can be used for initial checks.

Note that the top of the stem of any retaining wall should not be less than about 0.3 m. for proper placement of concrete. The depth, *D,* to the bottom of the base slab should be a minimum of 0.6m. However, the bottom of the base slab should be positioned below the seasonal frost line.

For counterfort retaining walls, the general proportion of the stem and the base slab is the same as for cantilever walls. However, the counterfort slabs may be about 0.3 m thick and spaced at center-to-center distances of 0.3*H* to 0.7*H*.

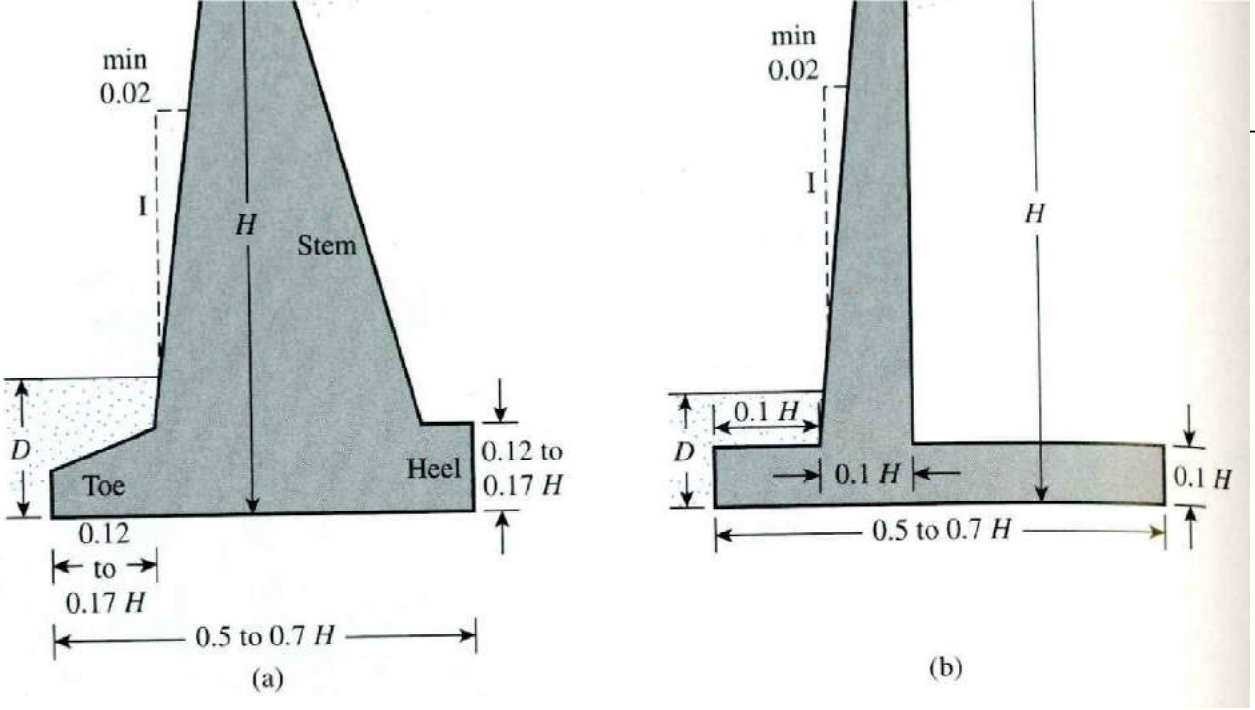

Figure 3.3 Approximate dimensions for various components of retaining wall for initial stability checks: (a) gravity wall; (b) cantilever wall

3.3 Application of Lateral Earth Pressure Theories to Design

The fundamental theories for calculating lateral earth pressure were presented in Chapter 2. To use these theories in design, an engineer must make several simple assumptions. In the case of cantilever walls, the use of the Rankine earth pressure theory for stability checks involves drawing a vertical line *AB* through point *A,* located at the edge of the heel of the base slab in Figure 3.4a. The Rankine active condition is assumed to exist along the vertical plane *AB*. Rankine active earth pressure equations may then be used to calculate the lateral pressure on the face *AB* of the wall. In the analysis of the wall's stability, the force $P_{a(\text{Rankine})}$, the weight of soil above the heel, and the weight W_c of the concrete all should be taken into consideration. The assumption for the development of Rankine active pressure along the soil face *AB* is theoretically correct if the shear zone bounded by the line *AC* is not obstructed by the stem of the wall. The angle, *h*, that the line *AC* makes with the vertical is

$$\eta = 45 + \frac{\alpha}{2} - \frac{\phi'}{2} - \frac{1}{2}\sin^{-1}\left(\frac{\sin\alpha}{\sin\phi'}\right) \qquad (3\text{-}1)$$

A similar type of analysis may be used for gravity walls, as shown in Figure 3.4b. However, Coulomb's active earth pressure theory also may be used, as shown in Figure 3.4c. If it is used, the only forces to be considered are $P_{a(\text{Coulomb})}$ and the weight of the wall, W_c.

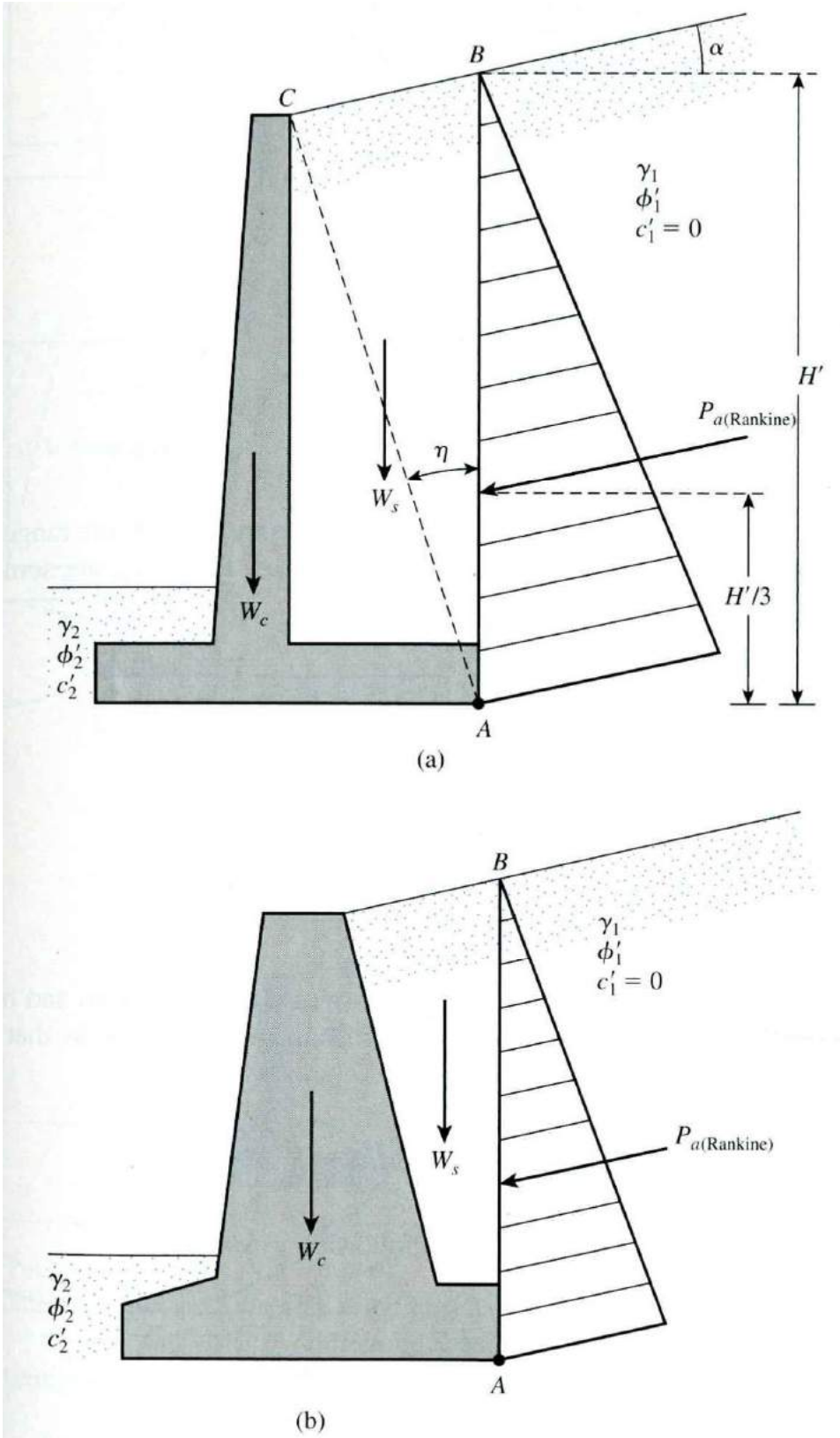

Figure 3.4 Assumption for the determination of lateral earth pressure: (a) cantilever wall; (b) and (c) gravity wall

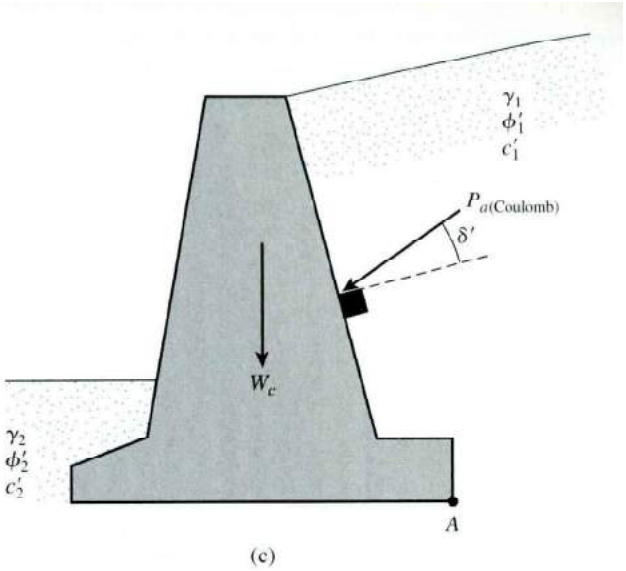

Figure 3.4 (*continued*)

If Coulomb's theory is used, it will be necessary to know the range of the wall friction angle δ' with various types of backfill material. Following are some ranges of wall friction angle for masonry or mass concrete walls:

Backfill material	Range of δ' (deg)
Gravel	27–30
Coarse sand	20–28
Fine sand	15–25
Stiff clay	15–20
Silty clay	12–16

In the case of ordinary retaining walls, water table problems and hence hydrostatic pressure are not encountered. Facilities for drainage from the soils that are retained are always provided.

3.4 Stability of Retaining Walls

A retaining wall may fail in any of the following ways:

- It may overturn about its toe. (See Figure 3.5a.)
- It may *slide* along its base. (See Figure 3.5b.)
- It may fail due to the loss of *bearing capacity* of the soil supporting the base. (See Figure 3.5c.)
- It may undergo deep-seated shear failure. (See Figure 3.5d.)
- It may go through excessive settlement.

The checks for stability against overturning, sliding, and bearing capacity failure will be described in Sections 3.5, 3.6, and 3.7. When a weak soil layer is located at a shallow depth—that is, within a depth of 1.5 times the width of the base slab of the retaining wall—the possibility of excessive settlement should be considered. In some cases, the use of lightweight backfill material behind the retaining wall may solve the problem.

Deep shear failure can occur along a cylindrical surface, such as *abc* shown in Figure 3.6, as a result of the existence of a weak layer of soil underneath the wall at a depth of about 1.5 times the width of the base slab of the retaining wall. In such cases, the critical cylindrical failure surface *abc* has to be determined by trial and error, using various centers such as *O*. The failure surface along which the minimum factor of safety is obtained is the *critical surface of sliding*. For the backfill slope with α less than about 10^{o}, the critical failure circle apparently passes through the edge of the heel slab (such as *def* in the figure). In this situation, the minimum factor of safety also has to be determined by trial and error by changing the center of the trial circle.

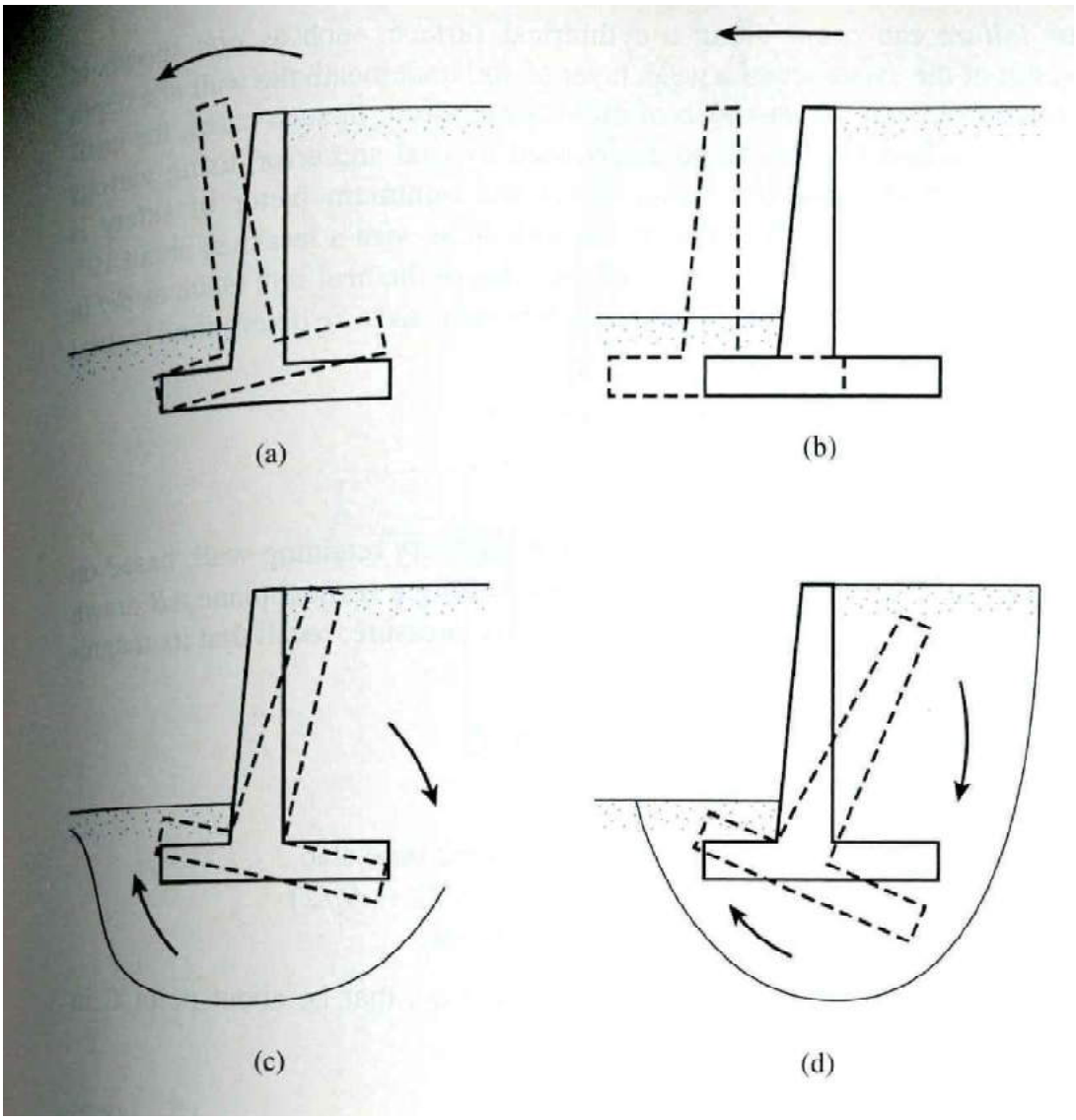

Figure 3.5 Failure of retaining wall: (a) by overturning; (b) by sliding; (c) by bearing capacity failure; (d) by deep-seated shear failure

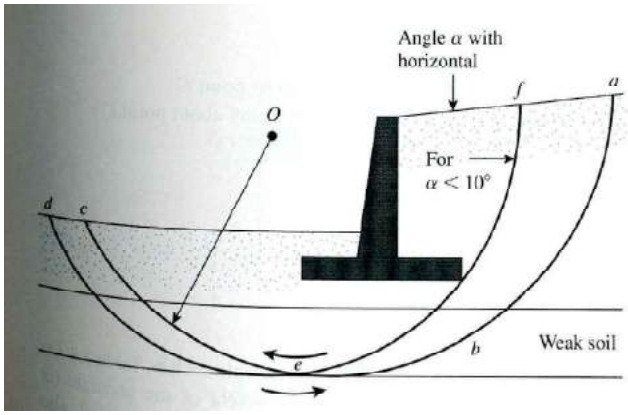

Figure 3.6 Deep-seated shear failure

3.5 Check for Overturning

Figure 3.7 shows the forces acting on a cantilever and a gravity retaining wall, based on the assumption that the Rankine active pressure is acting along a vertical plane *AB* drawn through the heel of the structure. P_p is the Rankine passive pressure; recall that its magnitude is

$$P_p = \frac{1}{2}K_p\gamma_2 D^2 + 2c_2'\sqrt{K_p D}$$

where
γ_2= unit weight of soil in front of the heel and under the base slab
K_p = Rankine passive earth pressure coefficient 5 tan2s45 1 *f*92y2d
c_2' , ϕ_2' = cohesion and effective soil friction angle, respectively

The factor of safety against overturning about the toe—that is, about point *C* in Figure 3.7—may be expressed as

$$FS_{(overturning)} = \frac{\sum M_R}{\sum M_o} \qquad (3\text{-}2)$$

where
$\sum M_R$= sum of the moments of forces tending to overturn about point *C*
$\sum M_o$ = sum of the moments of forces tending to resist overturning about point *C*

The overturning moment is

$$\Sigma M_o = P_h\left(\frac{H'}{3}\right) \qquad (3\text{-}3)$$

Where $P_h = P_a cos\alpha$

To calculate the resisting moment, $\sum M_R$ (neglecting P_p), a table such as Table 3.1 can be prepared. The weight of the soil above the heel and the weight of the concrete (or masonry) are both forces that contribute to the resisting moment. Note that the force P_v also contributes to the resisting moment. P_v is the vertical component of the active force P_a , or

$$P_v = P_a sin\alpha$$

The moment of the force P_v about *C* is

$$M_v = P_v B = P_a sin\alpha B \qquad (3\text{-}4)$$

where B = width of the base slab.

Once $\sum M_R$ is known, the factor of safety can be calculated as

$$\text{FS}_{(\text{overturning})} = \frac{M_1 + M_2 + M_3 + M_4 + M_5 + M_6 + M_v}{P_a \cos\alpha (H'/3)} \qquad (3\text{-}5)$$

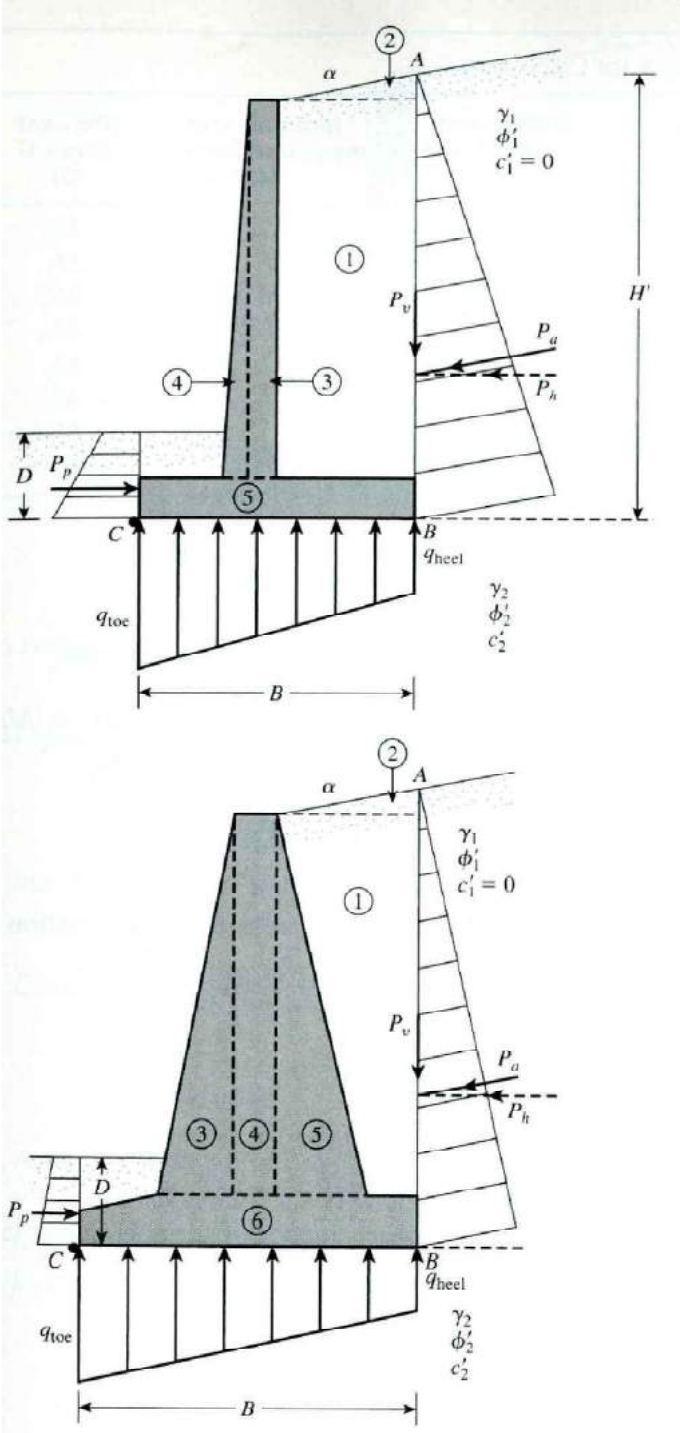

Figure 3.7 Check for overturning, assuming that the Rankine pressure is valid

Table 3.1 Procedure for Calculating $\sum M_R$

Section (1)	Area (2)	Weight/unit length of wall (3)	Moment arm measured from C (4)	Moment about C (5)
1	A_1	$W_1 = \gamma_1 \times A_1$	X_1	M_1
2	A_2	$W_2 = \gamma_1 \times A_2$	X_2	M_2
3	A_3	$W_3 = \gamma_c \times A_3$	X_3	M_3
4	A_4	$W_4 = \gamma_c \times A_4$	X_4	M_4
5	A_5	$W_5 = \gamma_c \times A_5$	X_5	M_5
6	A_6	$W_6 = \gamma_c \times A_6$	X_6	M_6
		P_v	B	M_v
		ΣV		ΣM_R

(*Note:* γ_l = unit weight of backfill
γ_c = unit weight of concrete)

The usual minimum desirable value of the factor of safety with respect to overturning is 2 to 3.

Some designers prefer to determine the factor of safety against overturning with the formula

$$FS_{(overturning)} = \frac{M_1 + M_2 + M_3 + M_4 + M_5 + M_6}{P_a \cos\alpha (H'/3) - M_v} \qquad (3\text{-}6)$$

3.6 Check for Sliding along the Base

The factor of safety against sliding may be expressed by the equation

$$FS_{(sliding)} = \frac{\sum F_R}{\sum F_d} \qquad (3\text{-}7)$$

where
$\sum F_R$ = sum of the horizontal resisting forces
$\sum F_d$ = sum of the horizontal driving forces

Figure 3.8 indicates that the shear strength of the soil immediately below the base slab may be represented as

$$s = \sigma' \tan \delta' + c'_a$$

where
δ' = angle of friction between the soil and the base slab

c_a' = adhesion between the soil and the base slab

Thus, the maximum resisting force that can be derived from the soil per unit length of the wall along the bottom of the base slab is

$$R' = s(\text{area of cross section}) = s(B \times 1) = B\sigma' \tan\delta' + Bc_a'$$

However,

$B\sigma'$ = sum of the vertical force = ΣV (see Table 3.1)

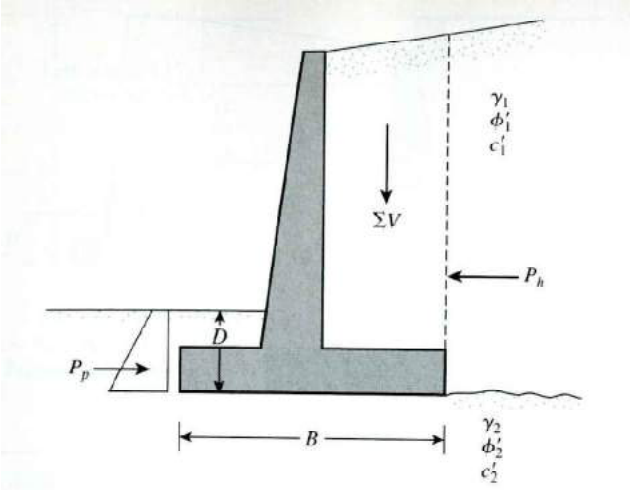

Figure 3.8 Check for sliding along the base

Figure 3.8 shows that the passive force P_p is also a horizontal resisting force. Hence,

$$\Sigma F_{R'} = (\Sigma V)\tan\delta' + Bc_a' + P_p \qquad (3\text{-}8)$$

The only horizontal force that will tend to cause the wall to slide (a *driving force*) is the horizontal component of the active force P_a , so

$$\Sigma F_d = P_a \cos\alpha \qquad (3\text{-}9)$$

Combining Eqs. (3.7), (3.8), and (3.9) yields

$$FS_{(\text{sliding})} = \frac{(\Sigma V)\tan\delta' + Bc_a' + P_p}{P_a \cos\alpha} \qquad (3\text{-}10)$$

A minimum factor of safety of 1.5 against sliding is generally required.

In many cases, the passive force P_p is ignored in calculating the factor of safety with respect to sliding. In general, we can write $\delta' = k_1\phi_2'$ and $c_a' = k_2 c_2'$. In most cases, k_1 and k_2 are in the range from 1/2 to 2/3. Thus,

$$FS_{(sliding)} = \frac{(\Sigma V)\tan(k_1\phi_2') + Bk_2c_2' + P_p}{P_a\cos\alpha} \qquad (3\text{-}11)$$

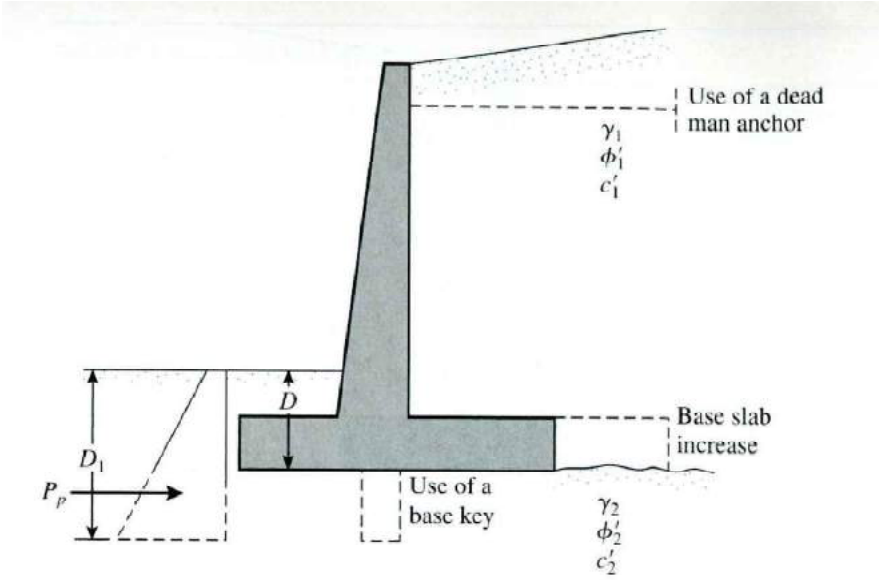

Figure 3.9 Alternatives for increasing the factor of safety with respect to sliding

If the desired value of $FS_{(sliding)}$ is not achieved, several alternatives may be investigated (see Figure 3.9):

- Increase the width of the base slab (i.e., the heel of the footing).
- Use a key to the base slab. If a key is included, the passive force per unit length of the wall becomes

$$P_p = \frac{1}{2}\gamma_2 D_1^2 K_p + 2c_2' D_1\sqrt{K_p}$$

where $K_p = \tan^2\left(45 + \frac{\phi_2'}{2}\right)$.

- Use a *deadman anchor* at the stem of the retaining wall.

3.7 Check for Bearing Capacity Failure

The vertical pressure transmitted to the soil by the base slab of the retaining wall should be checked against the ultimate bearing capacity of the soil. The nature of variation of the vertical pressure transmitted by the base slab into the soil is shown in Figure 3.11. Note that q_{toe} and q_{heel} are the *maximum* and the *minimum* pressures occurring at the ends of the toe and heel sections, respectively. The magnitudes of q_{toe} and q_{heel} can be determined in the following manner:

The sum of the vertical forces acting on the base slab is $\sum V$ (see column 3 of Table 3.1), and the horizontal force P_h is $P_a \cos\alpha$. Let

$$R = \sum V + P_h \qquad (3\text{-}12)$$

be the resultant force. The net moment of these forces about point *C* in Figure 3.11 is

$$M_{net} = \Sigma M_R - \Sigma M_o \qquad (3\text{-}`13)$$

Note that the values of $\sum M_R$ and $\sum M_o$ were previously determined. [See Column 5 of Table 3.1 and Eq. (3.3)]. Let the line of action of the resultant *R* intersect the base slab at *E*. Then the distance

$$\overline{CE} = \overline{X} = \frac{M_{net}}{\Sigma V} \qquad (3\text{-}14)$$

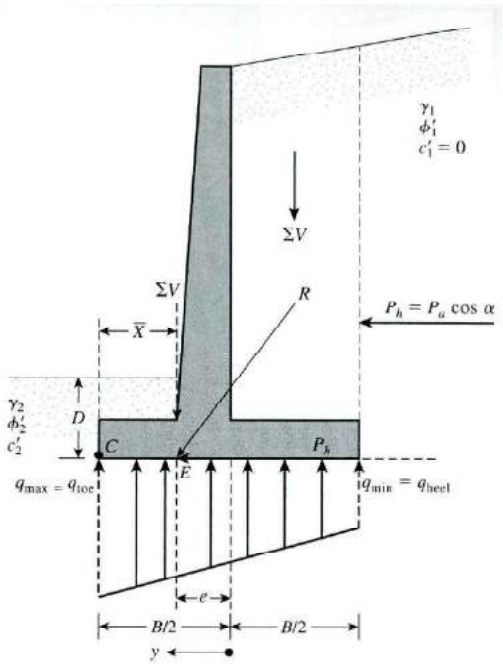

Figure 3.11 Check for bearing capacity failure

Hence, the eccentricity of the resultant R may be expressed as

$$e = \frac{B}{2} - \overline{CE} \qquad (3.15)$$

The pressure distribution under the base slab may be determined by using simple principles from the mechanics of materials. First, we have

$$q = \frac{\Sigma V}{A} \pm \frac{M_{net} y}{I} \qquad (3.16)$$

where
M_{net} =moment =($\sum V$)e
I = moment of inertia per unit length of the base section = 1/12(1)(B^2)

For maximum and minimum pressures, the value of y in Eq. (3.16) equals $B/2$. Substituting into Eq. (3.16) gives

$$q_{max} = q_{toe} = \frac{\Sigma V}{(B)(1)} + \frac{e(\Sigma V)\frac{B}{2}}{\left(\frac{1}{12}\right)(B^3)} = \frac{\Sigma V}{B}\left(1 + \frac{6e}{B}\right) \qquad (3.17)$$

Similarly

$$q_{min} = q_{heel} = \frac{\Sigma V}{B}\left(1 - \frac{6e}{B}\right) \qquad (3.18)$$

Note that $\sum V$ includes the weight of the soil, as shown in Table 3.1, and that when the value of the eccentricity e becomes greater than $B/6$, q_{min} [Eq. (3.18)] becomes negative. Thus, there will be some tensile stress at the end of the heel section. This stress is not desirable, because the tensile strength of soil is very small. If the analysis of a design shows that e . $B/6$, the design should be reproportioned and calculations redone. The relationships pertaining to the ultimate bearing capacity of a shallow foundation were discussed in previous Chapter . Recall that

$$q_u = c'_2 N_c F_{cd} F_{ci} + q N_q F_{qd} F_{qi} + \tfrac{1}{2}\gamma_2 B' N_\gamma F_{\gamma d} F_{\gamma i} \qquad (3.19)$$

where

$$q = \gamma_2 D$$

$$B' = B - 2e$$

$$F_{cd} = F_{qd} - \frac{1 - F_{qd}}{N_c \tan \phi'_2}$$

$$F_{qd} = 1 + 2 \tan \phi'_2 (1 - \sin \phi'_2)^2 \frac{D}{B'}$$

$$F_{\gamma d} = 1$$

$$F_{ci} = F_{qi} = \left(1 - \frac{\psi^\circ}{90^\circ}\right)^2$$

$$F_{\gamma i} = \left(1 - \frac{\psi^\circ}{\phi'^\circ_2}\right)^2$$

$$\psi^\circ = \tan^{-1}\left(\frac{P_a \cos\alpha}{\Sigma V}\right)$$

Note that the shape factors F_{cs} , F_{qs} , and $F_{\gamma s}$ given in previous Chapter are all equal to unity, because they can be treated as a continuous foundation. For this reason, the shape factors are not shown in Eq. (13.19).

Once the ultimate bearing capacity of the soil has been calculated by using Eq. (13.19), the factor of safety against bearing capacity failure can be determined:

$$\text{FS}_{(\text{bearing capacity})} = \frac{q_u}{q_{\max}} \qquad (3.20)$$

Generally, a factor of safety of 3 is required. We noted that the ultimate bearing capacity of shallow foundations occurs at a settlement of about 10% of the foundation width. In the case of retaining walls, the width B is large. Hence, the ultimate load q_u will occur at a fairly large foundation settlement. A factor of safety of 3 against bearing capacity failure may not ensure that settlement of the structure will be within the tolerable limit in all cases. Thus, this situation needs further investigation.

Example 1

Example 2

3.8 Construction Joints and Drainage from Backfill

Construction Joints

A retaining wall may be constructed with one or more of the following joints:

1. ***Construction joints*** **(see Figure 3.12a)** are vertical and horizontal joints that are placed between two successive pours of concrete. To increase the shear at the joints, keys may be used. If keys are not used, the surface of the first pour is cleaned and roughened before the next pour of concrete.

2. ***Contraction joints*** **(Figure 3.12b)** are vertical joints (grooves) placed in the face of a wall (from the top of the base slab to the top of the wall) that allow the concrete to shrink without noticeable harm. The grooves may be about 6 to 8 mm wide and 12 to 16 mm deep.

3. ***Expansion joints*** **(Figure 3.12c)** allow for the expansion of concrete caused by temperature changes; vertical expansion joints from the base to the top of the wall may also be used. These joints may be filled with flexible joint fillers. In most cases, horizontal reinforcing steel bars running across the stem are continuous through all joints. The steel is greased to allow the concrete to expand.

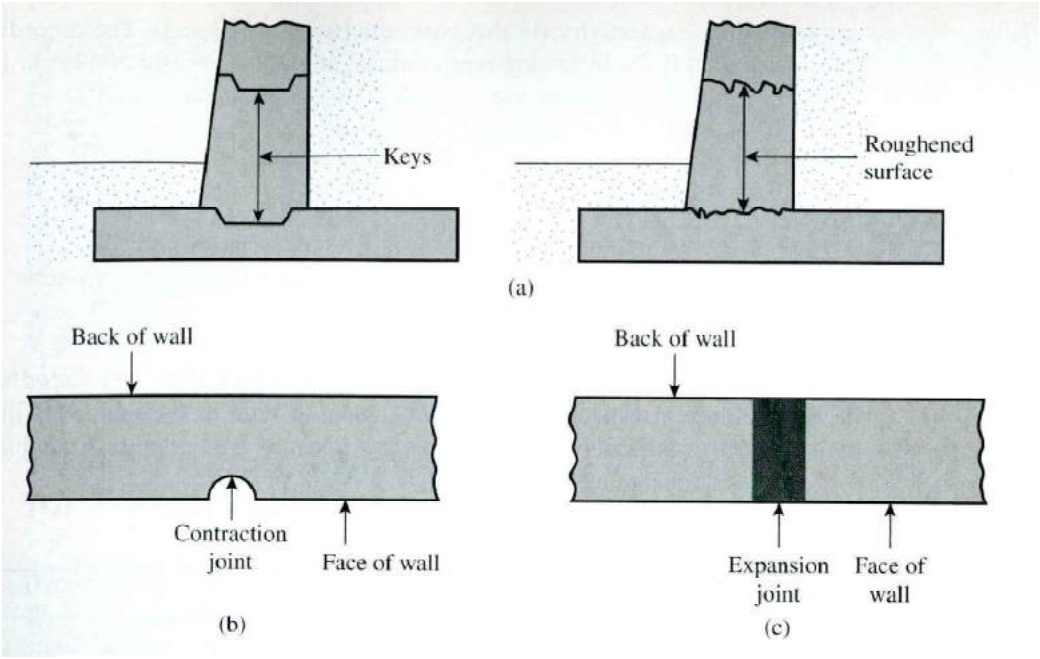

Figure 3.12 (a) Construction joints; (b) contraction joint; (c) expansion joint

Drainage from the Backfill

As the result of rainfall or other wet conditions, the backfill material for a retaining wall may become saturated, thereby increasing the pressure on the wall and perhaps creating an unstable condition. For this reason, adequate drainage must be provided by means of *weep holes* or *perforated drainage pipes*. (See Figure 3.13.)

When provided, weep holes should have a minimum diameter of about 0.1 m and be adequately spaced. Note that there is always a possibility that backfill material may be washed into weep holes or drainage pipes and ultimately clog them. Thus, a filter conductivity (in this case, the backfill material). The preceding conditions can be satisfied if the following requirements are met (Terzaghi and Peck, 1967):

$$\frac{D_{15(F)}}{D_{85(B)}} < 5 \quad [to\ satisfy\ condition(a)] \qquad (3.21)$$

$$\frac{D_{15(F)}}{D_{15(B)}} > 4 \quad [to\ satisfy\ condition(b)] \qquad (3.22)$$

In these relations, the subscripts F and B refer to the *filter* and the *base* material (i.e., the backfill soil), respectively. Also, D_{15} and D_{85} refer to the diameters through which 15% and 85% of the soil (filter or base, as the case may be) will pass. Example 3.3 gives the procedure for designing a filter.

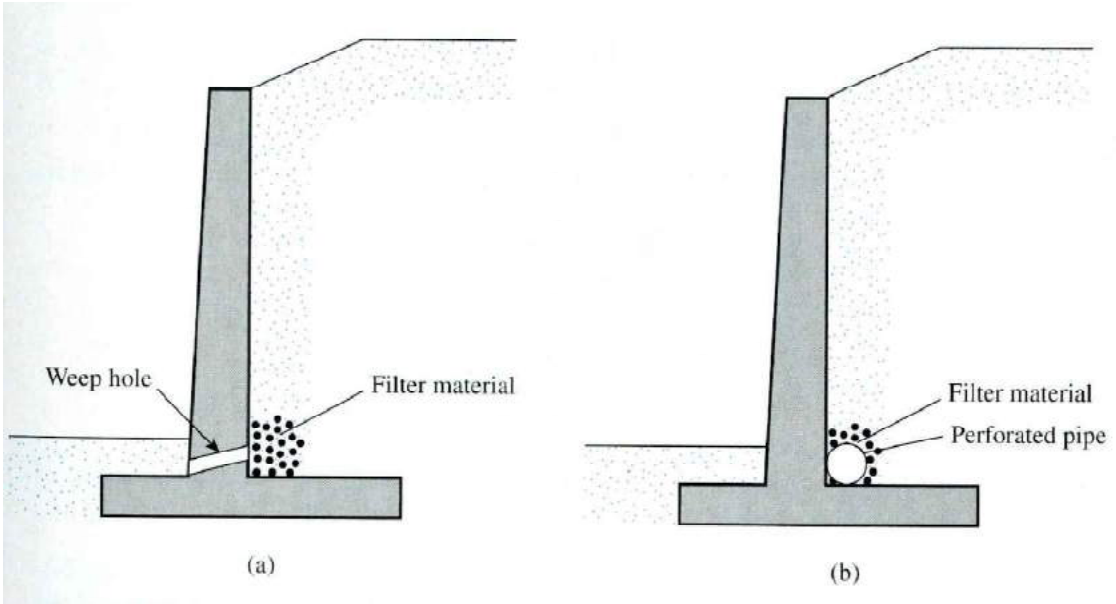

Figure 3.13 Drainage provisions for the backfill of a retaining wall: (a) by weep holes; (b) by a perforated drainage pipe

University of Anbar
Engineering College
Civil Engineering Department

CHAPTER FOUR

SHEET PILE WALLS

LECTURE
DR. AHMED H. ABDULKAREEM
2017

4.1. Introduction

Connected or semi-connected sheet piles are often used to build continuous walls for waterfront structures that range from small waterfront pleasure boat launching facilities to large dock facilities. (See Figure 4.1). In contrast to the construction of other types of retaining wall, the building of sheet-pile walls does not usually require dewatering of the site. Sheet piles are also used for some temporary structures, such as braced cuts. (See Chapter 5). The principles of sheet-pile wall design are discussed in the current chapter.

Several types of sheet pile are commonly used in construction:

(a) wooden sheet piles,
(b) precast concrete sheet piles, and
(c) steel sheet piles.

Aluminum sheet piles are also marketed.

(a)Wooden sheet piles are used only for temporary, light structures that are above the water table. The most common types are ordinary wooden planks and ***Wakefield piles***. The wooden planks are about 50 mm × 300 mm (2 in. × 12 in.) in cross section and are driven edge to edge (Figure 4.2a). Wakefield piles are made by nailing three planks together, with the middle plank offset by 50 to 75 mm (2 to 3 in.) (Figure 4.2b). Wooden planks can also be milled to form *tongue-and-groove piles,* as shown in Figure 4.2c. Figure 4.2d shows another type of wooden sheet pile that has precut grooves. Metal ***splines*** are driven into the grooves of the adjacent sheetings to hold them together after they are sunk into the ground.

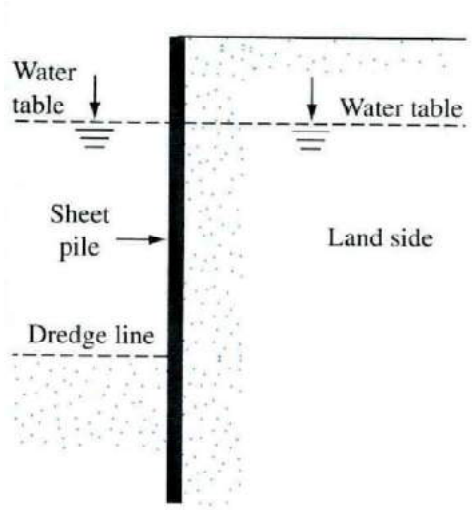

Figure 4.1 Example of waterfront sheet-pile wall.

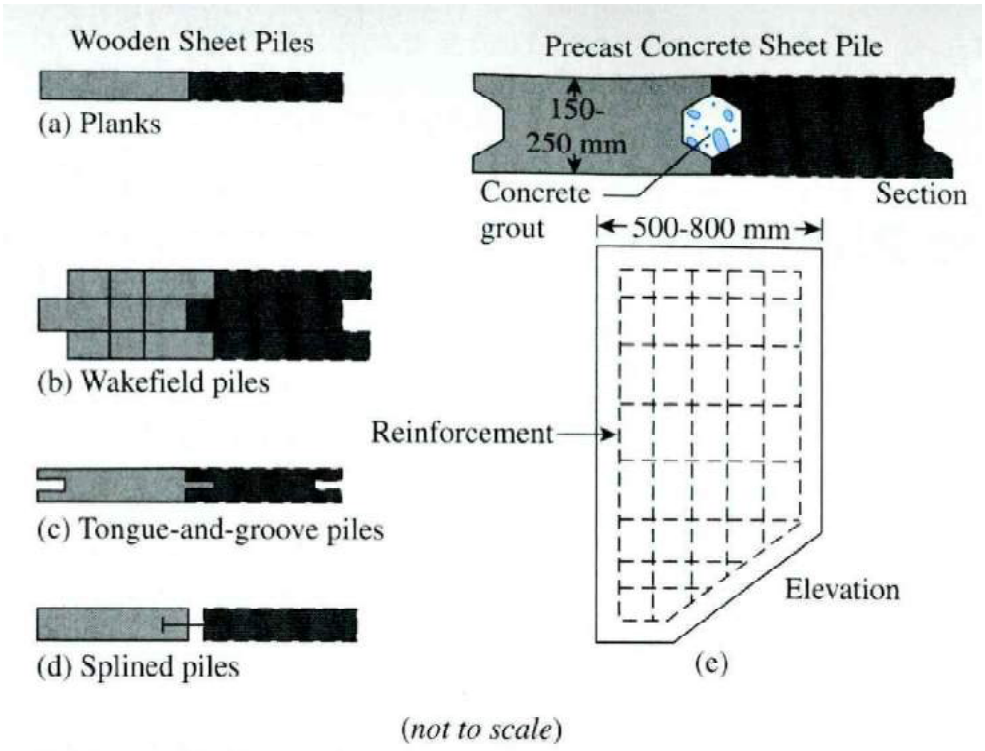

Figure 4.2 Various types of wooden and concrete sheet pile

Precast concrete sheet piles are heavy and are designed with reinforcements to withstand the permanent stresses to which the structure will be subjected after construction and also to handle the stresses produced during construction. In cross section, these piles are about 500 to 800 mm (20 to 32 in.) wide and 150 to 250 mm (6 to 10 in.) thick. Figure 4.2e is a schematic diagram of the elevation and the cross section of a reinforced concrete sheet pile.

Steel sheet piles in the United States are about 10 to 13 mm (0.4 to 0.5 in.) thick. European sections may be thinner and wider. Sheet-pile sections may be ***Z, deep arch, low arch,*** **or** ***straight web*** sections. The interlocks of the sheet-pile sections are shaped like a ***thumb-and-finger*** or ***ball-and-socket*** joint for watertight connections. Figure 4.3a is a schematic diagram of the thumb-and-finger type of interlocking for straight web sections. The ball-and-socket type of interlocking for *Z* section piles is shown in Figure 4.3b. Figure 4.4 shows some sheet piles at a construction site. Figure 4.5 shows a small enclosure with steel sheet piles for an excavation work. Table 4.1 lists the properties of the steel sheet-pile sections produced by Hammer & Steel, Inc. of Hazelwood, Missouri. The allowable design flexural stress for the steel sheet piles is as follows:

Type of steel	Allowable stress	
ASTM A-328	170 MN/m^2	(25,000 lb/in^2)
ASTM A-572	210 MN/m^2	(30,000 lb/in^2)
ASTM A-690	210 MN/m^2	(30,000 lb/in^2)

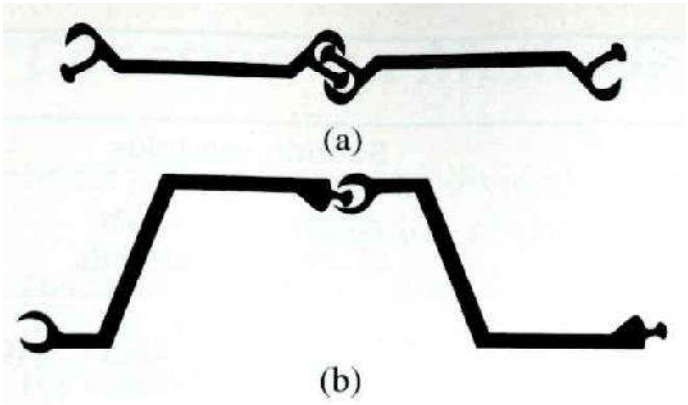

Figure 4.3 (a) Thumb-and-finger type sheet-pile connection; (b) ball-and-socket type sheet-pile connection

\

Figure 4.4 Some steel sheet piles at a construction site (*Courtesy of N. Sivakugan, James Cook University, Australia*)

Figure 4.5 A small enclosure with steel sheet piles for an excavation work (*Courtesy of N. Sivakugan, James Cook University, Australia*)

Table 4.1 Properties of Some Sheet-Pile Sections Production by Bethlehem Steel Corporation

Section designation	Sketch of section	Section modulus		Moment of inertia	
		m^3/m of wall	in^3/ft of wall	m^4/m of wall	in^4/ft of wall
PZ-40	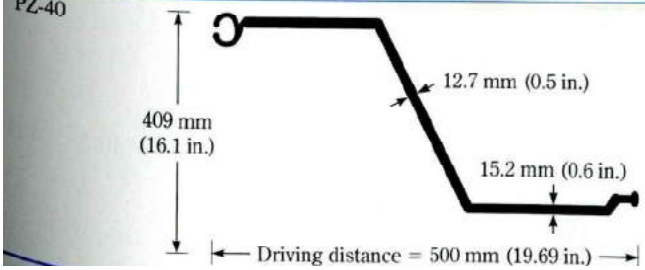	326.4×10^{-5}	60.7	670.5×10^{-6}	490.8
PZ-35	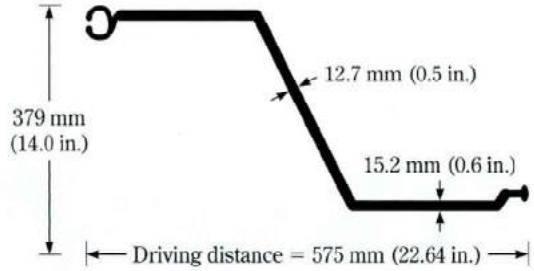	260.5×10^{-5}	48.5	493.4×10^{-6}	361.2
PZ-27	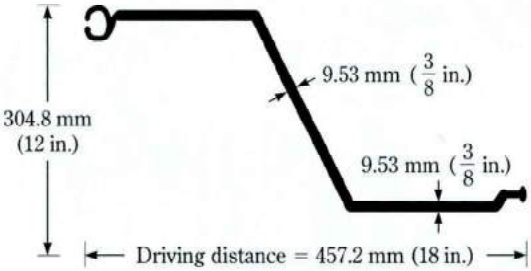	162.3×10^{-5}	30.2	251.5×10^{-6}	184.2
PZ-22	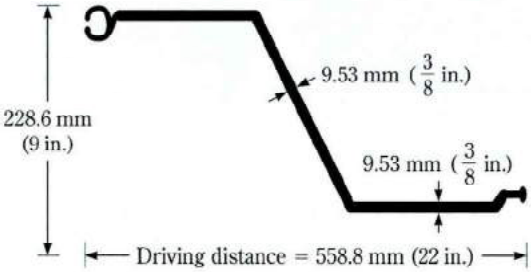	97×10^{-5}	18.1	115.2×10^{-6}	84.4
PSA-31	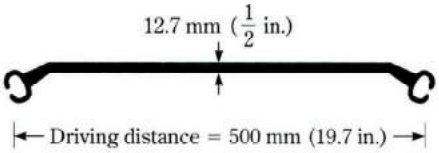	10.8×10^{-5}	2.01	4.41×10^{-6}	3.23
PSA-23	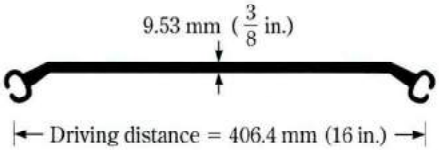	12.8×10^{-5}	2.4	5.63×10^{-6}	4.13

4.2 Construction Methods

Sheet-pile walls may be divided into two basic categories:
(a) cantilever and
(b) anchored.

In the construction of sheet-pile walls, the sheet pile may be driven into the ground and then the backfill placed on the land side, or the sheet pile may first be driven into the ground and the soil in front of the sheet pile dredged. In either case, the soil used for backfill behind the sheet-pile wall is usually granular. The soil below the dredge line may be sandy or clayey. The surface of soil on the water side is referred to as the *mud line* or *dredge line.*
Thus, construction methods generally can be divided into two categories (Tsinker, 1983):

1. Backfilled structure
2. Dredged structure

The sequence of construction for a *backfilled structure* is as follows (see Figure 4.6):

Step 1. Dredge the *in situ* soil in front and back of the proposed structure.
Step 2. Drive the sheet piles.
Step 3. Backfill up to the level of the anchor, and place the anchor system.
Step 4. Backfill up to the top of the wall.

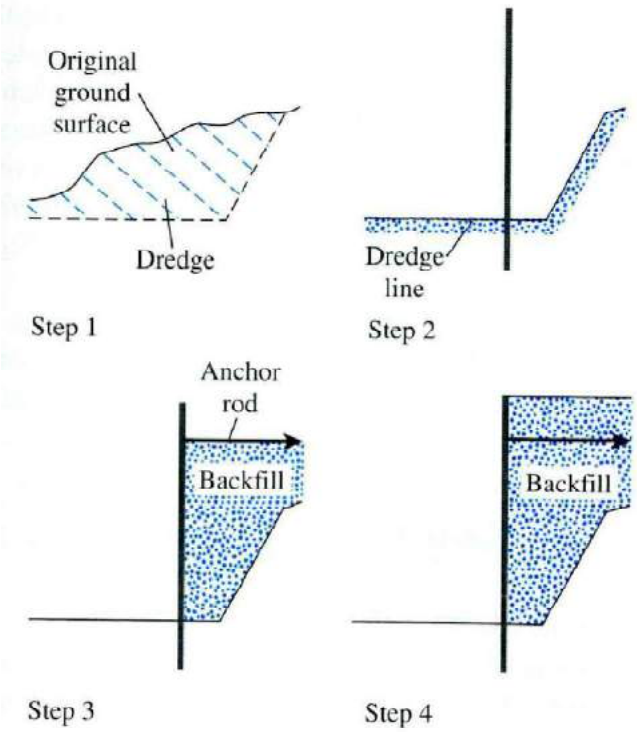

Figure 4.6 Sequence of construction for a backfilled structure

For a cantilever type of wall, only Steps 1, 2, and 4 apply. The sequence of construction for a *dredged structure* is as follows (see Figure 4.7):

Step 1. Drive the sheet piles.

Step 2. Backfill up to the anchor level, and place the anchor system.

Step 3. Backfill up to the top of the wall.

Step 4. Dredge the front side of the wall.

With cantilever sheet-pile walls, Step 2 is not required.

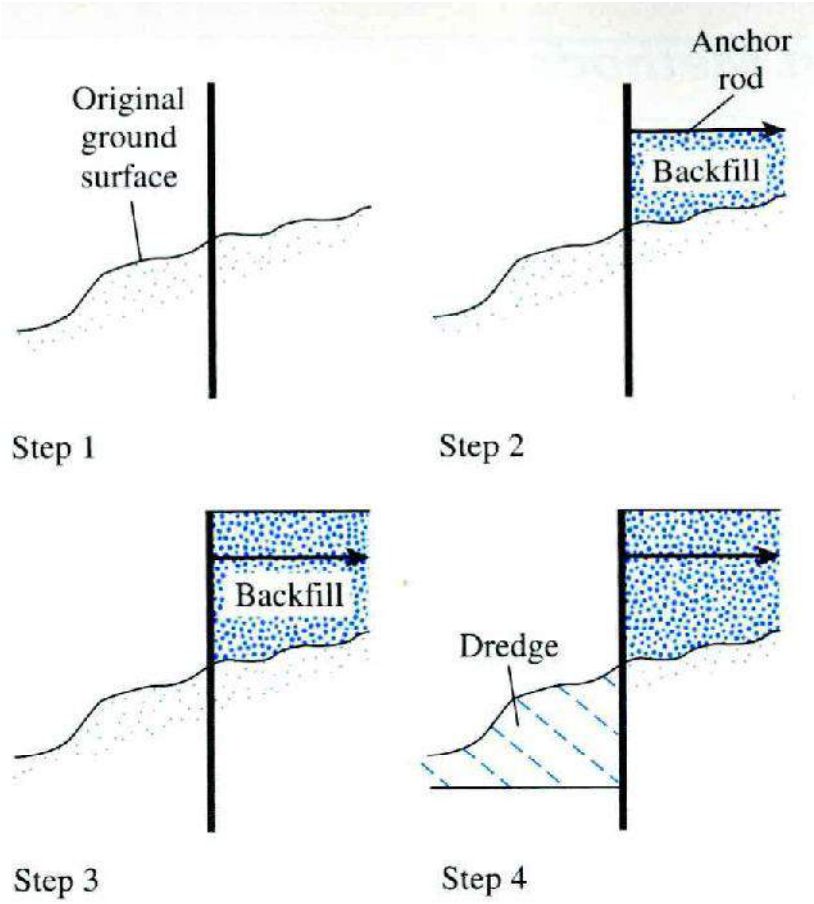

Figure 4.7 Sequence of construction for a dredged structure

4.3 Cantilever Sheet-Pile Walls

Cantilever sheet-pile walls are usually recommended for walls of moderate height—about 6 m or less, measured above the dredge line. In such walls, the sheet piles act as a wide cantilever beam above the dredge line. The basic principles for estimating net lateral pressure distribution on a cantilever sheet-pile wall can be explained with the aid of Figure 4.8. The figure shows the nature of lateral yielding of a cantilever wall penetrating sand layer below the dredge line. The wall rotates about point *O* (Figure 4.8a). Because the hydrostatic pressures at any depth from both sides of the wall will cancel each other, we consider only the effective lateral soil pressures. In zone *A,* the lateral pressure is just the active pressure from the land side. In zone *B,* because of the nature of yielding of the wall, there will be active pressure from the land side and passive pressure from the water side. The condition is reversed in zone *C*—that is, below the point of rotation, *O.* The net actual pressure distribution on the wall is like that shown in Figure 4.8b. However, for design purposes, Figure 4.8c shows a simplified version.

Sections 4.4 through 4.7 present the mathematical formulation of the analysis of cantilever sheet-pile walls. Note that, in some waterfront structures, the water level may fluctuate as the result of tidal effects. Care should be taken in determining the water level that will affect the net pressure diagram.

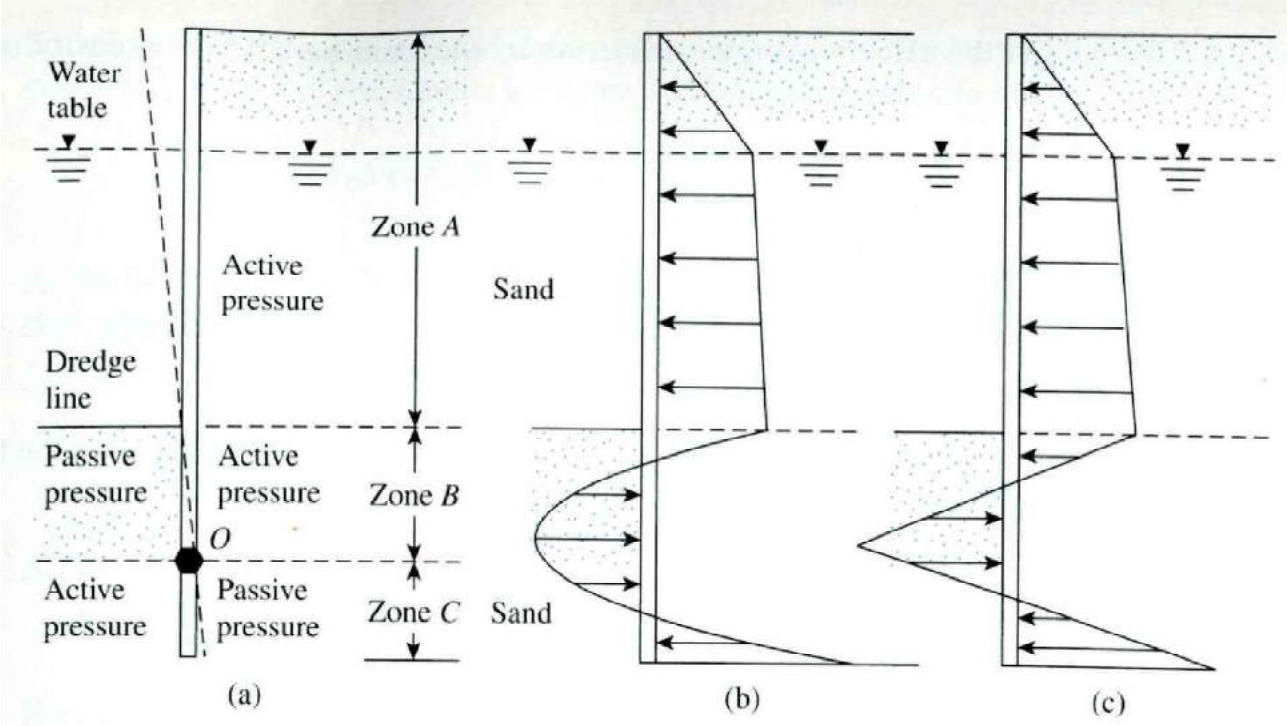

Figure 4.8 Cantilever sheet pile penetrating sand

4.4 Cantilever Sheet Piling Penetrating Sandy Soils

To develop the relationships for the proper depth of embedment of sheet piles driven into a granular soil, examine Figure 4.9a. The soil retained by the sheet piling above the dredge line also is sand. The water table is at a depth L_1 below the top of the wall. Let the effective angle of friction of the sand be ϕ'. The intensity of the active pressure at a depth z = L_1 is

$$\sigma_1' = \gamma L_1 K_a \qquad (4.1)$$

where

K_a = Rankine active pressure coefficient = $tan^2(45 - \frac{\phi'}{2})$

γ = unit weight of soil above the water table

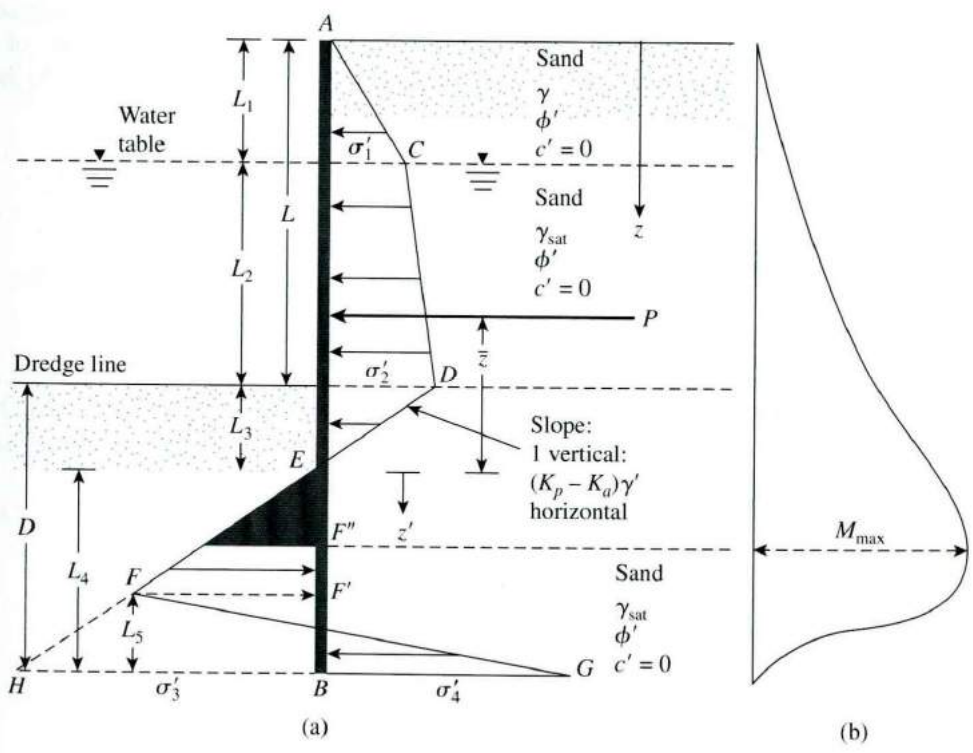

Figure 4.9 Cantilever sheet pile penetrating sand: (a) variation of net pressure diagram; (b) variation of moment

Similarly, the active pressure at a depth z = $L_1 + L_2$ (i.e., at the level of the dredge line) is

$$\sigma_2' = (\gamma L_1 + \gamma' L_2) K_a \qquad (4.2)$$

where γ' = effective unit weight of soil = $\gamma_{sat} - \gamma_w$.

Note that, at the level of the dredge line, the hydrostatic pressures from both sides of

the wall are the same magnitude and cancel each other.

To determine the net lateral pressure below the dredge line up to the point of rotation, *O,* as shown in Figure 4.8a, an engineer has to consider the passive pressure acting from the left side (the water side) toward the right side (the land side) of the wall and also the active pressure acting from the right side toward the left side of the wall. For such cases, ignoring the hydrostatic pressure from both sides of the wall, the active pressure at depth z is

$$\sigma'_a = [\gamma L_1 + \gamma' L_2 + \gamma'(z - L_1 - L_2)]K_a \qquad (4.3)$$

Also, the passive pressure at depth z is

$$\sigma'_p = \gamma'(z - L_1 - L_2)K_p \qquad (4.4)$$

where K_p = Rankine passive pressure coefficient = $tan^2(45 + \frac{\phi'}{2})$

Combining Eqs. (4.3) and (4.4) yields the net lateral pressure, namely,

$$\sigma' = \sigma'_a - \sigma'_p = (\gamma L_1 + \gamma' L_2)K_a - \gamma'(z - L_1 - L_2)(K_p - K_a) \qquad (4.5)$$

$$= \sigma'_2 - \gamma'(z - L)(K_p - K_a)$$

where $L = L_1 + L_2$. The net pressure, σ' equals zero at a depth L_3 below the dredge line, so

$$\sigma'_2 - \gamma'(z - L)(K_p - K_a) = 0$$

or

$$(z - L) = L_3 = \frac{\sigma'_2}{\gamma'(K_p - K_a)} \qquad (4.6)$$

Equation (4.6) indicates that the slope of the net pressure distribution line *DEF* is 1 vertical to $(K_p - K_a)\,\gamma'$ horizontal, so, in the pressure diagram,

$$\overline{HB} = \sigma'_3 = L_4(K_p - K_a)\gamma' \qquad (4.7)$$

At the bottom of the sheet pile, passive pressure, σ'_p, acts from the right toward the left side, and active pressure acts from the left toward the right side of the sheet pile, so, at z = $L + D$,

$$\sigma'_p = (\gamma L_1 + \gamma' L_2 + \gamma' D)K_p \qquad (4.8)$$

At the same depth,

$$\sigma'_a = \gamma' D K_a \qquad (4.9)$$

Hence, the net lateral pressure at the bottom of the sheet pile is

$$\begin{aligned}\sigma'_p - \sigma'_a = \sigma'_4 &= (\gamma L_1 + \gamma' L_2) K_p + \gamma' D (K_p - K_a) \\ &= (\gamma L_1 + \gamma' L_2) K_p + \gamma' L_3 (K_p - K_a) + \gamma' L_4 (K_p - K_a) \\ &= \sigma'_5 + \gamma' L_4 (K_p - K_a)\end{aligned} \qquad (4.10)$$

Where

$$\sigma'_5 = (\gamma L_1 + \gamma' L_2) K_p + \gamma' L_3 (K_p - K_a) \qquad (4.11)$$

$$D = L_3 + L_4 \qquad (4.12)$$

For the stability of the wall, the principles of statics can now be applied:

$\sum$ horizontal forces per unit length of wall = 0

and

$\sum$ moment of the forces per unit length of wall about point B = 0

For the summation of the horizontal forces, we have

Area of the pressure diagram $ACDE$ - area of $EFHB$ + area of $FHBG$ = 0

Or

$$P - \tfrac{1}{2}\sigma'_3 L_4 + \tfrac{1}{2} L_5 (\sigma'_3 + \sigma'_4) = 0 \qquad (4.13)$$

where P = area of the pressure diagram $ACDE$.

Summing the moment of all the forces about point B yields

$$P(L_4 + \bar{z}) - \left(\frac{1}{2} L_4 \sigma'_3\right)\left(\frac{L_4}{3}\right) + \frac{1}{2} L_5 (\sigma'_3 + \sigma'_4)\left(\frac{L_5}{3}\right) = 0 \qquad (4.14)$$

From Eq.(4.13)

$$L_5 = \frac{\sigma'_3 L_4 - 2P}{\sigma'_3 + \sigma'_4} \qquad (4.15)$$

Combining Eqs. (4.7), (4.10), (4.14), and (4.15) and simplifying them further, we obtain the following fourth-degree equation in terms of L_4 :

$$L_4^4 + A_1 L_4^3 - A_2 L_4^2 - A_3 L_4 - A_4 = 0 \quad (4.16)$$

In this equation

$$A_1 = \frac{\sigma_5'}{\gamma'(K_p - K_a)} \quad (4.17)$$

$$A_2 = \frac{8P}{\gamma'(K_p - K_a)} \quad (4.18)$$

$$A_3 = \frac{6P[2\bar{z}\gamma'(K_p - K_a) + \sigma_5']}{\gamma'^2(K_p - K_a)^2} \quad (4.19)$$

$$A_4 = \frac{P(6\bar{z}\sigma_5' + 4P)}{\gamma'^2(K_p - K_a)^2} \quad (4.20)$$

Step-by-Step Procedure for Obtaining the Pressure Diagram

Based on the preceding theory, a step-by-step procedure for obtaining the pressure diagram for a cantilever sheet-pile wall penetrating a granular soil is as follows:

Step 1. Calculate K_a and K_p .
Step 2. Calculate σ_1' [Eq. (4.1)] and σ_2' [Eq. (4.2)]. (*Note:* L_1 and L_2 will be given.)
Step 3. Calculate L_3 [Eq. (4.6)].
Step 4. Calculate P.
Step 5. Calculate z (i.e., the center of pressure for the area $ACDE$) by taking the moment about E.
Step 6. Calculate σ_5' [Eq. (4.11)].
Step 7. Calculate A_1 , A_2 , A_3 , and A_4 [Eqs. (4.17) through (4.20)].
Step 8. Solve Eq. (4.16) by trial and error to determine L_4 .
Step 9. Calculate σ_4' [Eq. (4.10)].
Step 10. Calculate σ_3' [Eq. (4.7)].
Step 11. Obtain L_5 from Eq. (4.15).
Step 12. Draw a pressure distribution diagram like the one shown in Figure 4.9a.

Step 13. Obtain the theoretical depth [see Eq. (4.12)] of penetration as $L_3 + L_4$.The actual depth of penetration is increased by about 20 to 30%.

Note that some designers prefer to use a factor of safety on the passive earth pressure coefficient at the beginning. In that case, in Step 1,

$$K_{p(\text{design})} = \frac{K_p}{\text{FS}}$$

where FS = factor of safety (usually between 1.5 and 2).

For this type of analysis, follow Steps 1 through 12 with the value of $K_a = tan^2(45 - \frac{\phi'}{2})$ and $K_{p(\text{design})}$ (instead of K_p). The actual depth of penetration can now be determined by adding L_3 , obtained from Step 3, and L_4 , obtained from Step 8.

Calculation of Maximum Bending Moment

The nature of the variation of the moment diagram for a cantilever sheet-pile wall is shown in Figure 4.9b. The maximum moment will occur between points E and F'. Obtaining the maximum moment $(M_{\max})$ per unit length of the wall requires determining the point of zero shear. For a new axis z' (with origin at point E) for zero shear,

$$P = \tfrac{1}{2}(z')^2(K_p - K_a)\gamma'$$

Or

$$z' = \sqrt{\frac{2P}{(K_p - K_a)\gamma'}} \qquad (4.21)$$

Once the point of zero shear force is determined (point F'' in Figure 4.9a), the magnitude of the maximum moment can be obtained as

$$M_{\max} = P(\bar{z} + z') - [\tfrac{1}{2}\gamma' z'^2(K_p - K_a)](\tfrac{1}{3})z' \qquad (4.22)$$

The necessary profile of the sheet piling is then sized according to the allowable flexural stress of the sheet pile material, or

$$S = \frac{M_{\max}}{\sigma_{\text{all}}} \qquad (4.23)$$

where
S = section modulus of the sheet pile required per unit length of the structure
σ_{all} = allowable flexural stress of the sheet pile

Example 4.1

Figure 4.10 shows a cantilever sheet-pile wall penetrating a granular soil. Here, L_1= 2 m, L_2= 3 m, γ = 15.9 kN/m^3, γ_{sat} = 19.33 kN/m^3, and ϕ'= 32°.

a. What is the theoretical depth of embedment, D?
b. For a 30% increase in D, what should be the total length of the sheet piles?
c. What should be the minimum section modulus of the sheet piles? Use σ_{all}=172 MN/m^2.

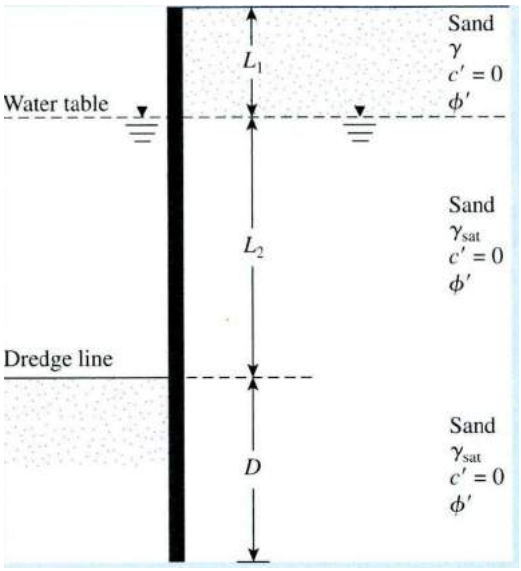

Figure 4.10 Cantilever sheet-pile wall

Part a

Using Figure 4.9a for the pressure distribution diagram, one can now prepare the following table for a step-by-step calculation.

Quantity required	Eq. no.	Equation and calculation
K_a	—	$\tan^2\left(45 - \frac{\phi'}{2}\right) = \tan^2\left(45 - \frac{32}{2}\right) = 0.307$
K_p	—	$\tan^2\left(45 + \frac{\phi'}{2}\right) = \tan^2\left(45 + \frac{32}{2}\right) = 3.25$
σ_1'	9.1	$\gamma L_1 K_a = (15.9)(2)(0.307) = 9.763\ \text{kN/m}^2$
σ_2'	9.2	$(\gamma L_1 + \gamma' L_2)K_a = [(15.9)(2) + (19.33 - 9.81)(3)](0.307) = 18.53\ \text{kN/m}^2$
L_3	9.6	$\frac{\sigma_2'}{\gamma'(K_p - K_a)} = \frac{18.53}{(19.33 - 9.81)(3.25 - 0.307)} = 0.66\ \text{m}$
P	—	$\frac{1}{2}\sigma_1' L_1 + \sigma_1' L_2 + \frac{1}{2}(\sigma_2' - \sigma_1')L_2 + \frac{1}{2}\sigma_2' L_3$ $= (\frac{1}{2})(9.763)(2) + (9.763)(3) + (\frac{1}{2})(18.53 - 9.763)(3)$ $+ (\frac{1}{2})(18.53)(0.66)$ $= 9.763 + 29.289 + 13.151 + 6.115 = 58.32\ \text{kN/m}$
$\bar{z}$	—	$\frac{\Sigma M_E}{P} = \frac{1}{58.32}\left[\begin{array}{l} 9.763(0.66 + 3 + \frac{2}{3}) + 29.289(0.66 + \frac{3}{2}) \\ + 13.151(0.66 + \frac{3}{3}) + 6.115(0.66 \times \frac{2}{3}) \end{array}\right] = 2.23\ \text{m}$
σ_5'	9.11	$(\gamma L_1 + \gamma' L_2)K_p + \gamma' L_3(K_p - K_a) = [(15.9)(2) + (19.33 - 9.81)(3)](3.25)$ $+ (19.33 - 9.81)(0.66)(3.25$ $- 0.307) = 214.66\ \text{kN/m}^2$
A_1	9.17	$\frac{\sigma_5'}{\gamma'(K_p - K_a)} = \frac{214.66}{(19.33 - 9.81)(3.25 - 0.307)} = 7.66$
A_2	9.18	$\frac{8P}{\gamma'(K_p - K_a)} = \frac{(8)(58.32)}{(19.33 - 9.81)(3.25 - 0.307)} = 16.65$

A_3	9.19	$\dfrac{6P[2\bar{z}\gamma'(K_p - K_a) + \sigma'_5]}{\gamma'^2(K_p - K_a)^2}$ $= \dfrac{(6)(58.32)[(2)(2.23)(19.33 - 9.81)(3.25 - 0.307) + 214.66]}{(19.33 - 9.81)^2(3.25 - 0.307)^2}$ $= 151.93$
A_4	9.20	$\dfrac{P(6\bar{z}\sigma'_5 + 4P)}{\gamma'^2(K_p - K_a)^2} = \dfrac{58.32[(6)(2.23)(214.66) + (4)(58.32)]}{(19.33 - 9.81)^2(3.25 - 0.307)^2}$ $= 230.72$
L_4	9.16	$L_4^4 + A_1L_4^3 - A_2L_4^2 - A_3L_4 - A_4 = 0$ $L_4^4 + 7.66L_4^3 - 16.65L_4^2 - 151.93L_4 - 230.72 = 0;\ L_4 \approx 4.8$ m

Thus,

$$D_{\text{theory}} = L_3 + L_4 = 0.66 + 4.8 = \mathbf{5.46\ m}$$

Part b

The total length of the sheet piles is

$$L_1 + L_2 + 1.3(L_3 + L_4) = 2 + 3 + 1.3(5.46) = \mathbf{12.1\ m}$$

Part c

Finally, we have the following table.

Quantity required	Eq. no.	Equation and calculation
z'	9.21	$\sqrt{\dfrac{2P}{(K_p - K_a)\gamma'}} = \sqrt{\dfrac{(2)(58.32)}{(3.25 - 0.307)(19.33 - 9.81)}} = 2.04$ m
$M_{\max}$	9.22	$P(\bar{z} + z') - \left[\dfrac{1}{2}\gamma' z'^2(K_p - K_a)\right]\dfrac{z'}{3} = (58.32)(2.23 + 2.04)$ $-\left[\left(\dfrac{1}{2}\right)(19.33 - 9.81)(2.04)^2(3.25 - 0.307)\right]\dfrac{2.04}{3}$ $= 209.39\ \text{kN}\cdot\text{m/m}$
S	9.29	$\dfrac{M_{\max}}{\sigma_{\text{all}}} = \dfrac{209.39\ \text{kN}\cdot\text{m}}{172 \times 10^3\ \text{kN/m}^2} = \mathbf{1.217 \times 10^{-3}\ m^3/m\ of\ wall}$ ■

4.5 Cantilever Sheet Piling Penetrating Clay

At times, cantilever sheet piles must be driven into a clay layer possessing an undrained cohesion (ϕ=0). The net pressure diagram will be somewhat different from that shown in Figure 4.9a. Figure 4.13 shows a cantilever sheet-pile wall driven into clay with a backfill of granular soil above the level of the dredge line. The water table is at a depth L_1 below the top of the wall. As before, Eqs. (4.1) and (4.2) give the intensity of the net pressures σ_1' and σ_2' , and the diagram for pressure distribution above the level of the dredge line can be drawn. The diagram for net pressure distribution below the dredge line can now be determined as follows.

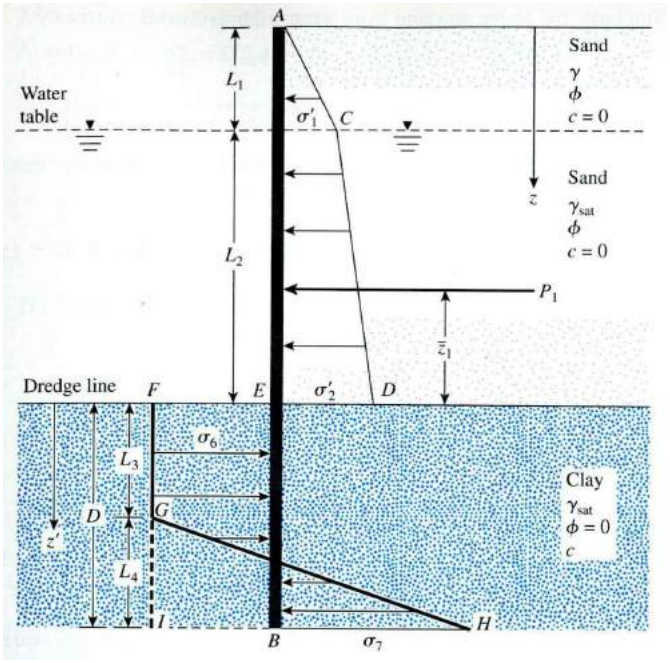

Figure 4.13 Cantilever sheet pile penetrating clay

At any depth greater than $L_1 + L_2$, for ϕ=0, the Rankine active earth-pressure coefficient K_a= 1. Similarly, for ϕ=0, the Rankine passive earth-pressure coefficient K_p=1. Thus, above the point of rotation (point *O* in Figure 4.8a), the active pressure, from right to left is

$$\sigma_a = [\gamma L_1 + \gamma' L_2 + \gamma_{sat}(z - L_1 - L_2)] - 2c \qquad (4.24)$$

Similarly, the passive pressure from left to right may be expressed as

$$\sigma_p = \gamma_{sat}(z - L_1 - L_2) + 2c \qquad (4.25)$$

Thus, the net pressure is

$$\begin{aligned}\sigma_6 = \sigma_p - \sigma_a &= [\gamma_{sat}(z - L_1 - L_2) + 2c] \\ &\quad - [\gamma L_1 + \gamma' L_2 + \gamma_{sat}(z - L_1 - L_2)] + 2c \\ &= 4c - (\gamma L_1 + \gamma' L_2) \qquad (4.26)\end{aligned}$$

At the bottom of the sheet pile, the passive pressure from right to left is

$$\sigma_p = (\gamma L_1 + \gamma' L_2 + \gamma_{sat} D) + 2c \qquad (4.27)$$

Similarly, the active pressure from left to right is

$$\sigma_a = \gamma_{sat} D - 2c \qquad (4.28)$$

Hence, the net pressure is

$$\sigma_7 = \sigma_p - \sigma_a = 4c + (\gamma L_1 + \gamma' L_2) \qquad (4.29)$$

For equilibrium analysis, $\sum F_H = 0$; that is, the area of the pressure diagram *ACDE* minus the area of *EFIB* plus the area of *GIH* = 0, or

$$P_1 - [4c - (\gamma L_1 + \gamma' L_2)]D + \tfrac{1}{2} L_4[4c - (\gamma L_1 + \gamma' L_2) + 4c + (\gamma L_1 + \gamma' L_2)] = 0$$

where P_1 = area of the pressure diagram *ACDE*.

Simplifying the preceding equation produces

$$L_4 = \frac{D[4c - (\gamma L_1 + \gamma' L_2)] - P_1}{4c} \qquad (4.30)$$

Now, taking the moment about point *B* ($\sum M_B = 0$) yields

$$P_1(D + \bar{z}_1) - [4c - (\gamma L_1 + \gamma' L_2)]\frac{D^2}{2} + \frac{1}{2} L_4 (8c)\left(\frac{L_4}{3}\right) = 0 \qquad (4.31)$$

where $\bar{z}_1$ = distance of the center of pressure of the pressure diagram *ACDE*, measured from the level of the dredge line.

Combining Eqs. (4.30) and (4.31) yields

$$D^2[4c - (\gamma L_1 + \gamma' L_2)] - 2DP_1 - \frac{P_1(P_1 + 12c\bar{z}_1)}{(\gamma L_1 + \gamma' L_2) + 2c} = 0 \qquad (4.32)$$

Equation (4.32) may be solved to obtain *D,* the theoretical depth of penetration of the clay layer by the sheet pile.

Step-by-Step Procedure for Obtaining the Pressure Diagram

Step 1. Calculate K_a for the granular soil (backfill).
Step 2. Obtain σ'_1 and σ'_2 . [See Eqs. (4.1) and (4.2).]
Step 3. Calculate P_1 and z_1 .
Step 4. Use Eq. (4.32) to obtain the theoretical value of D.
Step 5. Using Eq. (4.30), calculate L_4.
Step 6. Calculate σ_6 and σ_7 . [See Eqs. (4.26) and (4.29).]

Step 7. Draw the pressure distribution diagram as shown in Figure 4.13.
Step 8. The actual depth of penetration is

$$D_{\text{actual}} = 1.4 \text{ to } 1.6(D_{\text{theoretical}})$$

Maximum Bending Moment

According to Figure 4.13, the maximum moment (zero shear) will be between $L_1 + L_2 < z < L_1 + L_2 + L_3$. Using a new coordinate system $z9$ (with $z' = 0$ at the dredge line) for zero shear gives

$$P_1 - \sigma_6 z' = 0$$

or

$$z' = \frac{P_1}{\sigma_6} \qquad (4.33)$$

The magnitude of the maximum moment may now be obtained:

$$M_{\max} = P_1(z' + \bar{z}_1) - \frac{\sigma_6 z'^2}{2} \qquad (4.34)$$

Knowing the maximum bending moment, we determine the section modulus of the sheet-pile section from Eq. (4.23).

Example 4.2:

In Figure 4.14, for the sheet-pile wall, determine
a. The theoretical and actual depth of penetration. Use $D_{\text{actual}} = 1.5D_{\text{theory}}$.
b. The minimum size of sheet-pile section necessary. Use $\sigma_{\text{all}} = 172.5$ MN/m^2.

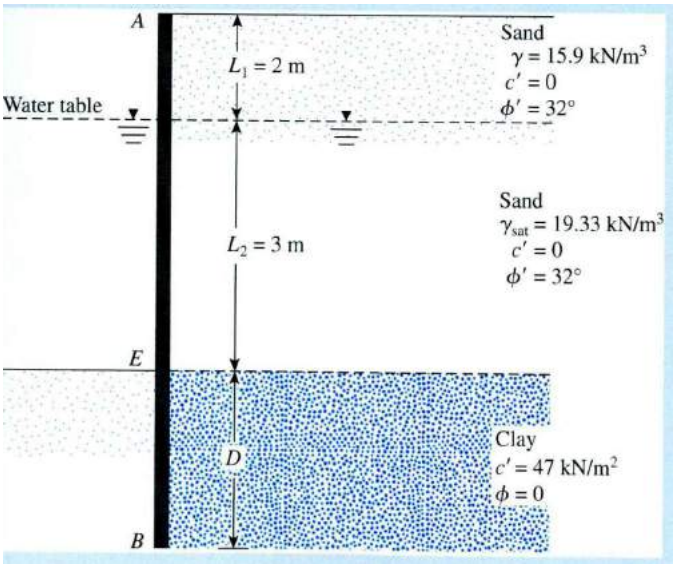

Figure 4.14 Cantilever sheet pile penetrating into saturated clay

Solution

We will follow the step-by-step procedure given in Section 9.6:

Step 1.

$$K_a = \tan^2\left(45 - \frac{\phi'}{2}\right) = \tan^2\left(45 - \frac{32}{2}\right) = 0.307$$

Step 2.

$$\sigma_1' = \gamma L_1 K_a = (15.9)(2)(0.307) = 9.763 \text{ kN/m}^2$$

$$\sigma_2' = (\gamma L_1 + \gamma' L_2) K_a = [(15.9)(2) + (19.33 - 9.81)3]0.307$$

$$= 18.53 \text{ kN/m}^2$$

Step 3. From the net pressure distribution diagram given in Figure 9.12, we have

$$P_1 = \frac{1}{2}\sigma_1' L_1 + \sigma_1' L_2 + \frac{1}{2}(\sigma_2' - \sigma_1') L_2$$

$$= 9.763 + 29.289 + 13.151 = 52.2 \text{ kN/m}$$

and

$$\bar{z}_1 = \frac{1}{52.2}\left[9.763\left(3 + \frac{2}{3}\right) + 29.289\left(\frac{3}{2}\right) + 13.151\left(\frac{3}{3}\right)\right]$$

$$= 1.78 \text{ m}$$

Step 4. From Eq. (9.48),

$$D^2[4c - (\gamma L_1 + \gamma' L_2)] - 2DP_1 - \frac{P_1(P_1 + 12c\bar{z}_1)}{(\gamma L_1 + \gamma' L_2) + 2c} = 0$$

Substituting proper values yields

$$D^2\{(4)(47) - [(2)(15.9) + (19.33 - 9.81)3]\} - 2D(52.2)$$

$$- \frac{52.2[52.2 + (12)(47)(1.78)]}{[(15.9)(2) + (19.33 - 9.81)3] + (2)(47)} = 0$$

or

$$127.64D^2 - 104.4D - 357.15 = 0$$

Solving the preceding equation, we obtain $D = 2.13$ m.

Step 5. From Eq. (9.46),

$$L_4 = \frac{D[4c - (\gamma L_1 + \gamma' L_2)] - P_1}{4c}$$

and

$$4c - (\gamma L_1 + \gamma' L_2) = (4)(47) - [(15.9)(2) + (19.33 - 9.81)3]$$

So,

$$L_4 = \frac{2.13(127.64) - 52.2}{(4)(47)} = 1.17 \text{ m}$$

Step 6.

$$\sigma_6 = 4c - (\gamma L_1 + \gamma' L_2) = 127.64 \text{ kN/m}^2$$

$$\sigma_7 = 4c + (\gamma L_1 + \gamma' L_2) = 248.36 \text{ kN/m}^2$$

Step 7. The net pressure distribution diagram can now be drawn, as shown in Figure 9.12.

Step 8. $D_{\text{actual}} \approx 1.5 D_{\text{theoretical}} = 1.5(2.13) \approx \mathbf{3.2\ m}$

Maximum-Moment Calculation

From Eq. (9.49),

$$z' = \frac{P_1}{\sigma_6} = \frac{52.2}{127.64} \approx 0.41 \text{ m}$$

Again, from Eq. (9.49),

$$M_{\max} = P_1(z' + \bar{z}_1) - \frac{\sigma_6 z'^2}{2}$$

So

$$M_{\max} = 52.2(0.41 + 1.78) - \frac{127.64(0.41)^2}{2}$$

$$= 114.32 - 10.73 = 103.59 \text{ kN-m/m}$$

The minimum required section modulus (assuming that $\sigma_{\text{all}} = 172.5 \text{ MN/m}^2$) is

$$S = \frac{103.59 \text{ kN-m/m}}{172.5 \times 10^3 \text{ kN/m}^2} = \mathbf{0.6 \times 10^{-3}\ m^3/m\ of\ the\ wall}$$

■

4.6 Anchored Sheet-Pile Walls

When the height of the backfill material behind a cantilever sheet-pile wall exceeds about 6 m, tying the wall near the top to anchor plates, anchor walls, or anchor piles becomes more economical. This type of construction is referred to as ***anchored sheet-pile wall*** **or an** ***anchored bulkhead***. Anchors minimize the depth of penetration required by the sheet piles and also reduce the cross-sectional area and weight of the sheet piles needed for construction. However, the tie rods and anchors must be carefully designed.

The two basic methods of designing anchored sheet-pile walls are

(a) the *free earth support* method and

(b) the *fixed earth support* method.

Figure 4.17 shows the assumed nature of deflection of the sheet piles for the two methods.

The free earth support method involves a minimum penetration depth. Below the dredge line, no pivot point exists for the static system. The nature of the variation of the bending moment with depth for both methods is also shown in Figure 4.17. Note that

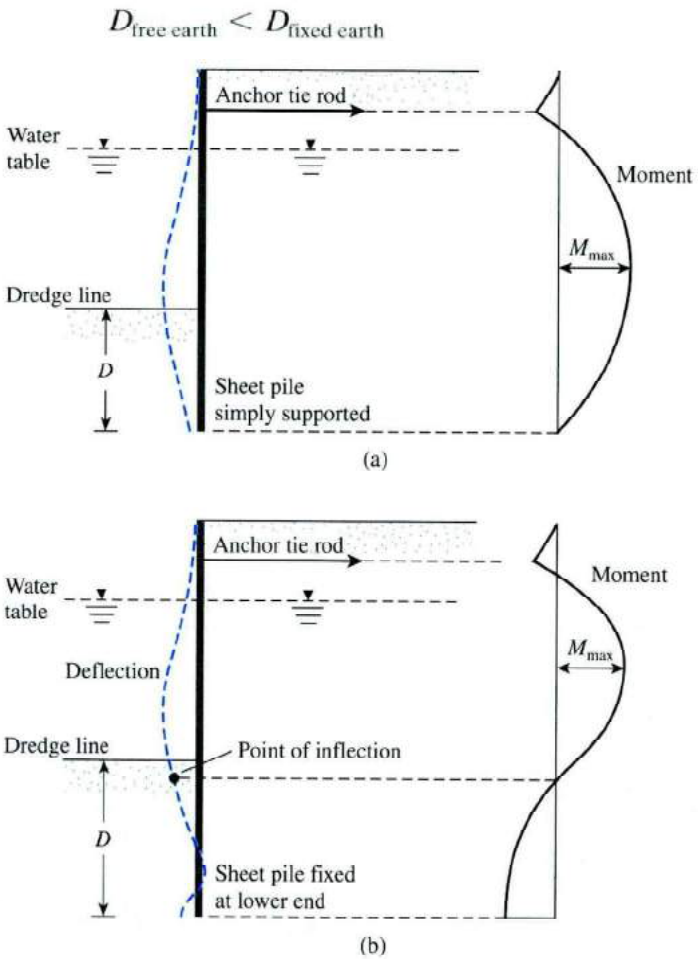

Figure 4.17 Nature of variation of deflection and moment for anchored sheet piles: (a) free earth support method (b) fixed earth support method

4.7 Free Earth Support Method for Penetration of Sandy Soil

Figure 4.18 shows an anchor sheet-pile wall with a granular soil backfill; the wall has been driven into a granular soil. The tie rod connecting the sheet pile and the anchor is located at a depth *l*1 below the top of the sheet-pile wall.

The diagram of the net pressure distribution above the dredge line is similar to that shown in Figure 4.9. At depth $z = L_1$, $\sigma'_1 = \gamma L_1 K_a$, and at $z = L_1 + L_2$, $\sigma'_2 = (\gamma L_1 + \gamma' L_2) K_a$. Below the dredge line, the net pressure will be zero at $z + L_1 + L_2 + L_3$. The relation for L_3 is given by Eq. (4.6), or

$$L_3 = \frac{\sigma'_2}{\gamma'(K_p - K_a)}$$

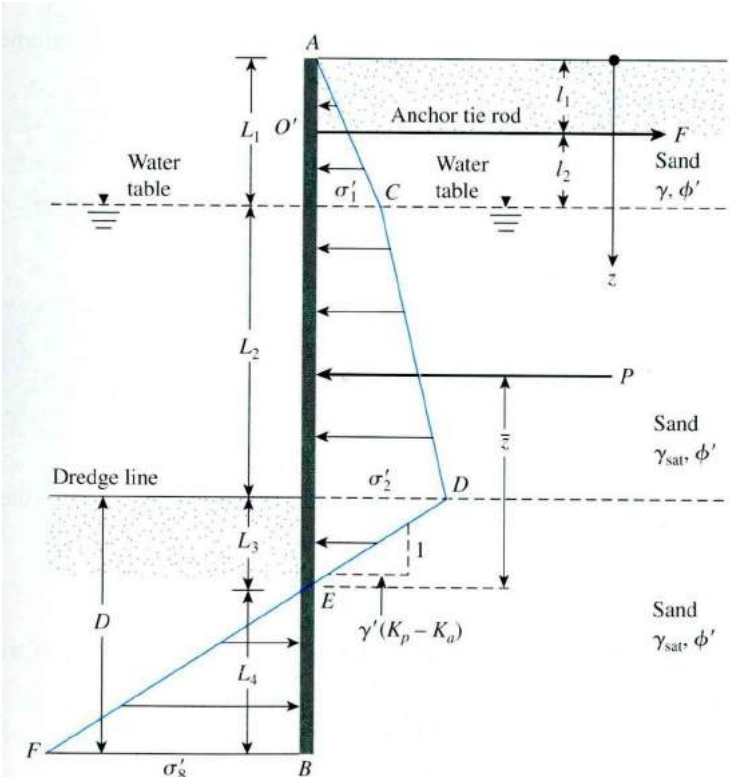

Figure 4.18 Anchored sheet-pile wall penetrating sand

At $z = L_1 + L_2 + L_3 + L_4$, the net pressure is given by

$$\sigma'_8 = \gamma'(K_p - K_a) L_4 \qquad (4.35)$$

Note that the slope of the line *DEF* is 1 vertical to $\gamma'(K_p - K_a)$ horizontal. For equilibrium of the sheet pile, $\sum$ horizontal forces = 0, and $\sum$ moment about $O' = 0$. (*Note:* Point O' is located at the level of the tie rod.)

Summing the forces in the horizontal direction (per unit length of the wall) gives

Area of the pressure diagram *ACDE* - area of *EBF* - *F* = 0

where F=5 tension in the tie rod/unit length of the wall, or

$$P - \tfrac{1}{2}\sigma'_8 L_4 - F = 0$$

or

$$F = P - \tfrac{1}{2}[\gamma'(K_p - K_a)]L_4^2 \qquad (4.36)$$

where P = area of the pressure diagram $ACDE$.

Now, taking the moment about point O' gives

$$-P[(L_1 + L_2 + L_3) - (\bar{z} + l_1)] + \tfrac{1}{2}[\gamma'(K_p - K_a)]L_4^2(l_2 + L_2 + L_3 + \tfrac{2}{3}L_4) = 0$$

Or

$$L_4^3 + 1.5L_4^2(l_2 + L_2 + L_3) - \frac{3P[(L_1 + L_2 + L_3) - (\bar{z} + l_1)]}{\gamma'(K_p - K_a)} = 0 \qquad (4.37)$$

Equation (4.37) may be solved by trial and error to determine the theoretical depth, L_4:

$$D_{\text{theoretical}} = L_3 + L_4$$

The theoretical depth is increased by about 30 to 40% for actual construction, or

$$D_{\text{actual}} = 1.3 \text{ to } 1.4\ D_{\text{theoretical}} \qquad (4.38)$$

The step-by-step procedure in Section 4.4 indicated that a factor of safety can be applied to K_p at the beginning [i.e., $K_{p(\text{designd})} = K_p/\text{FS}$]. If that is done, there is no need to increase the theoretical depth by 30 to 40%. This approach is often more conservative.

The maximum theoretical moment to which the sheet pile will be subjected occurs at a depth between $z = L_1$ and $z = L_1 + L_2$. The depth z for zero shear and hence maximum moment may be evaluated from

$$\tfrac{1}{2}\sigma'_1 L_1 - F + \sigma'_1(z - L_1) + \tfrac{1}{2}K_a\gamma'(z - L_1)^2 = 0 \qquad (4.39)$$

Once the value of z is determined, the magnitude of the maximum moment is easily obtained.

4.8 Moment Reduction for Anchored Sheet-Pile

Walls Penetrating into Sand Sheet piles are flexible, and hence sheet-pile walls yield (i.e., become displaced laterally), which redistributes the lateral earth pressure. This change tends to reduce the maximum bending moment, M_{max} , as calculated by the procedure outlined in Section 4.7. For that reason, Rowe (1952, 1957) suggested a procedure for reducing the maximum design moment on the sheet-pile walls *obtained from the* ***free earth support method***. This section discusses the procedure of moment reduction for sheet piles *penetrating into sand.*

In Figure 4.25, which is valid for the case of a sheet pile penetrating sand, the following notation is used:

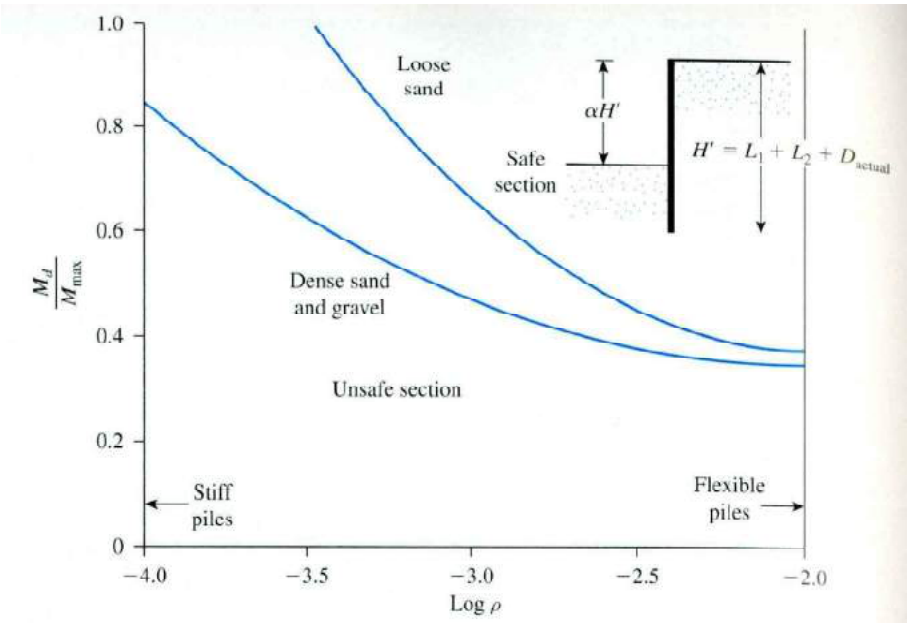

Figure 4.25 Plot of log ρ against M_d /M_{max} for sheet-pile walls penetrating sand (after, P. W. (1952).

1. H' = 5 total height of pile driven (i.e., $L_1 + L_2 + D_{actual}$)

2. $$\text{Relative flexibility of pile} = \rho = 10.91 \times 10^{-7}\left(\frac{H'^4}{EI}\right) \qquad (4.40)$$

where

H' is in meters

E = modulus of elasticity of the pile material (MN/ m^2)

I = moment of inertia of the pile section per meter of the wall (m^4/m of wall)

3. M_d = design moment

4. M_{max} = maximum theoretical moment

The procedure for the use of the moment reduction diagram (see Figure 4.25) is as follows:

Step 1. Choose a sheet-pile section (e.g., from among those given in Table 4.1).

Step 2. Find the modulus S of the selected section (Step 1) per unit length of the wall.
Step 3. Determine the moment of inertia of the section (Step 1) per unit length of the wall.
Step 4. Obtain H' and calculate r [see Eq. (4.40)].
Step 5. Find log r.
Step 6. Find the moment capacity of the pile section chosen in Step 1 as $M_d = \sigma_{all} S$.
Step 7. Determine M_d/M_{max} . Note that M_{max} is the maximum theoretical moment determined before.
Step 8. Plot log r (Step 5) and M_d/M_{max} in Figure 4.25.
Step 9. Repeat Steps 1 through 8 for several sections. The points that fall above the curve (in loose sand or dense sand, as the case may be) are *safe sections*.

The points that fall below the curve are *unsafe sections*. The cheapest section may now be chosen from those points which fall above the proper curve. Note that the section chosen will have an M_d , M_{max}.

Example 4.3:

Let $L_1 = 3.05$ m, $L_2 = 6.1$ m, $l_1 = 1.53$ m, $l_2 = 1.52$ m, $c' = 0$, $\phi' = 30°$, $\gamma = 16$ kN/m^3, $\gamma_{sat} = 19.5$ kN/m^3, and $E = 207 \times 10^3$ MN/m^2 in Figure 9.17.

a. Determine the theoretical and actual depths of penetration. (*Note*: $D_{actual} = 1.3D_{theory}$.)

b. Find the anchor force per unit length of the wall.

c. Determine the maximum moment, M_{max}.

Solution

Part a

We use the following table.

Quantity required	Eq. no.	Equation and calculation
K_a	—	$\tan^2\left(45 - \frac{\phi'}{2}\right) = \tan^2\left(45 - \frac{30}{2}\right) = \frac{1}{3}$
K_P	—	$\tan^2\left(45 + \frac{\phi'}{2}\right) = \tan^2\left(45 + \frac{30}{2}\right) = 3$
$K_p - K_a$	—	$3 - 0.333 = 2.667$
γ'	—	$\gamma_{sat} - \gamma_w = 19.5 - 9.81 = 9.69$ kN/m^3
σ_1'	9.1	$\gamma L_1 K_a = (16)(3.05)(\frac{1}{3}) = 16.27$ kN/m^2
σ_2'	9.2	$(\gamma L_1 + \gamma' L_2) K_a = [(16)(3.05) + (9.69)(6.1)]\frac{1}{3} = 35.97$ kN/m^2
L_3	9.6	$\frac{\sigma_2'}{\gamma'(K_p - K_a)} = \frac{35.97}{(9.69)(2.667)} = 1.39$ m
P	—	$\frac{1}{2}\sigma_1' L_1 + \sigma_2' L_2 + \frac{1}{2}(\sigma_2' - \sigma_1') L_2 + \frac{1}{2}\sigma_2' L_3 = (\frac{1}{2})(16.27)(3.05) + (16.27)(6.1) + (\frac{1}{2})(35.97 - 16.27)(6.1) + (\frac{1}{2})(35.97)(1.39) = 24.81 + 99.25 + 60.01 + 25.0 = 209.07$ kN/m
$\bar{z}$	—	$\frac{\Sigma M_E}{P} = \left[\begin{array}{l}(24.81)\left(1.39 + 6.1 + \frac{3.05}{3}\right) + (99.25)\left(1.39 + \frac{6.1}{2}\right) \\ + (60.01)\left(1.39 + \frac{6.1}{3}\right) + (25.0)\left(\frac{2 \times 1.39}{3}\right)\end{array}\right]\frac{1}{209.07} = 4.21$ m

L_4	9.67	$L_4^3 + 1.5L_4^2(l_2 + L_2 + L_3) - \dfrac{3P[(L_1 + L_2 + L_3) - (\bar{z} + l_1)]}{\gamma'(K_p - K_a)} = 0$
		$L_4^3 + 1.5L_4^2(1.52 + 6.1 + 1.39)$
		$- \dfrac{(3)(209.07)[(3.05 + 6.1 + 1.39) - (4.21 + 1.53)]}{(9.69)(2.667)} = 0$
		$L_4 = 2.7$ m
D_{theory}	—	$L_3 + L_4 = 1.39 + 2.7 = 4.09 \approx$ **4.1 m**
D_{actual}	—	$1.3D_{\text{theory}} = (1.3)(4.1) =$ **5.33 m**

Part b

The anchor force per unit length of the wall is

$$F = P - \tfrac{1}{2}\gamma'(K_p - K_a)L_4^2$$
$$= 209.07 - \left(\tfrac{1}{2}\right)(9.69)(2.667)(2.7)^2 = 114.87 \text{ kN/m} \approx \mathbf{115\ kN/m}$$

Part c

From Eq. (9.69), for zero shear,

$$\tfrac{1}{2}\sigma_1' L_1 - F + \sigma_1'(z - L_1) + \tfrac{1}{2}K_a\gamma'(z - L_1)^2 = 0$$

Let $z - L_1 = x$, so that

$$\tfrac{1}{2}\sigma_1' l_1 - F + \sigma_1' x + \tfrac{1}{2}K_a\gamma' x^2 = 0$$

or

$$\left(\tfrac{1}{2}\right)(16.27)(3.05) - 115 + (16.27)(x) + \left(\tfrac{1}{2}\right)\left(\tfrac{1}{3}\right)(9.69)x^2 = 0$$

giving $x^2 + 10.07x - 55.84 = 0$

Now, $x = 4$ m and $z = x + L_1 = 4 + 3.05 = 7.05$ m. Taking the moment about the point of zero shear, we obtain

$$M_{\max} = -\frac{1}{2}\sigma_1' L_1\left(x + \frac{3.05}{3}\right) + F(x + 1.52) - \sigma_1'\frac{x^2}{2} - \frac{1}{2}K_a\gamma' x^2\left(\frac{x}{3}\right)$$

or

$$M_{\max} = -\left(\frac{1}{2}\right)(16.27)(3.05)\left(4 + \frac{3.05}{3}\right) + (115)(4 + 1.52) - (16.27)\left(\frac{4^2}{2}\right)$$
$$-\left(\frac{1}{2}\right)\left(\frac{1}{3}\right)(9.69)(4)^2\left(\frac{4}{3}\right) = \mathbf{344.9\ kN \cdot m/m}$$

Example 4.4:

Refer to Example 9.5. Use Rowe's moment reduction diagram (Figure 9.24) to find an appropriate sheet pile section. For the sheet pile, use $E = 207 \times 10^3\ \text{MN/m}^2$ and $\sigma_{all} = 172{,}500\ \text{kN/m}^2$.

Solution

$$H' = L_1 + L_2 + D_{actual} = 3.05 + 6.1 + 5.33 = 14.48\ \text{m}$$

$M_{max} = 344.9\ \text{kN} \cdot \text{m/m}$. Now the following table can be prepared.

Section	$I(\text{m}^4/\text{m})$	$H'(\text{m})$	$\rho = 10.91 \times 10^{-7}\left(\frac{H'^4}{EI}\right)$	$\log \rho$	$S(\text{m}^3/\text{m})$	$M_d = S\sigma_{all}$ (kN · m/m)	$\frac{M_d}{M_{max}}$
PZ-22	115.2×10^{-6}	14.48	20.11×10^{-4}	−2.7	97×10^{-5}	167.33	0.485
PZ-27	251.5×10^{-6}	14.48	9.21×10^{-4}	−3.04	162.3×10^{-5}	284.84	0.826

Figure 9.25 gives a plot of M_d/M_{max} versus ρ. It can be seen that **PZ-27** will be sufficient.

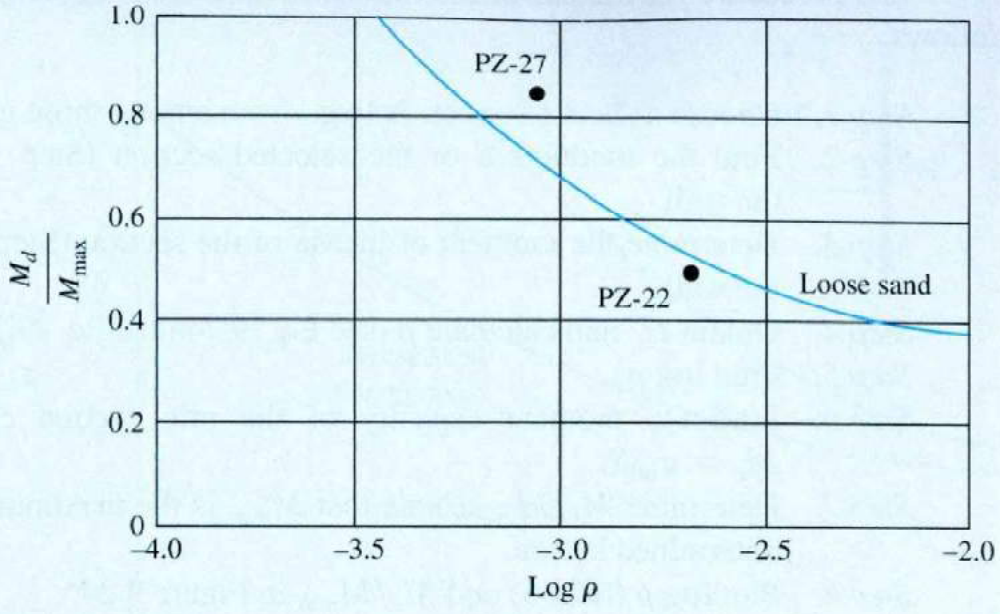

Figure 9.25 Plot of M_d/M_{max} versus $\log \rho$

4.9 Free Earth Support Method for Penetration of Clay

Figure 4.32 shows an anchored sheet-pile wall penetrating a clay soil and with a granular soil backfill. The diagram of pressure distribution above the dredge line is similar to that shown in Figure 4.9. From Eq. (4.26), the net pressure distribution below the dredge line (from $z = L_1 + L_2$ to $z = L_1 + L + D$) is

$$\sigma_6 = 4c - (\gamma L_1 + \gamma' L_2)$$

For static equilibrium, the sum of the forces in the horizontal direction is

$$P_1 - \sigma_6 D = F \qquad (4.41)$$

where

P_1 = area of the pressure diagram ACD

F = anchor force per unit length of the sheet-pile wall

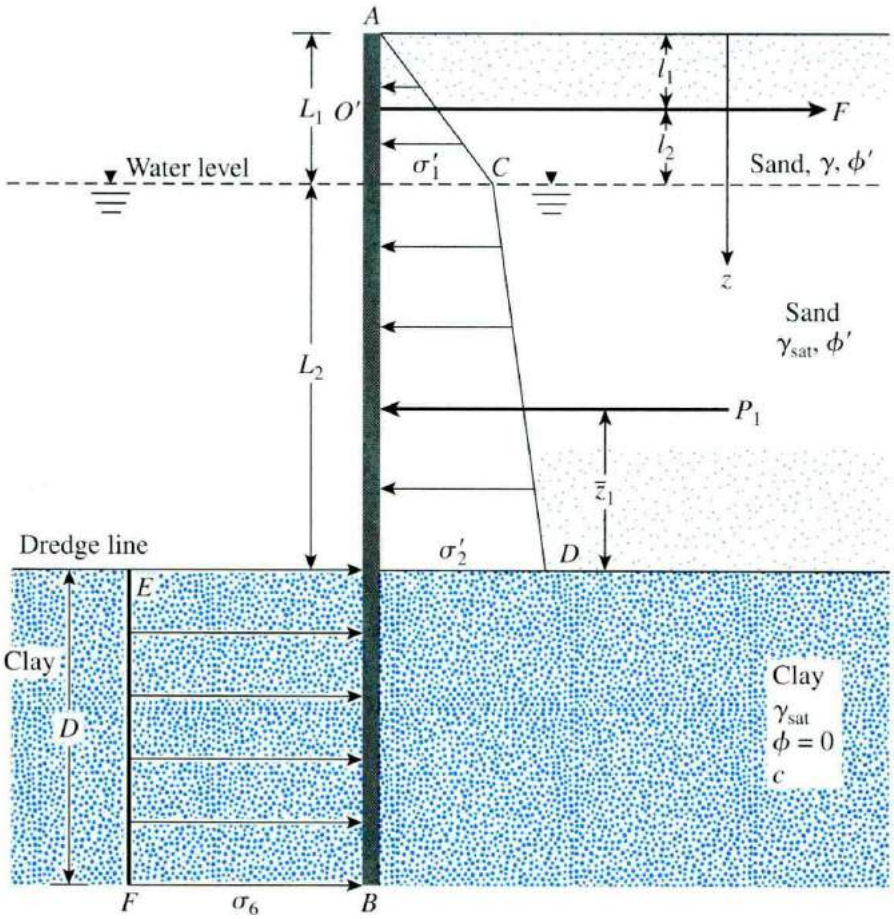

Figure 4.32 Anchored sheet-pile wall penetrating clay

Again, taking the moment about O' produces

$$P_1(L_1 + L_2 - l_1 - \bar{z}_1) - \sigma_6 D\left(l_2 + L_2 + \frac{D}{2}\right) = 0$$

Simplification yields

$$\sigma_6 D^2 + 2\sigma_6 D(L_1 + L_2 - l_1) - 2P_1(L_1 + L_2 - l_1 - \bar{z}_1) = 0 \qquad (4.42)$$

Equation (4.42) gives the theoretical depth of penetration, D.

As in Section 4.7, the maximum moment in this case occurs at a depth L_1 , z , $L_1 + L_2$. The depth of zero shear (and thus the maximum moment) may be determined from Eq. (4.39).

A moment reduction technique similar to that in Section 14.11 for anchored sheet piles penetrating into clay has also been developed by Rowe (1952, 1957). This technique is presented in Figure 4.33, in which the following notation is used:

1. The stability number is

$$S_n = 1.25\frac{c}{(\gamma L_1 + \gamma' L_2)} \qquad (4.43)$$

where c = undrained cohesion (ϕ=0). For the definition of γ, γ', L_1 , and L_2 , see Figure 4.32.

2. The nondimensional wall height is

$$\alpha = \frac{L_1 + L_2}{L_1 + L_2 + D_{\text{actual}}} \qquad (4.44)$$

3. The flexibility number is ρ [see Eq. (4.40)]

4. M_d = design moment

$M_{\max}$ = maximum theoretical moment

The procedure for moment reduction, using Figure 4.33, is as follows:

Step 1. Obtain $H' = L_1 + L_2 + D_{\text{actual}}$.

Step 2. Determine $\alpha = (L_1 + L_2)/H'$.

Step 3. Determine S_n [from Eq. (4.43)].

Step 4. For the magnitudes of α and S_n obtained in Steps 2 and 3, determine $M_d/M_{\max}$ for various values of log ρ from Figure 4.33, and plot $M_d/M_{\max}$ against logρ.

Step 5. Follow Steps 1 through 9 as outlined for the case of moment reduction of sheet-pile walls penetrating granular soil. (See Section 4.8.)

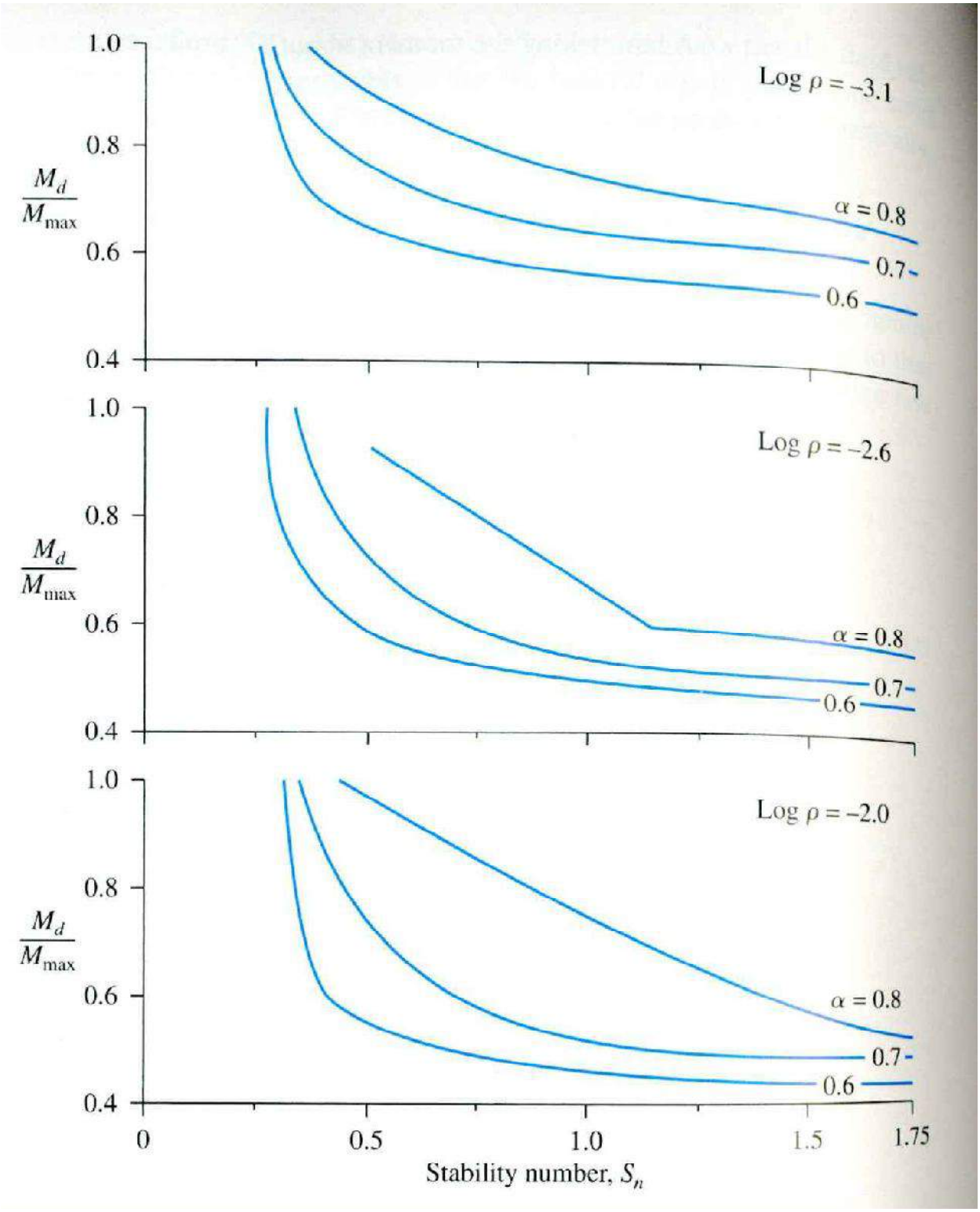

Figure 4.33 Plot of *Md*y*M*max against stability number for sheetpile wall penetrating clay [after Rowe, (1957].

Example 4.5:

In Figure 9.34, let $L_1 = 3$ m, $L_2 = 6$ m, and $l_1 = 1.5$ m. Also, let $\gamma = 17$ kN/m^3, $\gamma_{sat} = 20$ kN/m^3, $\phi' = 35°$, and $c = 41$ kN/m^2.

a. Determine the theoretical depth of embedment of the sheet-pile wall.
b. Calculate the anchor force per unit length of the wall.

Solution

Part a
We have

$$K_a = \tan^2\left(45 - \frac{\phi'}{2}\right) = \tan^2\left(45 - \frac{35}{2}\right) = 0.271$$

and

$$K_p = \tan^2\left(45 + \frac{\phi'}{2}\right) = \tan^2\left(45 + \frac{35}{2}\right) = 3.69$$

From the pressure diagram in Figure 9.36,

$$\sigma_1' = \gamma L_1 K_a = (17)(3)(0.271) = 13.82 \text{ kN/m}^2$$

$$\sigma_2' = (\gamma L_1 + \gamma' L_2) K_a = [(17)(3) + (20 - 9.81)(6)](0.271) = 30.39 \text{ kN/m}^2$$

$$P_1 = \text{areas } 1 + 2 + 3 = 1/2(3)(13.82) + (13.82)(6) + 1/2(30.39 - 13.82)(6)$$
$$= 20.73 + 82.92 + 49.71 = 153.36 \text{ kN/m}$$

and

$$\bar{z}_1 = \frac{(20.73)\left(6 + \frac{3}{3}\right) + (82.92)\left(\frac{6}{2}\right) + (49.71)\left(\frac{6}{3}\right)}{153.36} = 3.2 \text{ m}$$

From Eq. (9.85),

$$\sigma_6 D^2 + 2\sigma_6 D(L_1 + L_2 - l_1) - 2P_1(L_1 + L_2 - l_1 - \bar{z}_1) = 0$$

$$\sigma_6 = 4c - (\gamma L_1 + \gamma' L_2) = (4)(41) - [(17)(3) + (20 - 9.81)(6)] = 51.86 \text{ kN/m}^2$$

So,

$$(51.86)D^2 + (2)(51.86)(D)(3 + 6 - 1.5) - (2)(153.36)(3 + 6 - 1.5 - 3.2) = 0$$

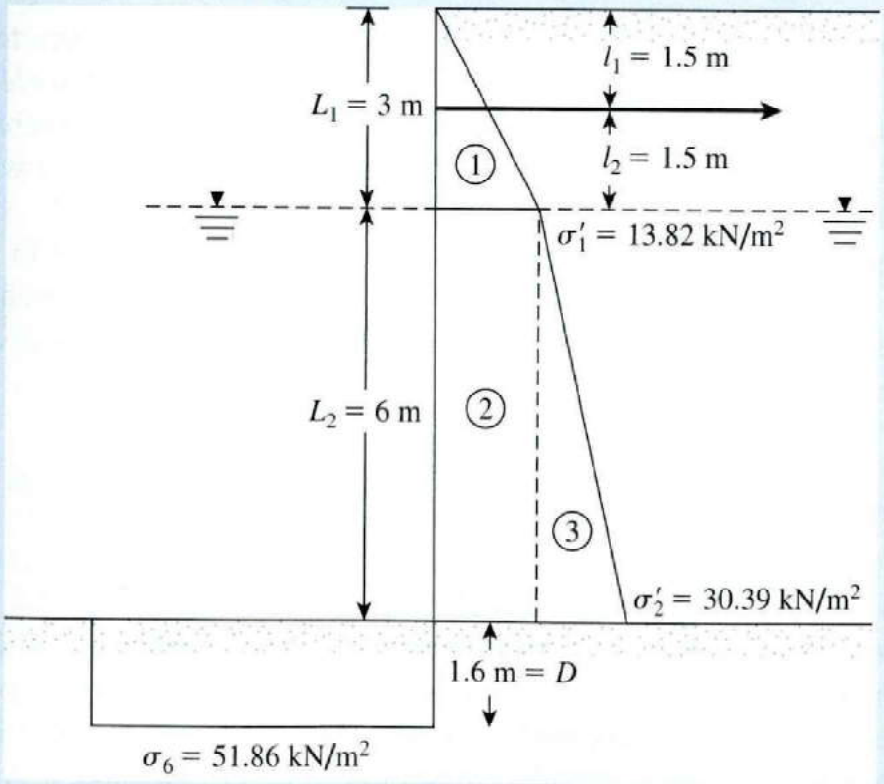

Figure 9.36 Free earth support method, sheet pile penetrating into clay

or

$$D^2 + 15D - 25.43 = 0$$

Hence,

$$D \approx \mathbf{1.6\ m}$$

Part b

From Eq. (9.84),

$$F = P_1 - \sigma_6 D = 153.36 - (51.86)(1.6) = \mathbf{70.38\ kN/m}$$

4.10 Anchors

Sections 4.7 through 4.9 gave an analysis of anchored sheet-pile walls and discussed how to obtain the force F per unit length of the sheet-pile wall that has to be sustained by the anchors. The current section covers in more detail the various types of anchor generally used and the procedures for evaluating their ultimate holding capacities.

The general types of anchor used in sheet-pile walls are as follows:

1. **Anchor plates and beams (deadman)**
2. **Tie backs**
3. **Vertical anchor piles**
4. **Anchor beams supported by batter (compression and tension) piles**

Anchor plates and beams are generally made of cast concrete blocks. (See Figure 4.36a.) The anchors are attached to the sheet pile by *tie rods*. A ***wale*** is placed at the front or back face of a sheet pile for the purpose of conveniently attaching the tie rod to the wall. To protect the tie rod from corrosion, it is generally coated with paint or asphaltic materials.

In the construction of ***tiebacks***, bars or cables are placed in predrilled holes (see Figure 4.36b) with concrete grout (cables are commonly high-strength, prestressed steel tendons). Figures 4.36c and 4.36d show a vertical anchor pile and an anchor beam with batter piles.

Placement of Anchors

The resistance offered by anchor plates and beams is derived primarily from the passive force of the soil located in front of them. Figure 4.36a, in which AB is the sheet-pile wall, shows the best location for maximum efficiency of an anchor plate. If the anchor is placed inside wedge ABC, which is the Rankine active zone, it would not provide any resistance to failure. Alternatively, the anchor could be placed in zone $CFEH$. Note that line DFG is the slip line for the Rankine passive pressure. If part of the passive wedge is located inside the active wedge ABC, full passive resistance of the anchor cannot be realized upon failure of the sheet-pile wall. However, if the anchor is placed in zone ICH, the Rankine passive zone in front of the anchor slab or plate is located completely outside the Rankine active zone ABC. In this case, full passive resistance from the anchor can be realized.

Figures 4.36b, 4.36c, and 4.36d also show the proper locations for the placement of tiebacks, vertical anchor piles, and anchor beams supported by batter piles.

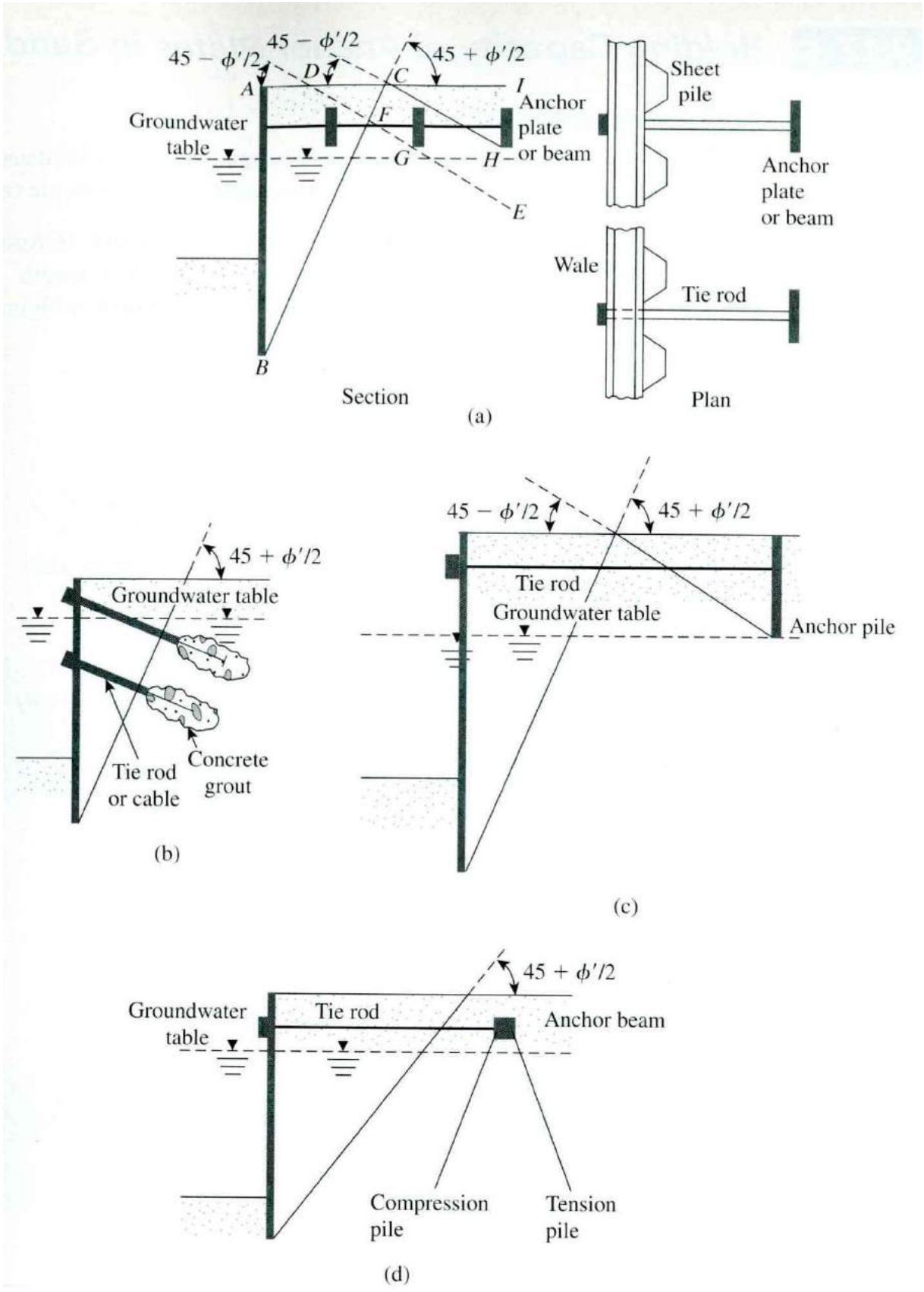

Figure 4.36 Various types of anchoring for sheet-pile walls: (a) anchor plate or beam; (b) tieback; (c) vertical anchor pile; (d) anchor beam with batter piles

Capacity of Deadman (After Teng, 1969)

A series of deadmen (anchor beams, anchor blocks or anchor plates) are normally placed at intervals parallel to the sheet pile walls. These anchor blocks may be constructed near the ground surface or at great depths, and in short lengths or in one continuous beam. The holding capacity of these anchorages is discussed below.

Continuous Anchor Beam Near Ground Surface (Teng, 1969)

If the length of the beam is considerably greater than its depth, it is called^ a continuous deadman. Fig. 4.37(a) shows a deadman. If the depth to the top of the deadman, *h,* is less than about onethird to one-half of *H* (where *H* is depth to the bottom of the deadman), the capacity may be calculated by assuming that the top of the deadman extends to the ground surface. The ultimate capacity of a deadman may be obtained from (per unit length)

For granular soil (c = 0)

$$T_u = P_p - P_a = \frac{1}{2}\gamma H^2 K_p - \frac{1}{2}\gamma H^2 K_A \qquad (4.45)$$

or $$T_u = \frac{1}{2}\gamma H^2 (K_P - K_A) \qquad (4.46)$$

For clay soil ($\phi = 0$)

$$T_u = P_p - P_a = q_u H + \frac{1}{2}\gamma H^2 - \frac{1}{2}\gamma H^2 - q_u H + \frac{2c^2}{\gamma} = 2q_u H - \frac{2c^2}{\gamma} \qquad (4.47)$$

where q_u = unconfmed compressive strength of soil,

γ = effective unit weight of soil, and

K_p, K_a = Rankine's active and passive earth pressure coefficients.

It may be noted here that the active earth pressure is assumed to be zero at a depth = *2c/y* which is the depth of the tension cracks. It is likely that the magnitude and distribution of earth pressure may change slowly with time. For lack of sufficient data on this, the design of deadmen in cohesive soils should be made with a conservative factor of safety.

Short Deadman Near Ground Surface in Granular Soil (Fig. 4.37b)

If the length of a deadman is shorter than *5h (h* = height of deadman) there will be an end effect with regards to the holding capacity of the anchor. The equation suggested by Teng for computing the ultimate tensile capacity T_u is

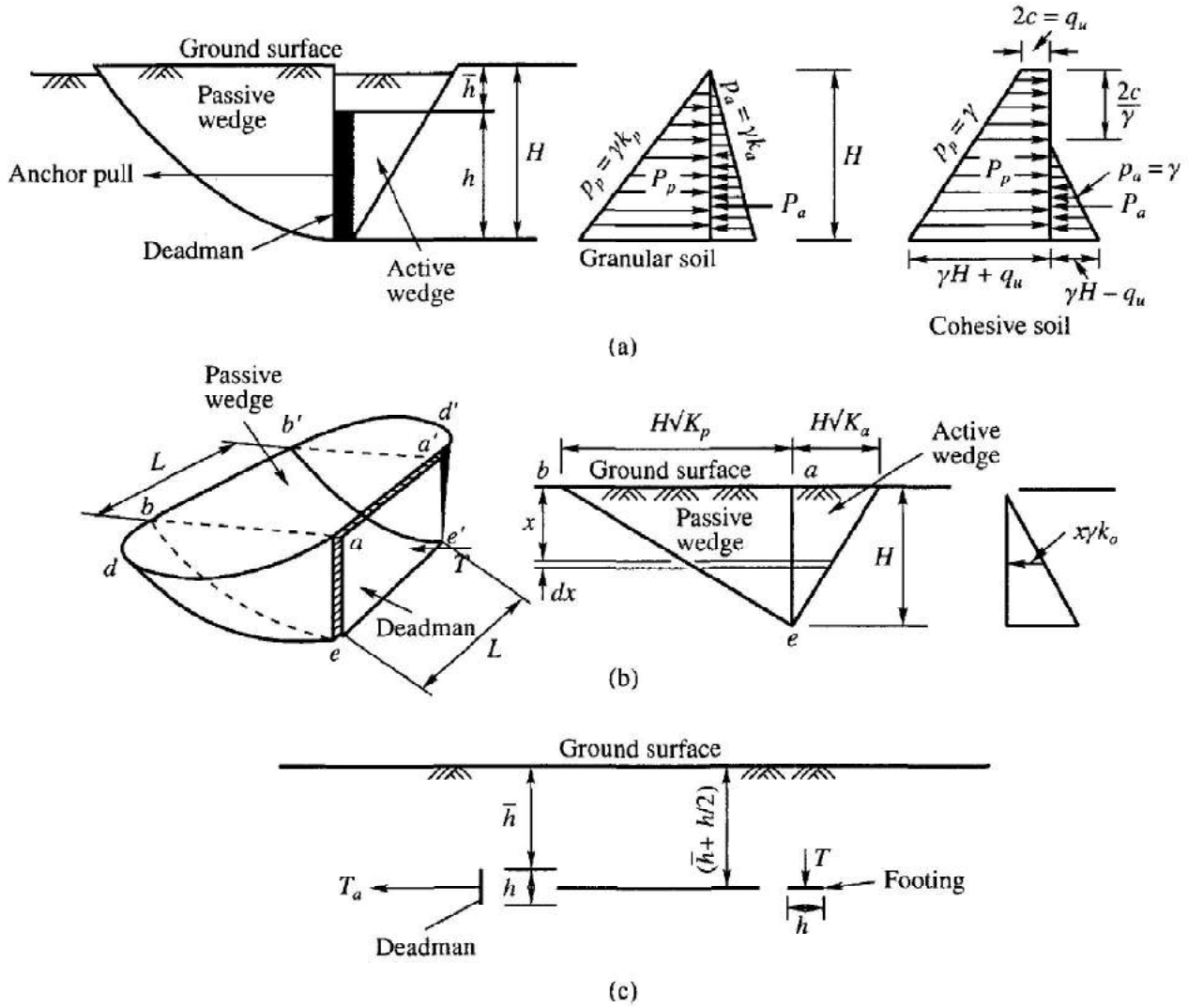

Figure 4.37 Capacity of deadmen: (a) continuous deadmen near ground surface ($\bar{h}/H$ < 1/3 ~ 1/2); (b) short deadmen near ground surface; (c) deadmen at great depth below ground surface (after Teng, 1969)

$$T_u = L(P_p - P_a) + \frac{1}{3}K_o\gamma(\sqrt{K_P} + \sqrt{K_A})H^3\tan\phi \qquad (4.48)$$

where
h= height of deadman
$\bar{h}$= depth to the top of deadman
L= length of deadman
H= depth to the bottom of the dead man from the ground surface
P_p ,P_a = total passive and active earth pressures per unit length
K_o= coefficient of earth pressures at-rest, taken equal to 0.4
γ= effective unit weight of soil
K_p, K_a= Rankine's coefficients of passive and active earth pressures

ϕ= angle of internal friction

Anchor Capacity of Short Deadman in Cohesive Soil Near Ground Surface

In cohesive soils, the second term of Eq. (4.48) should be replaced by the cohesive resistance

$$T_u = L\left(P_p - P_a\right) + q_u H^2 \qquad (4.49)$$

where q_u = unconfmed compressive strength of soil.

Deadman at Great Depth

The ultimate capacity of a deadman at great depth below the ground surface as shown in Fig. (4.37c) is approximately equal to the bearing capacity of a footing whose base is located at a depth ($\bar{h}$ + h/2), corresponding to the mid height of the deadman (Terzaghi, 1943).

University of Anbar
Engineering College
Civil Engineering Department

CHAPTER FIVE

BRACED CUTS

LECTURE
DR. AHMED H. ABDULKAREEM
2017

5.1 Introduction

Sometimes construction work requires ground excavations with vertical or near-vertical faces—for example, basements of buildings in developed areas or underground transportation facilities at shallow depths below the ground surface (a cut-and-cover type of construction). The vertical faces of the cuts need to be protected by temporary bracing systems to avoid failure that may be accompanied by considerable settlement or by bearing capacity failure of nearby foundations.

Figure 5.1 shows two types of braced cut commonly used in construction work. One type uses the ***soldier beam*** (Figure 5.1a), which is driven into the ground before excavation and is a vertical steel or timber beam. ***Laggings***, which are horizontal timber planks, are placed between soldier beams as the excavation proceeds. When the excavation reaches the desired depth, ***wales*** and ***struts*** (horizontal steel beams) are installed. The struts are compression members. Figure 5.1b shows another type of braced excavation. In this case, interlocking *sheet piles* are driven into the soil before excavation. Wales and struts are inserted immediately after excavation reaches the appropriate depth.

Figure 5.2 shows the braced-cut construction used for the Chicago subway in 1940. Timber lagging, timber struts, and steel wales were used. Figure 5.3 shows a braced cut made during the construction of the Washington, DC, metro in 1974. In this cut, timber lagging, steel H-soldier piles, steel wales, and pipe struts were used.

To design braced excavations (i.e., to select wales, struts, sheet piles, and soldier beams), an engineer must estimate the lateral earth pressure to which the braced cuts will be subjected. The theoretical aspects of the lateral earth pressure on a braced cut is discussed in Section 5.2. The total active force per unit length of the wall (P_a) can be calculated by using the general wedge theory. However, that analysis will not provide the relationships required for estimating the variation of lateral pressure with depth, which is a function of several factors, such as the type of soil, the experience of the construction crew, the type of construction equipment used, and so forth. For that reason, empirical pressure envelopes developed from field observations are used for the design of braced cuts. This procedure is discussed in the following sections.

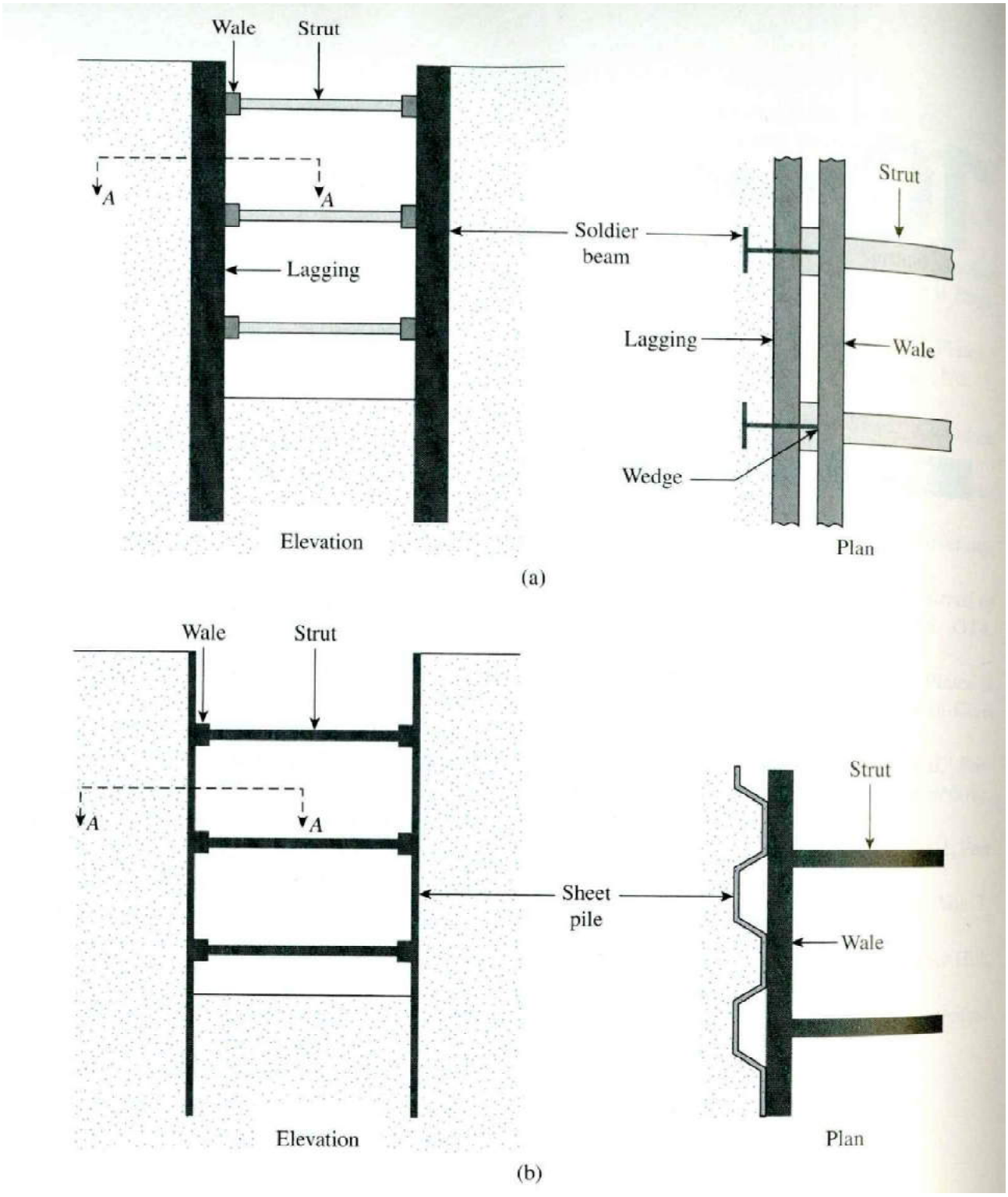

Figure 5.1 Types of braced cut: (a) use of soldier beams; (b) use of sheet piles

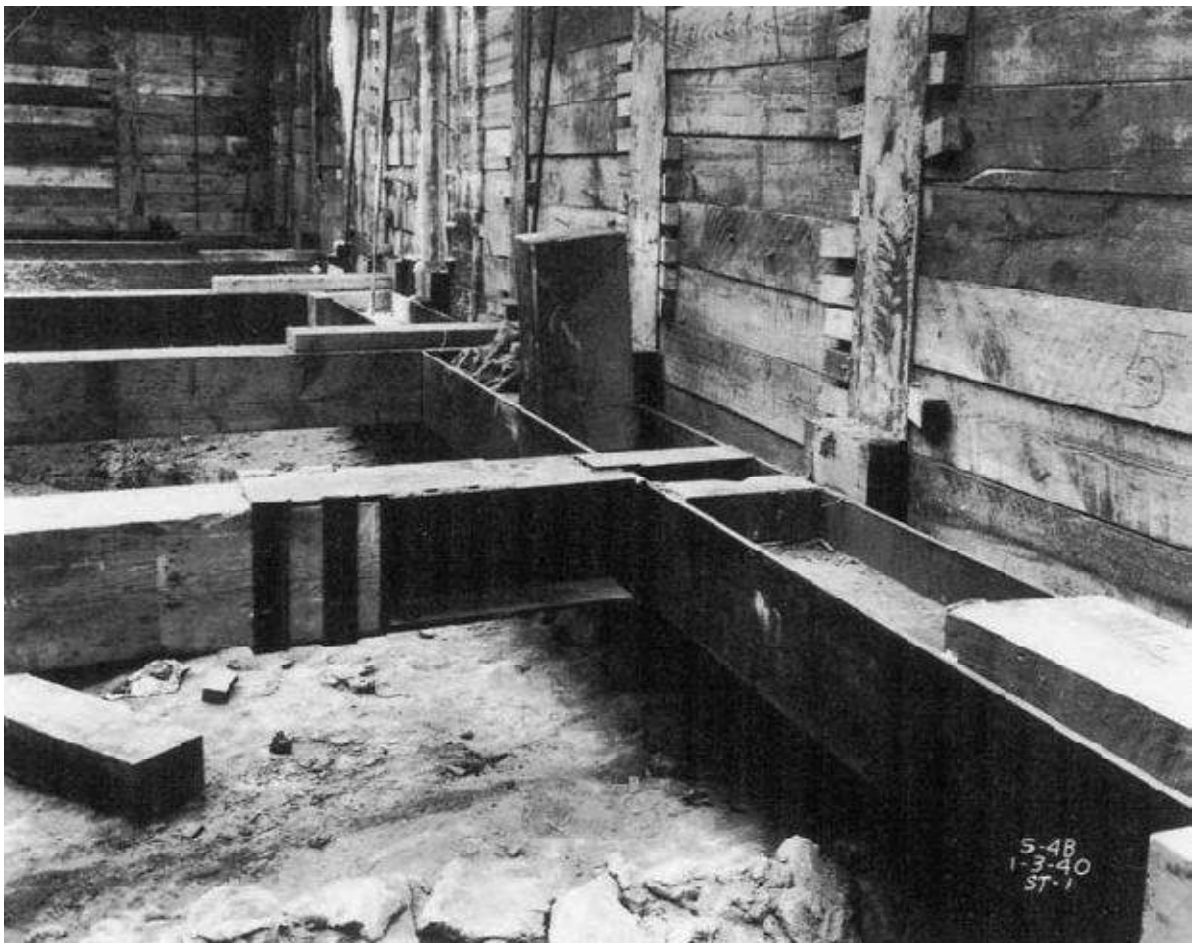

Figure 5.2 Braced cut in Chicago Subway construction, January 1940 (*Courtesy of Ralph B. Peck*)

Figure 5.3 Braced cut in the construction of Washington, D.C. Metro, May 1974 (Courtesy of Ralph B. Peck)

5.2 Pressure Envelope for Braced-Cut Design

As mentioned in Section 5.1, the lateral earth pressure in a braced cut is dependent on the type of soil, construction method, and type of equipment used. The lateral earth pressure changes from place to place. Each strut should also be designed for the maximum load to which it may be subjected. Therefore, the braced cuts should be designed using apparent-pressure diagrams that are envelopes of all the pressure diagrams determined from measured strut loads in the field. Figure 5.4 shows the method for obtaining the apparent-pressure diagram at a section from strut loads. In this figure, let P_1 , P_2 , P_3 , P_4 , …. be the measured strut loads. The apparent horizontal pressure can then be calculated as

$$\sigma_1 = \frac{P_1}{(s)\left(d_1 + \frac{d_2}{2}\right)}$$

$$\sigma_2 = \frac{P_2}{(s)\left(\frac{d_2}{2} + \frac{d_3}{2}\right)}$$

$$\sigma_3 = \frac{P_3}{(s)\left(\frac{d_3}{2} + \frac{d_4}{2}\right)}$$

$$\sigma_4 = \frac{P_4}{(s)\left(\frac{d_4}{2} + \frac{d_5}{2}\right)}$$

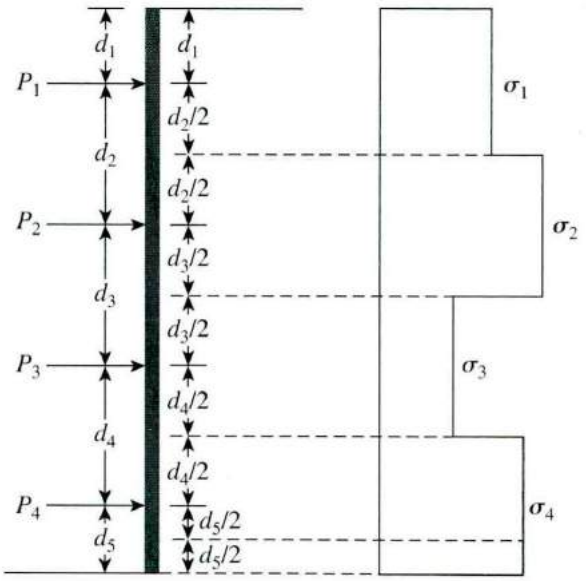

Figure 5.4 Procedure for calculating apparent-pressure diagram from measured strut loads

where

σ_1 , σ_2 , σ_3 , σ_4 = apparent pressures

S= center-to-center spacing of the struts

Using the procedure just described for strut loads observed from the Berlin subway cut, Munich subway cut, and New York subway cut, Peck (1969) provided the envelope of apparent-lateral-pressure diagrams for design of cuts in *sand.* This envelope is illustrated in Figure 5.5, in which

$$\sigma_a = 0.65\gamma H K_a \qquad \textbf{(5.1)}$$

where

γ = unit weight

H = height of the cut

K_a = Rankine active pressure coefficient = $(\tan^2(45+\phi'/2)$

ϕ' = effective friction angle of sand

Cuts in Clay

In a similar manner, Peck (1969) also provided the envelopes of apparent-lateral-pressure diagrams for cuts in *soft to medium clay* and in *stiff clay.* The pressure envelope for soft to medium clay is shown in Figure 5.6 and is applicable to the condition

$$\frac{\gamma H}{c} > 4$$

where c = undrained cohesion ϕ=0.

The pressure, σ_a , is the larger of

$$\sigma_a = \gamma H\left[1 - \left(\frac{4c}{\gamma H}\right)\right] \qquad (5.2)$$

and

$$\sigma_a = 0.3\gamma H$$

where γ = unit weight of clay.

The pressure envelope for cuts in stiff clay is shown in Figure 5.7, in which

$$\sigma_a = 0.2\gamma H \text{ to } 0.4\gamma H \qquad (\text{with an average of } 0.3\gamma H) \qquad (5.3)$$

is applicable to the condition $\gamma H/c \leq 4$.

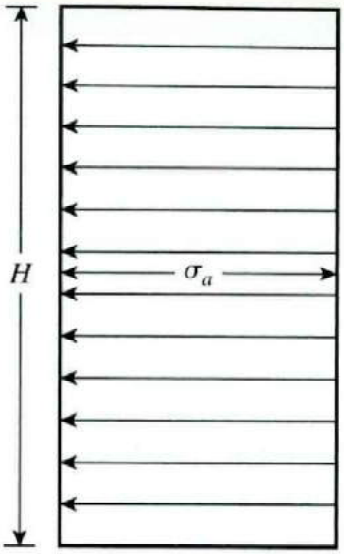

Figure 10.5 Peck's (1969) apparent-pressure envelope for cuts in sand

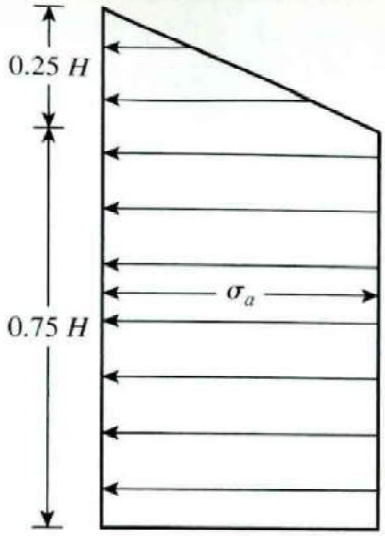

Figure 10.6 Peck's (1969) apparent-pressure envelope for cuts in soft to medium clay

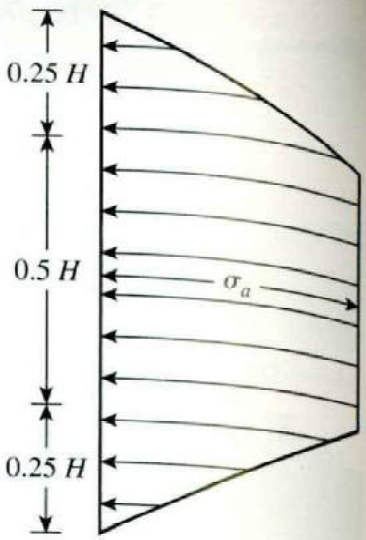

Figure 10.7 Peck's (1969) apparent-pressure envelope for cuts in stiff clay

When using the pressure envelopes just described, keep the following points in mind:

1. They apply to excavations having depths greater than about 6m(≈20ft).
2. They are based on the assumption that the water table is below the bottom of the cut.
3. Sand is assumed to be drained with zero pore water pressure.
4. Clay is assumed to be undrained and pore water pressure is not considered.

5.3 Pressure Envelope for Cuts in Layered Soil

Sometimes, layers of both sand and clay are encountered when a braced cut is being constructed. In this case, Peck (1943) proposed that an equivalent value of cohesion (ϕ=0) should be determined according to the formula (see Figure 5.8a).

$$c_{av} = \frac{1}{2H}[\gamma_s K_s H_s^2 \tan \phi_s' + (H - H_s) n' q_u] \qquad (5.4)$$

where

H = total height of the cut

γ_s = unit weight of sand

H_s= height of the sand layer

K_s= a lateral earth pressure coefficient for the sand layer (≈1)

ϕ'_s=5 effective angle of friction of sand
q_u= unconfined compression strength of clay
n = a coefficient of progressive failure (ranging from 0.5 to 1.0; average value 0.75)

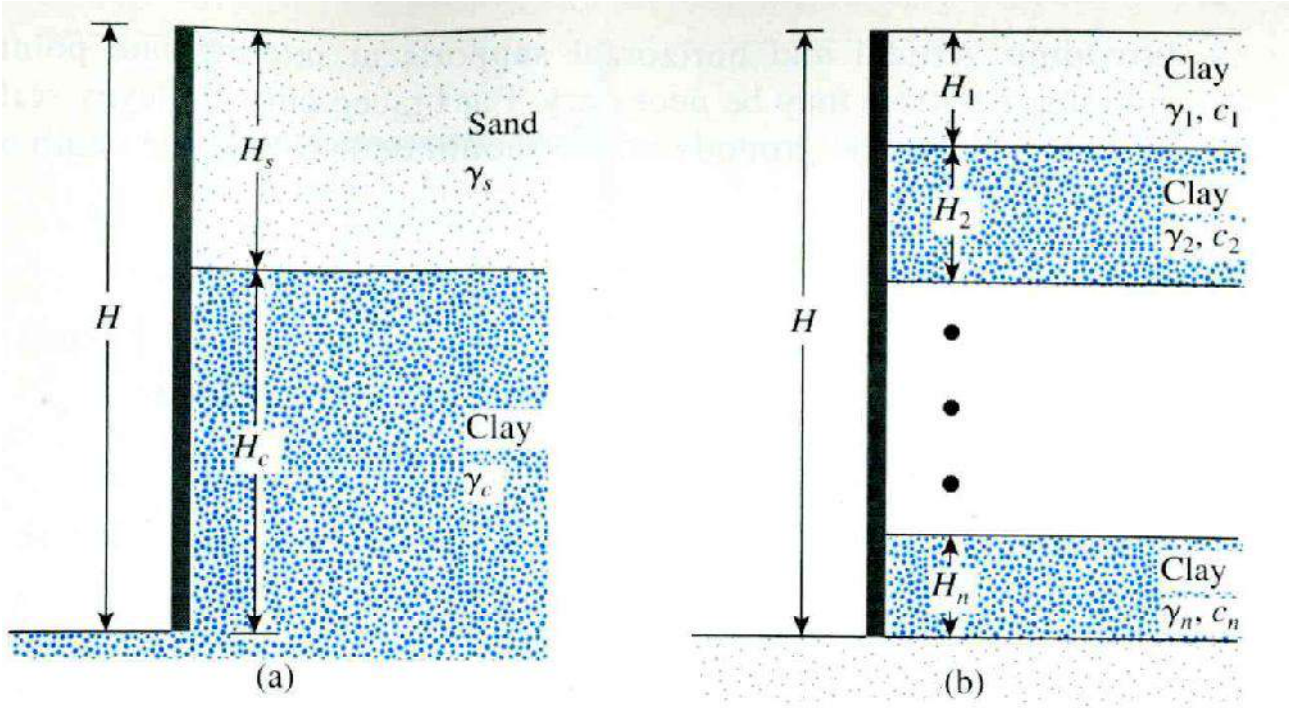

Figure 5.8 Layered soils in braced cuts

The average unit weight of the layers may be expressed as

$$\gamma_a = \frac{1}{H}[\gamma_s H_s + (H - H_s)\gamma_c] \qquad (5.5)$$

where γ_c = saturated unit weight of clay layer.

Once the average values of cohesion and unit weight are determined, the pressure envelopes in clay can be used to design the cuts.

Similarly, when several clay layers are encountered in the cut (Figure 5.8b), the average undrained cohesion becomes

$$c_{av} = \frac{1}{H}(c_1 H_1 + c_2 H_2 + \cdots + c_n H_n) \qquad (5.6)$$

where
c_1 , c_2 , …, c_n = undrained cohesion in layers 1, 2, … , n
H_1 , H_2 , … , H_n = thickness of layers 1, 2, … , n

The average unit weight is now

$$\gamma_a = \frac{1}{H}(\gamma_1 H_1 + \gamma_2 H_2 + \gamma_3 H_3 + \cdots + \gamma_n H_n) \qquad (5.7)$$

5.4 Design of Various Components of a Braced Cut Struts

In construction work, struts should have a minimum vertical spacing of about 2.75 m (9 ft) or more. Struts are horizontal columns subject to bending. The load-carrying capacity of columns depends on their *slenderness ratio,* which can be reduced by providing vertical and horizontal supports at intermediate points. For wide cuts, splicing the struts may be necessary. For braced cuts in clayey soils, the depth of the first strut below the ground surface should be less than the depth of tensile crack, z_c. From Eq. (5.7),

$$\sigma'_a = \gamma z K_a - 2c'\sqrt{K_a}$$

where K_a = coefficient of Rankine active pressure.

For determining the depth of tensile crack,

$$\sigma'_a = 0 = \gamma z_c K_a - 2c'\sqrt{K_a}$$

or

$$z_c = \frac{2c'}{\sqrt{K_a}\gamma}$$

With $\phi = 0$, $K_a = \tan^2(45 - \phi/2) = 1$, so

$$z_c = \frac{2c}{\gamma}$$

A simplified conservative procedure may be used to determine the strut loads. Although this procedure will vary, depending on the engineers involved in the project, the following is a step-by-step outline of the general methodology (see Figure 5.9):

Step 1. Draw the pressure envelope for the braced cut. (See Figures 5.5, 5.6, and 5.7.) Also, show the proposed strut levels. Figure 5.9a shows a pressure envelope for a sandy soil; however, it could also be for a clay. The strut levels are marked *A, B, C,* and *D.* The sheet piles (or soldier beams) are assumed to be hinged at the strut levels, except for the top and bottom ones. In Figure 5.9a, the hinges are at the level of struts *B* and *C.* (Many

designers also assume the sheet piles or soldier beams to be hinged at all strut levels except for the top.)

Step 2. Determine the reactions for the two simple cantilever beams (top and bottom) and all the simple beams between. In Figure 5.9b, these reactions are A, B_1 , B_2 , C_1 , C_2 , and D.

Step 3. The strut loads in the figure may be calculated via the formulas

$$P_A = (A)(s)$$
$$P_B = (B_1 + B_2)(s)$$
$$P_C = (C_1 + C_2)(s) \qquad (5.8)$$

and

$$P_D = (D)(s)$$

where

P_A , P_B , P_C , P_D = loads to be taken by the individual struts at levels A,B, C, and D, respectively

A, B_1 , B_2 , C_1 , C_2 , D = reactions calculated in Step 2 (note the unit: force/unit length of the braced cut)

s = horizontal spacing of the struts (see plan in Figure 5.9a)

Step 4. Knowing the strut loads at each level and the intermediate bracing conditions allows selection of the proper sections from the steel manual

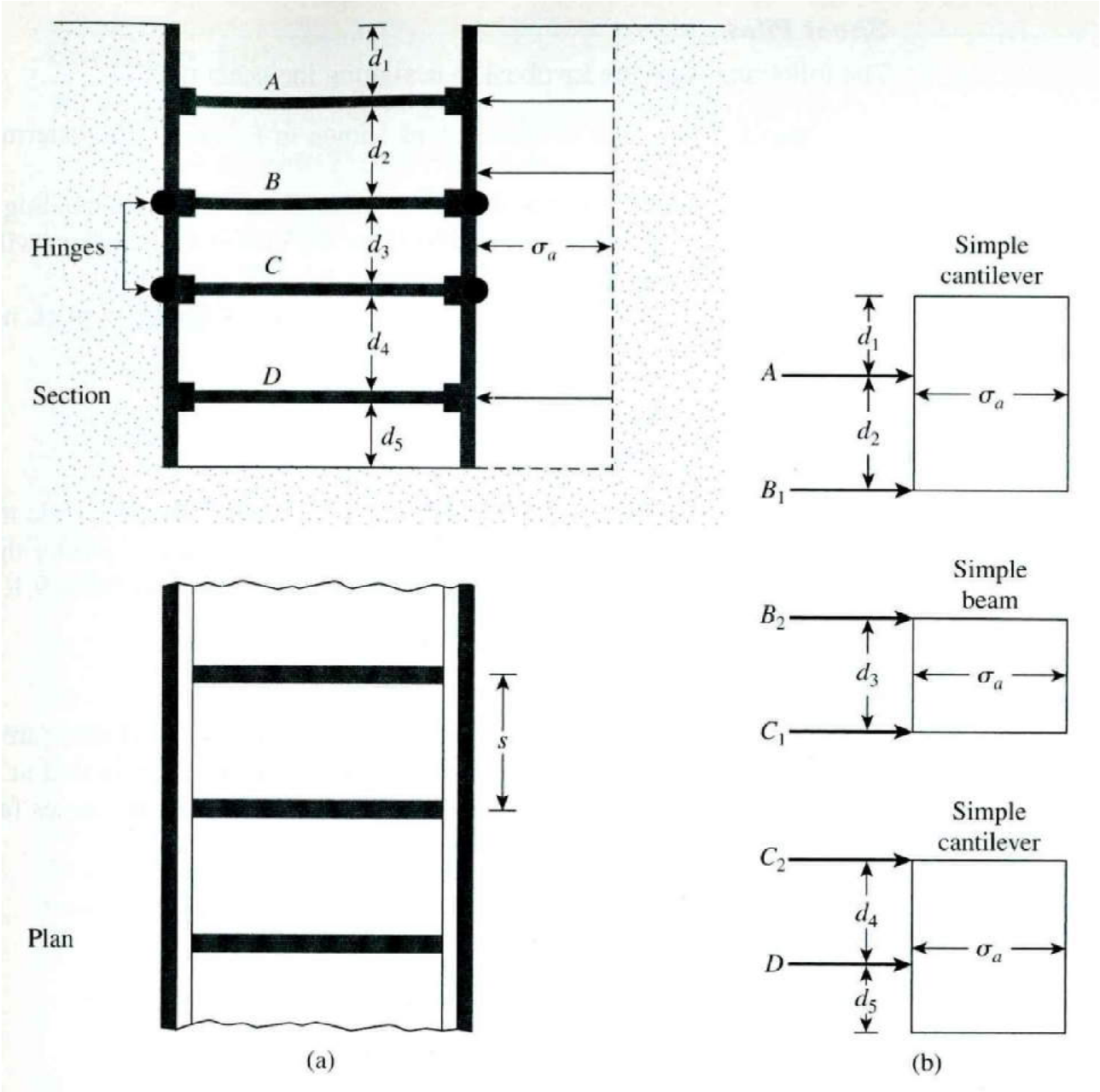

Figure 5.9 Determination of strut loads: (a) section and plan of the cut; (b) method for determining strut loads

Sheet Piles

The following steps are involved in designing the sheet piles:

Step 1. For each of the sections shown in Figure 15.11b, determine the maximum bending moment.

Step 2. Determine the maximum value of the maximum bending moments (M_{max}) obtained in Step 1. Note that the unit of this moment will be, for example, kN-m/m length of the wall.

Step 3. Obtain the required section modulus of the sheet piles, namely,

$$S = \frac{M_{max}}{\sigma_{all}} \qquad (5.9)$$

where σ_{all} = allowable flexural stress of the sheet-pile material.

Step 4. Choose a sheet pile having a section modulus greater than or equal to the required section modulus from a table such as Table 4.1.

Wales

Step1. Wales may be treated as continuous horizontal members if they are spliced properly. Conservatively, they may also be treated as though they are pinned at the struts. For the section shown in Figure 5.9a, the maximum moments for the wales (assuming that they are pinned at the struts) are,

$$\text{At level } A, \quad M_{max} = \frac{(A)(s^2)}{8}$$

$$\text{At level } B, \quad M_{max} = \frac{(B_1 + B_2)s^2}{8}$$

$$\text{At level } C, \quad M_{max} = \frac{(C_1 + C_2)s^2}{8}$$

and

$$\text{At level } D, \quad M_{max} = \frac{(D)(s^2)}{8}$$

where A, B_1 , B_2 , C_1 , C_2 , and D are the reactions under the struts per unit length of the wall (see Step 2 of strut design).

Step 2. Determine the section modulus of the wales:

$$S = \frac{M_{\max}}{\sigma_{\text{all}}}$$

The wales are sometimes fastened to the sheet piles at points that satisfy the lateral support requirements.

Example 5.1:

The cross section of a long braced cut is shown in Figure 10.10a.

a. Draw the earth-pressure envelope.
b. Determine the strut loads at levels *A*, *B*, and *C*.
c. Determine the section modulus of the sheet pile section required.
d. Determine a design section modulus for the wales at level *B*.

(*Note:* The struts are placed at 3 m, center to center, in the plan.) Use

$$\sigma_{all} = 170 \times 10^3 \text{ kN/m}^2$$

Solution

Part a

We are given that $\gamma = 18 \text{ kN/m}^2$, $c = 35 \text{ kN/m}^2$, and $H = 7$ m. So,

$$\frac{\gamma H}{c} = \frac{(18)(7)}{35} = 3.6 < 4$$

Thus, the pressure envelope will be like the one in Figure 10.7. The envelope is plotted in Figure 10.10a with maximum pressure intensity, σ_a, equal to $0.3\gamma H = 0.3(18)(7) = \mathbf{37.8 \text{ kN/m}^2}$.

Part b

To calculate the strut loads, examine Figure 10.10b. Taking the moment about B_1, we have $\Sigma M_{B_1} = 0$, and

$$A(2.5) - \left(\frac{1}{2}\right)(37.8)(1.75)\left(1.75 + \frac{1.75}{3}\right) - (1.75)(37.8)\left(\frac{1.75}{2}\right) = 0$$

or

$$A = 54.02 \text{ kN/m}$$

Also, Σ vertical forces $= 0$. Thus,

$$\tfrac{1}{2}(1.75)(37.8) + (37.8)(1.75) = A + B_1$$

or

$$33.08 + 66.15 - A = B_1$$

So,

$$B_1 = 45.2 \text{ kN/m}$$

Due to symmetry,

$$B_2 = 45.2 \text{ kN/m}$$

and

$$C = 54.02 \text{ kN/m}$$

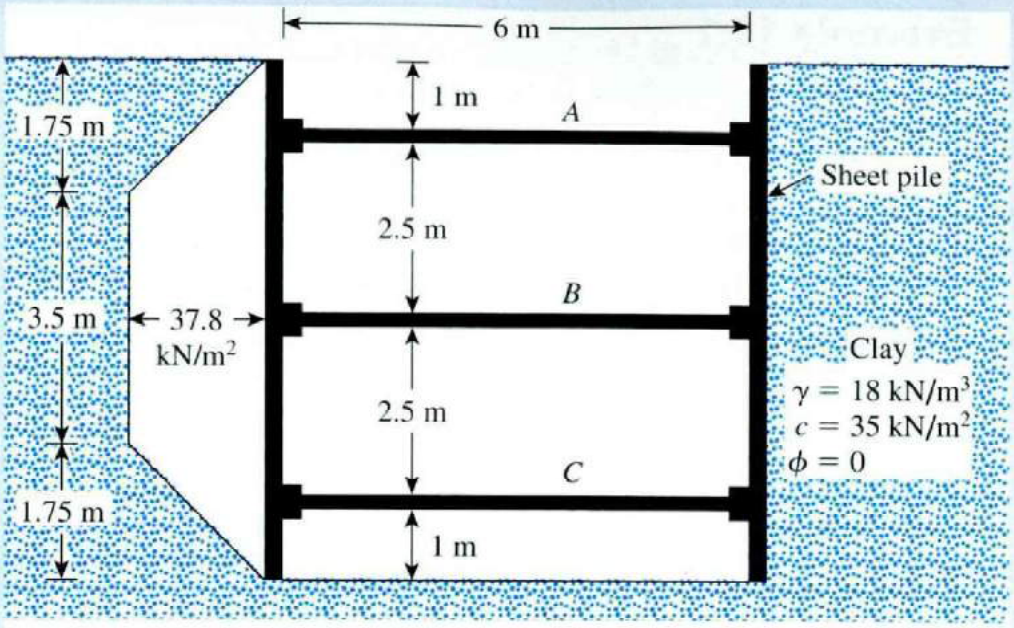

(a) Cross section

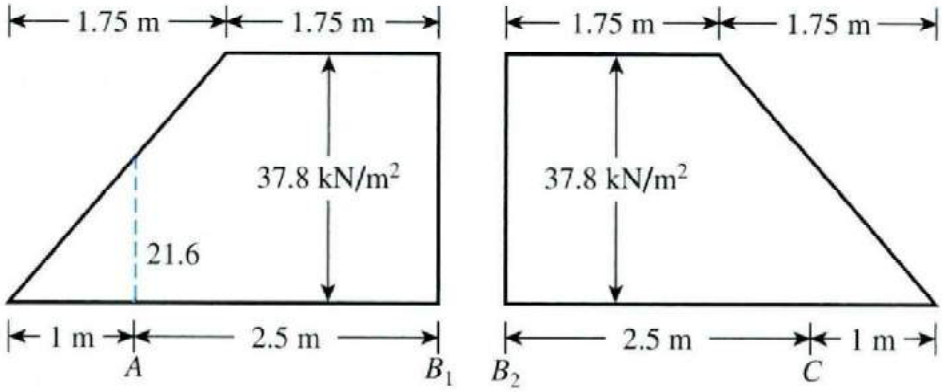

(b) Determination of reaction

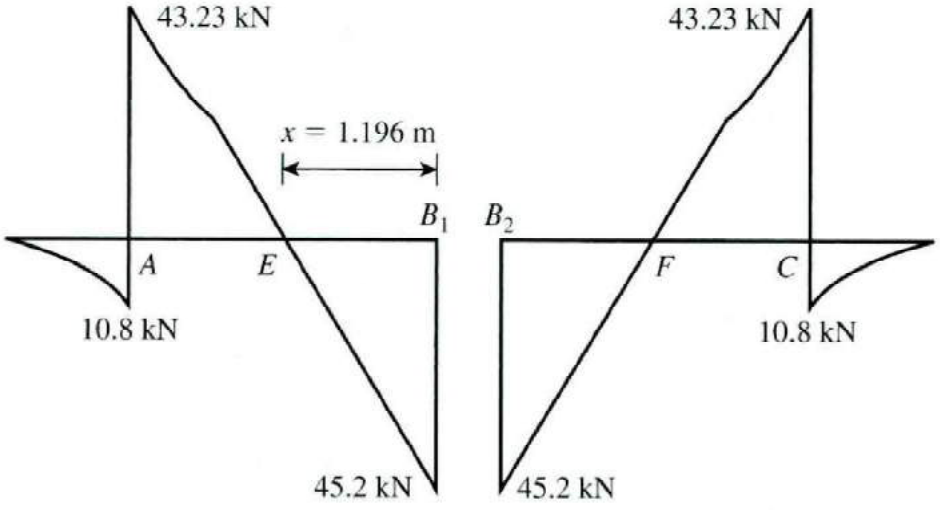

(c) Shear force diagram

Figure 10.10 Analysis of a braced cut

Hence, the strut loads at the levels indicated by the subscripts are

$$P_A = 54.02 \times \text{horizontal spacing, } s = 54.02 \times 3 = \mathbf{162.06\ kN}$$

$$P_B = (B_1 + B_2)3 = (45.2 + 45.2)3 = \mathbf{271.2\ kN}$$

and

$$P_C = 54.02 \times 3 = \mathbf{162.06\ kN}$$

Part c

At the left side of Figure 10.10b, for the maximum moment, the shear force should be zero. The nature of the variation of the shear force is shown in Figure 10.10c. The location of point E can be given as

$$x = \frac{\text{reaction at } B_1}{37.8} = \frac{45.2}{37.8} = 1.196 \text{ m}$$

Also,

$$\text{Magnitude of moment at } A = \frac{1}{2}(1)\left(\frac{37.8}{1.75} \times 1\right)\left(\frac{1}{3}\right)$$

$$= 3.6 \text{ kN-m/meter of wall}$$

and

$$\text{Magnitude of moment at } E = (45.2 \times 1.196) - (37.8 \times 1.196)\left(\frac{1.196}{2}\right)$$

$$= 54.06 - 27.03 = 27.03 \text{ kN-m/meter of wall}$$

Because the loading on the left and right sections of Figure 10.10b are the same, the magnitudes of the moments at F and C (see Figure 10.10c) will be the same as those at E and A, respectively. Hence, the maximum moment is 27.03 kN-m/meter of wall.

The section modulus of the sheet piles is thus

$$S = \frac{M_{max}}{\sigma_{all}} = \frac{27.03 \text{ kN-m}}{170 \times 10^3 \text{ kN/m}^2} = \mathbf{15.9 \times 10^{-5} m^3/m \text{ of the wall}}$$

Part d

The reaction at level B has been calculated in part b. Hence,

$$M_{max} = \frac{(B_1 + B_2)s^2}{8} = \frac{(45.2 + 45.2)3^2}{8} = 101.7 \text{ kN-m}$$

and

$$\text{Section modulus, } S = \frac{101.7}{\sigma_{all}} = \frac{101.7}{(170 \times 1000)}$$

$$= \mathbf{0.598 \times 10^{-3} m^3}$$

Example 10.2

Refer to the braced cut shown in Figure 10.11, for which $\gamma = 17\ \text{kN/m}^3$, $\phi' = 35°$, and $c' = 0$. The struts are located 4 m on center in the plan. Draw the earth-pressure envelope and determine the strut loads at levels A, B, and C.

Solution

For this case, the earth-pressure envelope shown in Figure 10.5 is applicable. Hence,

$$K_a = \tan^2\left(45 - \frac{\phi'}{2}\right) = \tan^2\left(45 - \frac{35}{2}\right) = 0.271$$

From Equation (10.1)

$$\sigma_a = 0.65\,\gamma H K_a = (0.65)(17)(9)(0.271) = 26.95\ \text{kN/m}^2$$

Figure 10.12a shows the pressure envelope. Refer to Figure 10.12b and calculate B_1:

$$\sum M_{B_1} = 0$$

$$A = \frac{(26.95)(5)\left(\frac{5}{2}\right)}{3} = 112.29\ \text{kN/m}$$

$$B_1 = (26.95)(5) - 112.29 = 22.46\ \text{kN/m}$$

Now, refer to Figure 10.12c and calculate B_2:

$$\sum M_{B_2} = 0$$

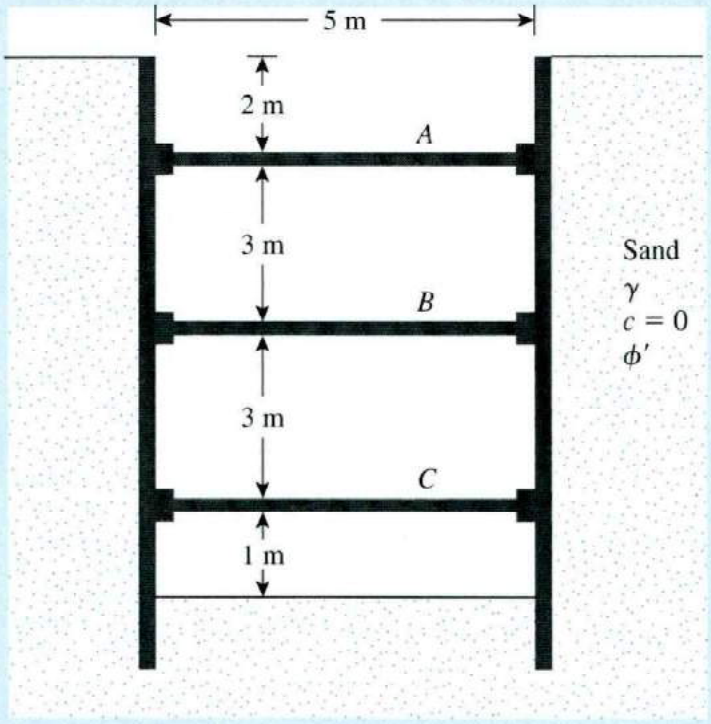

Figure 10.11

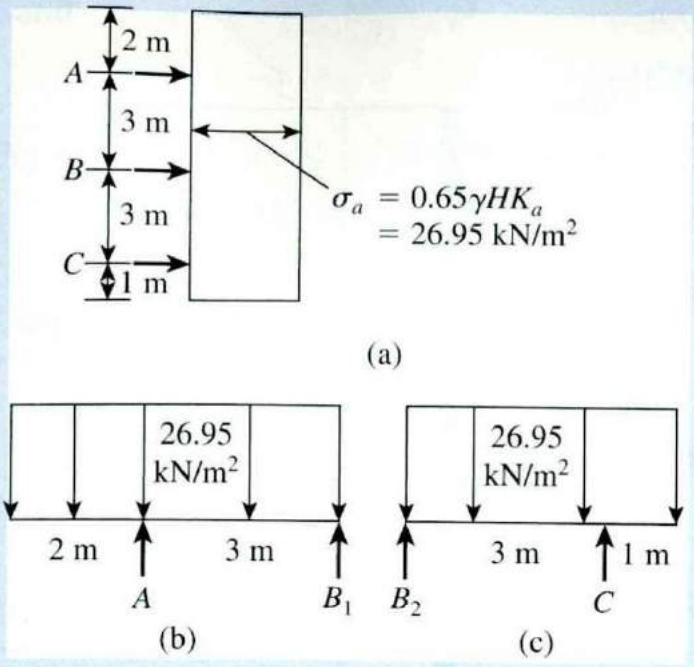

Figure 10.12 Load diagrams

$$C = \frac{(26.95)(4)\left(\frac{4}{2}\right)}{3} = 71.87 \text{ kN/m}$$

$$B_2 = (26.95)(4) - 71.87 = 35.93 \text{ kN/m}$$

The strut loads are

At A, $(112.29)(\text{spacing}) = (112.29)(4) = \mathbf{449.16\ kN}$

At B, $(B_1 + B_2)(\text{spacing}) = (22.46 + 35.93)(4) = \mathbf{233.56\ kN}$

At C, $(71.87)(\text{spacing}) = (71.87)(4) = \mathbf{287.48\ kN}$

University of Anbar
Engineering College
Civil Engineering Department

CHAPTER SIX

SLOPE STABILITY

LECTURE
DR. AHMED H. ABDULKAREEM
2017

Introduction

An exposed ground surface that stands at an angle with the horizontal is called an *unrestrained slope*. The slope can be natural or constructed. If the ground surface is not horizontal, a component of gravity will cause the soil to move downward, as shown in Figure 6.1. If the component of gravity is large enough, slope failure can occur; that is, the soil mass in zone *abcdea* can slide downward. The driving force overcomes the resistance from the shear strength of the soil along the rupture surface.

In many cases, civil engineers are expected to make calculations to check the safety of natural slopes, slopes of excavations, and compacted embankments. This process, called *slope stability analysis*, involves determining and comparing the shear stress developed along the most likely rupture surface with the shear strength of the soil.

The stability analysis of a slope is not an easy task. Evaluating variables such as the soil stratification and its in-place shear strength parameters may prove to be a formidable task. Seepage through the slope and the choice of a potential slip surface add to the complexity of the problem. This chapter explains the basic principles involved in slope stability analysis.

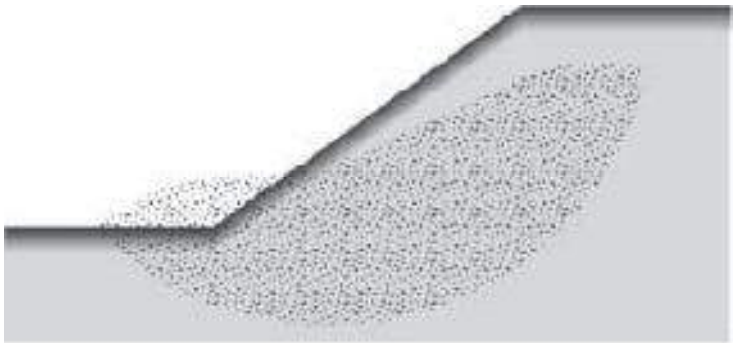

Figure 6.1 Slope failure

6.1 Factor of Safety

The task of the engineer charged with analyzing slope stability is to determine the factor of safety. Generally, the factor of safety is defined as

$$F_s = \frac{\tau_f}{\tau_d} \qquad (6\text{-}1)$$

where

FS_s = factor of safety with respect to strength

τ_f = average shear strength of the soil

τ_d = average shear stress developed along the potential failure surface

The shear strength of a soil consists of two components, cohesion and friction, and may be expressed as

$$\tau_f = c' + \sigma' \tan \phi' \qquad (6\text{-}2)$$

where
c' = cohesion
ϕ' = drained angle of friction
σ' = effective normal stress on the potential failure surface.

In a similar manner, we can also write

$$\tau_d = c'_d + \sigma' \tan \phi'_d \qquad (6\text{-}3)$$

where c'_d and ϕ'_d are, respectively, the effective cohesion and the angle of friction that develop along the potential failure surface. Substituting Eqs. (6.2) and (6.3) into Eq. (6.1), we get

$$F_s = \frac{c' + \sigma' \tan \phi'}{c'_d + \sigma' \tan \phi'_d} \qquad (6\text{-}4)$$

Now we can introduce some other aspects of the factor of safety-that is, the factor of safety with respect to cohesion, $FS_{c'}$, and the factor of safety with respect to friction, $FS_{\phi'}$ They are defined as follows:

$$F_{c'} = \frac{c'}{c'_d} \qquad (6\text{-}5)$$

and

$$F_{\phi'} = \frac{\tan \phi'}{\tan \phi'_d} \qquad (6\text{-}6\_$$

When Eqs. (6.4), (6.5), and (6.6) are compared, we see that when $FS_{c'}$ becomes equal to $FS_{\phi'}$, that is the factor of safety with respect to strength. Or, if

$$\frac{c'}{c'_d} = \frac{\tan \phi'}{\tan \phi'_d} \qquad (6\text{-}7)$$

we can write

$$F_s = F_{c'} = F_{\phi'}$$

When FS_s is equal to 1, the slope is in a state of impending failure. Generally, a value of 1.5 for the factor of safety with respect to strength is acceptable for the design of a stable slope.

6.2 Stability of Infinite Slopes

In considering the problem of slope stability, we may start with the case of an infinite slope, as shown in Figure 6.2. An infinite slope is one in which *H*is much greater than the slope height. The shear strength of the soil may be given by [Eq. (6.2)]

$$\tau_f = c' + \sigma' \tan \phi'$$

We will evaluate the factor of safety against a possible slope failure along a plane *AB* located at a depth *H* below the ground surface. The slope failure can occur by the movement of soil above the plane *AB* from right to left.

Let us consider a slope element, *abcd*, that has a unit length perpendicular to the plane of the section shown. The forces, *F*, that act on the faces *ab* and *cd* are

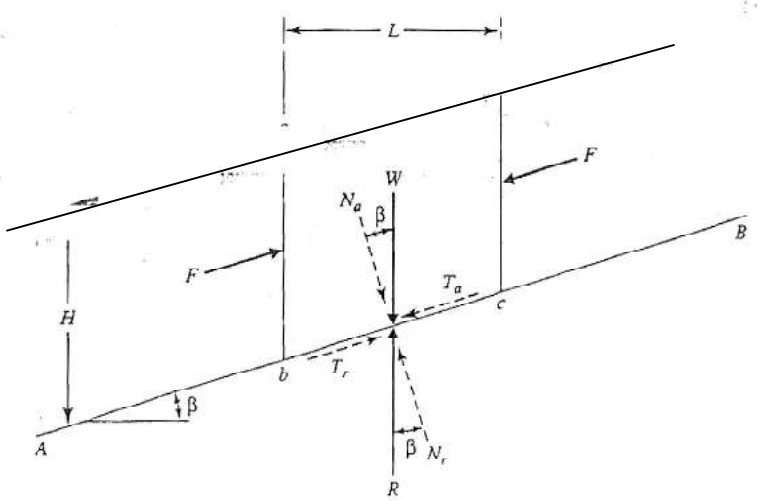

Figure 6.2 Analysis of infinite slope (without seepage)

equal and opposite and may be ignored. The effective weight of the soil element is (with pore water pressure equal to 0)

$$W = (\text{Volume of soil element}) \times (\text{Unit weight of soil}) = \gamma LH \qquad (6\text{-}8)$$

The weight W can be resolved into two components:

1. Force perpendicular to the plane $AB = N_a = W \cos\beta = \gamma LH \cos\beta$.
2. Force parallel to the plane $AB = T_a = W \sin\beta = \gamma LH \sin\beta$. Note that this is the force that tends to cause the slip along the plane.

Thus, the effective normal stress and the shear stress at the base of the slope element can be given, respectively, as

$$\sigma' = \frac{N_a}{\text{Area of base}} = \frac{\gamma LH \cos\beta}{\left(\frac{L}{\cos\beta}\right)} = \gamma H \cos^2\beta \qquad (6\text{-}9)$$

And

$$\tau = \frac{T_a}{\text{Area of base}} = \frac{\gamma LH \sin\beta}{\left(\frac{L}{\cos\beta}\right)} = \gamma H \cos\beta \sin\beta \qquad (6\text{-}10)$$

The reaction to the weight W is an equal and opposite force R. The normal and tangential components of R with respect to the plane AB are

$$N_r = R\cos\beta = W\cos\beta \qquad (6\text{-}11)$$

and

$$T_r = R\sin\beta = W\sin\beta \qquad (6\text{-}12)$$

For equilibrium, the resistive shear stress that develops at the base of the element is equal to $(T_r)/(\text{Area of base}) = \gamma H \sin\beta \cos\beta$. The resistive shear stress may also be written in the same form as Eq. (14.3):

$$\tau_d = c'_d + \sigma' \tan\phi'_d$$

The value of the effective normal stress is given by Eq. (6.9). Substitution of Eq. (6.9) into Eq. (6.3) yields

$$\tau_d = c'_d + \gamma H \cos^2\beta \tan\phi'_d \qquad (6\text{-}13)$$

This

$$\gamma H \sin\beta \cos\beta = c'_d + \gamma H \cos^2\beta \tan\phi'_d$$

Or

$$\frac{c'_d}{\gamma H} = \sin\beta\cos\beta - \cos^2\beta\tan\phi'_d$$

$$= \cos^2\beta(\tan\beta - \tan\phi'_d) \qquad (6\text{-}14)$$

The factor of safety with respect to strength was defined in Eq. (6.7), from which

$$\tan\phi'_d = \frac{\tan\phi'}{F_s} \quad \text{and} \quad c'_d = \frac{c'}{F_s}$$

Substituting the preceding relationships into Eq. (6.14), we obtain

$$F_s = \frac{c'}{\gamma H \cos^2\beta \tan\beta} + \frac{\tan\phi'}{\tan\beta} \qquad (6\text{-}15)$$

For granular soils, $c' = 0$, and the factor of safety, F_s, becomes equal to $(\tan\phi')/(\tan\beta)$. This indicates that in an infinite slope in sand, the value of F_s is independent of the height H and the slope is stable as long as $\beta < \phi'$.

If a soil possesses cohesion and friction, the depth of the plane along which critical equilibrium occurs may be determined by substituting $F_s = 1$ and $H = H_{cr}$ into Eq. (14.15). Thus,

$$H_{cr} = \frac{c'}{\gamma}\frac{1}{\cos^2\beta(\tan\beta - \tan\phi')} \qquad (6\text{-}16)$$

If there is seepage through the soil and the ground water level coincides with the ground surface as shown in Figure 6.3, the factor of safety with respect to strength can be obtained as

$$F_s = \frac{c'}{\gamma_{sat} H \cos^2\beta \tan\beta} + \frac{\gamma'}{\gamma_{sat}}\frac{\tan\phi'}{\tan\beta} \qquad (6\text{-}17)$$

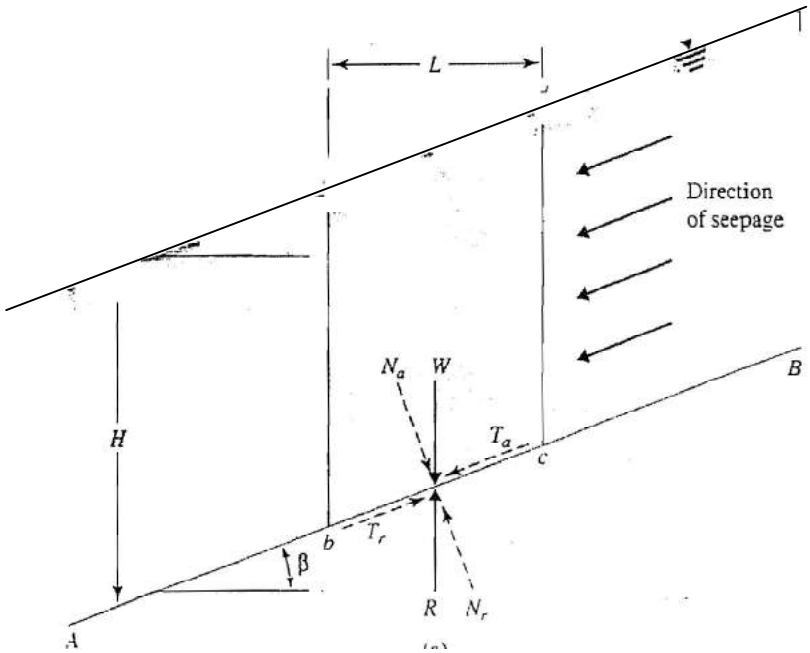

Figure 6.3Infinite slope with seepage

6.3 Finite Slopes

When the value of H_{cr} approaches the height of the slope, the slope is generally considered finite. When analyzing the stability of a finite slope in a homogeneous soil, for simplicity, we need to make an assumption about the general shape of the surface of potential failure. Although there is considerable evidence that slope failures usually occur on curved failure surfaces, Culmann (1875) approximated the surface of potential failure as a plane. The factor of safety, *FSs*, calculated using Culmann's approximation gives fairly good results for near-vertical slopes only.

After extensive investigation of slope failures in the 1920s, a Swedish geotechnical commission recommended that the actual surface of sliding may be approximated to be circularly cylindrical. Since that time, most conventional stability analyses of slopes have been made by assuming that the curve of potential sliding is an arc of a circle. However, in many circumstances (for example, zoned dams and foundations on weak strata), stability analysis using plane failure of sliding is more appropriate and yields excellent results.

Analysis of Finite Slope with Plane Failure Surface (Culmann's Method)

This analysis is based on the assumption that the failure of a slope occurs along a plane when the average shearing stress that tends to cause the slip is greater than the shear strength of the soil. Also, the most critical plane is the one that has a minimum ratio of the average shearing stress that tends to cause failure to the shear strength of soil.

Figure 6.4 shows a slope of height *H*. The slope rises at an angle _ with the horizontal. *AC* is a trial failure plane. If we consider a unit length perpendicular to the section of the slope, the weight of the wedge *ABC* = *W*:

$$W = \tfrac{1}{2}(H)(\overline{BC})(1)(\gamma) = \tfrac{1}{2}H(H\cot\theta - H\cot\beta)\gamma$$

$$= \frac{1}{2}\gamma H^2\left[\frac{\sin(\beta-\theta)}{\sin\beta\sin\theta}\right] \qquad (6\text{-}19)$$

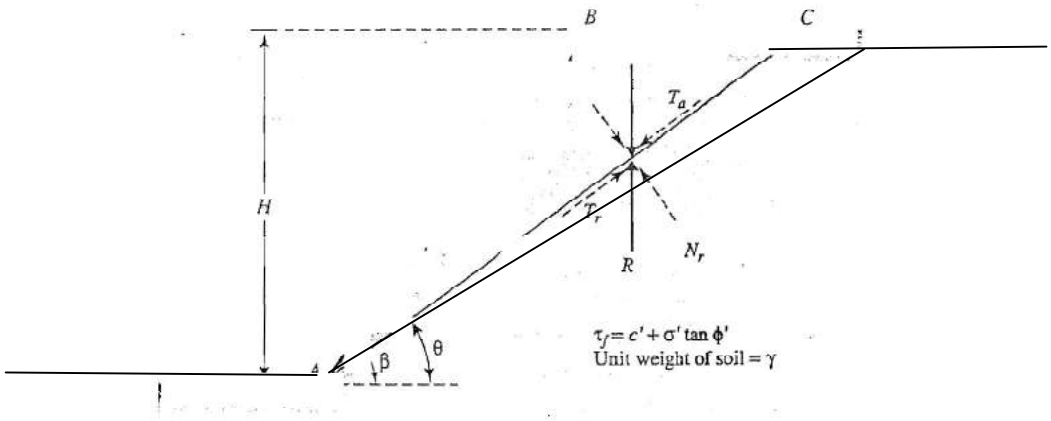

Figure 6.4 Finite slope analysis—Culmann's method

The normal and tangential components of W with respect to the plane AC are as follows:

$$N_a = \text{normal component} = W\cos\theta = \frac{1}{2}\gamma H^2\left[\frac{\sin(\beta-\theta)}{\sin\beta\sin\theta}\right]\cos\theta \quad (14.30)$$

$$T_a = \text{tangential component} = W\sin\theta = \frac{1}{2}\gamma H^2\left[\frac{\sin(\beta-\theta)}{\sin\beta\sin\theta}\right]\sin\theta \quad (14.31)$$

The average effective normal stress and the average shear stress on the plane AC are, respectively,

$$\sigma' = \frac{N_a}{(\overline{AC})(1)} = \frac{N_a}{\left(\frac{H}{\sin\theta}\right)}$$

$$= \frac{1}{2}\gamma H\left[\frac{\sin(\beta-\theta)}{\sin\beta\sin\theta}\right]\cos\theta\sin\theta \quad (14.32)$$

and

$$\tau = \frac{T_a}{(\overline{AC})(1)} = \frac{T_a}{\left(\frac{H}{\sin\theta}\right)}$$

$$= \frac{1}{2}\gamma H\left[\frac{\sin(\beta-\theta)}{\sin\beta\sin\theta}\right]\sin^2\theta \quad (14.33)$$

The average resistive shearing stress developed along the plane AC may also be expressed as

$$\tau_d = c'_d + \sigma'\tan\phi'_d$$

$$= c'_d + \frac{1}{2}\gamma H\left[\frac{\sin(\beta-\theta)}{\sin\beta\sin\theta}\right]\cos\theta\sin\theta\tan\phi'_d \quad (14.34)$$

Now, from Eqs. (14.33) and (14.34),

$$\frac{1}{2}\gamma H\left[\frac{\sin(\beta-\theta)}{\sin\beta\sin\theta}\right]\sin^2\theta = c'_d + \frac{1}{2}\gamma H\left[\frac{\sin(\beta-\theta)}{\sin\beta\sin\theta}\right]\cos\theta\sin\theta\tan\phi'_d \quad (14.35)$$

or

or

$$c_d = \frac{1}{2}\gamma H\left[\frac{\sin(\beta - \theta)(\sin\theta - \cos\theta \tan\phi'_d)}{\sin\beta}\right] \tag{14.36}$$

The expression in Eq. (14.36) is derived for the trial failure plane AC. In an effort to determine the critical failure plane, we must use the principle of maxima and minima (for a given value of ϕ'_d) to find the angle θ where the developed cohesion would be maximum. Thus, the first derivative of c_d with respect to θ is set equal to zero, or

$$\frac{\partial c'_d}{\partial \theta} = 0 \tag{14.37}$$

Because γ, H, and β are constants in Eq. (14.36), we have

$$\frac{\partial}{\partial \theta}[\sin(\beta - \theta)(\sin\theta - \cos\theta \tan\phi'_d)] = 0 \tag{14.38}$$

Solving Eq. (14.38) gives the critical value of θ, or

$$\theta_{cr} = \frac{\beta + \phi'_d}{2} \tag{14.39}$$

Substitution of the value of $\theta = \theta_{cr}$ into Eq. (14.36) yields

$$c'_d = \frac{\gamma H}{4}\left[\frac{1 - \cos(\beta - \phi'_d)}{\sin\beta \cos\phi'_d}\right] \tag{14.40}$$

The preceding equation can also be written as

$$\frac{c'_d}{\gamma H} = m = \frac{1 - \cos(\beta - \phi'_d)}{4 \sin\beta \cos\phi'_d} \tag{14.41}$$

where m = stability number.

The maximum height of the slope for which critical equilibrium occurs can be obtained by substituting $c'_d = c'$ and $\phi'_d = \phi'$ into Eq. (14.40). Thus,

$$H_{cr} = \frac{4c'}{\gamma}\left[\frac{\sin\beta \cos\phi'}{1 - \cos(\beta - \phi')}\right] \tag{14.42}$$